SUBSTRATE INSOLUBILITY DICTATES HSP104-DEPENDENTENDOPLASMIC RETICULUM ASSOCIATED DEGRADATION

by

George Michael Preston

BA in Biology, St. Mary's College of Maryland, 2009

Submitted to the Graduate Faculty of

the School of Medicine in partial fulfillment

of the requirements for the degree of

Doctor of Philosophy

University of Pittsburgh

UNIVERSITY OF PITTSBURGH

SCHOOL OF MEDICINE

This dissertation was presented

by

George Michael Preston

It was defended on

April 13, 2017

and approved by

Dr. Patrick Thibodeau, Assistant Professor, Department of Microbiology and Molecular Genetics

Dr. Arohan Subramanya, Assistant Professor, Department of Cell Biology and Molecular Physiology

Dr. Yong Wan, Professor, Department of Cell Biology and Molecular Physiology

Dr. Andrew VanDemark, Associate Professor, Department of Biological Sciences

Dissertation Advisor: Dr. Jeffrey L. Brodsky, Professor, Department of Biological Sciences

SUBSTRATE INSOLUBILITY DICTATES HSP104-DEPENDENT ENDOPLASMIC RETICULUM ASSOCIATED DEGRADATION

George Michael Preston, Ph.D.

University of Pittsburgh, 2017

Misfolded proteins that reside in the Endoplasmic Reticulum (ER) are degraded through a quality control process known as ER-associated degradation (ERAD). ERAD substrates are targeted to the 26S proteasome, but when proteasome function is compromised disease-associated ERAD substrates can aggregate in the cytoplasm. Under normal conditions, how are these misfolded substrates identified by ERAD factors? To address this question, a novel ERAD substrate, Q394X, was utilized. Q394X contains two transmembrane domains fused to a truncated, C-terminal Nucleotide Binding Domain (NBD) from the well-characterized ERAD substrate, Ste6p*. By exposing ER-enriched microsomes containing Q394X to the non-ionic detergent, dodecyl maltoside (DDM), Q394X was shown to be partially extracted from membranes and is less soluble than the wild type version of Q394X (Chimera A). However, Q394X solubility was restored after addition of 6M urea to similar levels as Chimera A. Interestingly, systematically truncating the NBD at sites both N-terminal and C-terminal to the truncation site in Q394X had varying effects on protein solubility and stability. Two of the truncation mutants were as soluble as Chimera A, while the others exhibited the decreased solubility that was evident for Q394X. By performing degradation assays, it was demonstrated that protein solubility and stability are positively correlated.

To define how cells process the less soluble substrate, Q394X, I next investigated which chaperones might mediate its degradation. I found that Q394X was stabilized in yeast when genes encoding members of the protein disaggregation machinery, including the AAA+ ATPase, Heat

Shock Protein of 104 kDa (Hsp104), were deleted. Under these conditions of Q394X stabilization in the absence of Hsp104, I determined that Q394X aggregates in the ER membrane. Furthermore, Hsp104 was shown to localize to punctae under these conditions, but formation of these punctae requires Q394X expression. This aggregation of Q394X leads to a decrease in Q394X retrotranslocation by Cdc48. These data provide evidence that Hsp104 acts to disaggregate Q394X in the ER membrane, which is required for efficient Q394X retrotranslocation and degradation.

TABLE OF CONTENTS

LIST OF TABLES

LIST OF FIGURES

LIST OF ABBREVIATIONS

αENAC	The alpha subunit of the heterotrimeric epithelial sodium channel
CF	Cystic Fibrosis
CFTR	cystic fibrosis transmembrane conductance regulator
CHIP	C-terminus of Hsc70- interacting protein
DDM	non-ionic detergent, dodecyl maltoside
DUBs	deubiquitinating enzymes
ER	Endoplasmic Reticulum
ERAD	Endoplasmic reticulum-associated degradation
ERAD-C	ER cytosolic lesion
ERAD-L	ER luminal lesion
HECT	homologous to the E6AP carboxyl terminus
HRD	Hmg CoA reductase degradation
HSP	heat-shock protein
Q394X/Q1249X	Chimera A^{Q394X}/ $Ste6^{Q1249X}$
RING	really interesting new gene
SCF	Skp1, Cullins, F-box proteins
SUMO	small ubiquitin-like modifier
UBX	ubiquitin regulatory X
UPS	ubiquitin-proteasome system

PREFACE

I would first like to express my sincerest gratitude to my thesis advisor, Dr. Jeffrey L. Brodsky. Throughout my graduate career, Jeff has been the best mentor for which I could have asked. He has supported me in every avenue of my life, for which I am forever grateful. Jeff has provided me with the ideal scientific environment, which has allowed me to become the scientist that I am. Jeff's willingness to allow me the opportunity to take ownership of my research, while also never failing to be available to help when needed, has shown me what being a great mentor entails. I know that the skills and lessons I have learned under Jeff's mentorship will help me to succeed in whatever avenue I choose to pursue in my scientific career.

I would also like to thank the members of the Brodsky lab, both past and present. The environment that the members of this lab create is one that helps facilitate great science and helped make my time in graduate school enjoyable. I would especially like to thank Dr. Christopher Guerriero, who trained me when I started in the lab and has been a great source of advice and support since. I would also like to thank Jennifer Goeckeler-Fried for being a great lab manager and helping to make my science go as smoothly as possible. Finally, I would like to thank my fellow graduate students in the Brodsky lab. I have greatly appreciated your friendship and support as we have navigated our way through graduate school together.

Next, I would like to thank the members of my thesis committee for their support and their influence in my research. Dr. Patrick Thibodeau, Dr. Arohan Subramanya, Dr. Yong Wan, and Dr. Andrew VanDemark have all helped to guide me towards success in my research. Their well-timed advice and readiness to help is sincerely appreciated. I would also like to thank all the members of the Department of Cell Biology and the Department of Biological Sciences at the

University of Pittsburgh. I have had the distinct honor of being able to interact with the members of both of these departments, giving me a huge resource throughout my graduate career. My interactions with these scientists will forever impact my career and for that I am grateful.

Finally, I would like to thank my family and friends. To my parents, George and Barbara Preston, I could not be where I am without your never-ending support and love. To my brother and sister, Jason and Elizabeth, I am extremely grateful for your love, support, and friendship. To my beautiful wife, Kristy, I am forever grateful for all that you have done to help me to achieve this accomplishment. The past 5 years would not have been possible without you by my side and I love you. To my beautiful daughter Avery, the past 10 weeks with you have taught me so much. You inspire me to be the best person I can be and you have helped me to finish graduate school with motivation and purpose. To the friends I have made both in and outside of graduate school, I thank you for your support and helping to keep me grounded. I will always value our friendships.

1.0 INTRODUCTION

In order to survive, cells must be capable of dealing with a variety of stresses, including temperature, oxidative stress, and mutations in their DNA. These stresses often lead to problems in protein folding, which is linked to multiple human diseases. In order to properly abrogate these stresses, cells possess a series of mechanisms, called quality control pathways. These quality control pathways help rid the cell of problematic proteins. One important quality control pathway is the endoplasmic reticulum associated degradation (ERAD) pathway (1).

While ERAD consists of multiple steps ultimately leading to a protein's degradation, one of the most important steps is the ubiquitination of misfolded proteins on the cytosolic face of the ER membrane. This act of attaching ubiquitin to a protein targets it for degradation by the 26S proteasome. In this introduction, I will discuss the foundation of what is known about the role of the ubiquitin-proteasome system (UPS) in ERAD. I will address how proteins fold, and in the event that they misfold, how ERAD destroys them. I will review the initial findings that have proven to be crucial for our current understanding of ERAD and how cells destroy misfolded proteins. Finally, I will present what is currently known about the important factors of the UPS that play a role in ERAD, along with some of the alternative mechanisms that can be utilized to achieve protein degradation.

1.1 THE UBIQUITINATION PATHWAY

The ubiquitination of a misfolded protein can represent a rate-limiting step during ERAD. But, before the substrate can be ubiquitinated, cells utilize an E1 ubiquitin-activating enzyme that hydrolyzes ATP to create a thiol-ester bond with the C-terminal carboxylate in ubiquitin (Figure 1) (2-4). After activation, an E2 ubiquitin-conjugating enzyme is utilized to transfer ubiquitin to a substrate that may be bound to an E3-ubiquitin ligase. In other cases, the substrate may be linked to the E3 by a molecular chaperone (see below). Currently, only 1 E1 ubiquitin-activating enzyme and 11 E2 ubiquitin-conjugating enzymes have been identified in yeast, whereas there are 2 E1 ubiquitin-activating enzymes and 35 E2 ubiquitin-conjugating enzymes that have been identified in humans (5, 6). In contrast, there are roughly 80 and 600 putative E3s in yeast and humans (7).

Among these many ligases, three classes of E3s function in ERAD: (1) RING domain, (2) HECT domain, and (3) U-box domain E3s. RING domain and U-box domain E3s facilitate the transfer of ubiquitin from the E2 ubiquitin-conjugating enzyme to the substrate, whereas HECT domain E3s are directly ubiquitinated before the ubiquitin is transferred (8-12). Once the substrate becomes mono-ubiquitinated, an ubiquitin chain can be synthesized and elongated. The most prominent Lys in ubiquitin that is elongated in this manner and used to target substrates for degradation is Lys-48 (4, 13-15). However, substrate ubiquitination via Lys-11-derived isopeptide linkages are also recognized by the proteasome (16). A more recently discovered class of components of the ubiquitination machinery are the ubiquitin chain elongation factors, called E4s (17). As the name implies, the activity of the E4 elongates the polyubiquitin chain in order to more effectively recruit factors that facilitate substrate degradation and expedite proteasomal degradation (18-20). After an ERAD substrate has been adequately ubiquitinated (Figures 2 and

3), the p97/Cdc48 complex is recruited to the substrate by its cofactors, Ufd1, Npl4, and in some cases Ubx2 (UBXD8 in mammalian cells) (21, 22).

Interestingly, the viral protein, US11, which promotes the ERAD of specific substrates (see below), interacts with p97 in a ubiquitin-independent manner in mammalian cells (23). However, most p97/Cdc48 substrates are ubiquitinated. The recruitment of the p97/Cdc48 complex leads to substrate 'retrotranslocation' (or 'dislocation' for membrane proteins) from the ER and into the cytosol, where it is bound and shuttled to the 26S proteasome by delivery factors, such as Rad23 and Dsk2, in yeast (24). Interaction of Rad23 with the Cdc48–Ufd1–Npl4 complex is mediated by another Cdc48 cofactor, the E4 Ufd2 (20). Once Rad23 and Dsk2 bind the Cdc48 complex, they link the complex to the proteasome through a component that resides on the proteasome 'cap' (also known as the 19S particle or PA700), Rpn1 (25). In addition to binding by Rad23–Dsk2– Rpn1, another component of the 19S cap, called Rpn10, can bind ubiquitin in an Rad23-independent manner (26). After substrate binding to the 19S particle of the proteasome, the proteasome-associated deubiquitinating enzymes (DUBs), Ubp6 and Rpn11, cleave the ubiquitin chain from the substrate, and the substrate is subsequently threaded into the 20S core particle and degraded (27-31). Entry into the 20S particle requires the activity of six AAA-ATPases that drive substrate entry into the core and facilitate the opening of an aperture that otherwise retains the 20S particle in a closed state (32, 33).

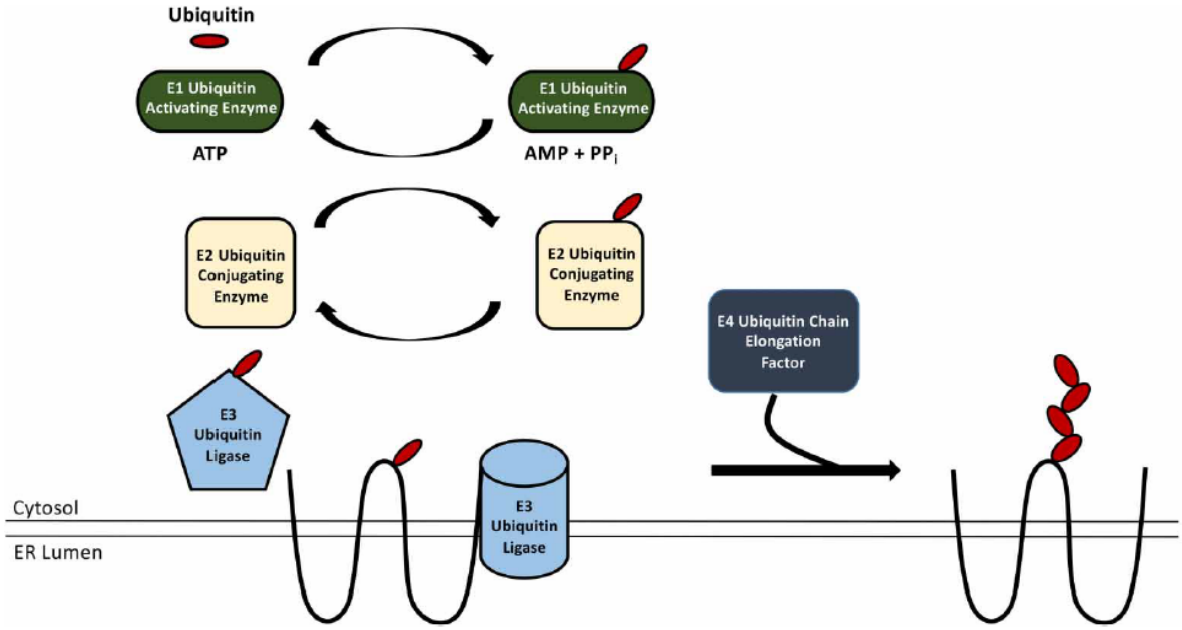

Figure 1. The ubiquitination pathway

The cytosolic E1 ubiquitin-activating enzyme hydrolyzes ATP to activate the ubiquitin molecule. ATP hydrolysis and the formation of a transient AMP-derivative lead to the formation of a thioester bond between the E1 and the C-terminus of ubiquitin. The E1 then transfers ubiquitin to one of the ~11 yeast or the ~35 mammalian E2 ubiquitin-conjugating enzymes. The covalently bound ubiquitin–E2 adduct then binds one of the ~80 yeast or the ~300 mammalian E3 ubiquitin ligases. The E3 enzymes may also be bound to the ERAD substrate and facilitate transfer of ubiquitin to the substrate, or a chaperone intermediate (not shown) may facilitate transfer. Some E3 ubiquitin ligases (e.g. HECT domain E3s) become covalently modified with ubiquitin during ERAD substrate modification, while other E3s (e.g. RING and U-box domain proteins) facilitate the transfer of ubiquitin from the E2 ubiquitin-conjugating enzyme to the substrate. Importantly, select E2 ubiquitin-conjugating enzymes and E3 ubiquitin ligases are cytoplasmic, while others reside at the ER membrane. Once a substrate is ubiquitinated by an E3 ubiquitin ligase, other enzymes, such as E4s, may further extend the ubiquitin chain on the ERAD substrate.

1.2 PROTEIN MISFOLDING AND ERAD

In cells, proteins must adopt a specific fold that allows them to perform their required functions. Early *in vitro* studies investigating protein folding demonstrated that the information needed for proteins to fold is contained in the amino acid sequence (34). However, it is not feasible for proteins to sample all potential partially folded conformations, as the time it would take to fold even small proteins would be well beyond the time-frame in which proteins are known to fold (35). Instead, it is believed that proteins adopt short-range interactions within their local environment, which helps to guide them to adopt their functional fold (36). These intramolecular interactions lead to the orientation of hydrophobic regions towards the interior of the protein, formation of and interactions between secondary structures within the protein, and the alignment of regions for post-translational modifications (37). Partial folding through intramolecular interactions leads to the adoption of more ordered structures, which then leads to the peptide residing in lower free energy states. By having large differences in free energy between intermediate folded forms and the native conformation, proteins are more likely to reside in their properly folded state (38). Using free energy differences to drive proper folding is important, because the lower free energy states have fewer potential alternative states, which allows proteins to fold more quickly and/or efficiently (36). However, it is still possible that native peptides sample these incompletely folded states, as some populations of protein folding intermediates have been observed *in vitro* (39). It has been suggested that these folding intermediates may help the protein to adopt its properly folded state; alternatively, they could represent misfolded, trapped states of the protein (40). Regardless, *in vitro* folding studies have been used to learn a lot about the dynamics of protein folding.

While many of the principles of protein folding are likely the same *in vivo* as have been observed *in vitro*, proteins face a different problem *in vivo*. In cells, proteins often fold co-

translationally or after being inserted into a specific organelle, such as the endoplasmic reticulum (ER) (41, 42). In these cellular environments, newly synthesized peptides are exposed to a variety of factors that affect protein folding, including varying ion concentrations, oxidative states, etc… (43, 44). However, one aspect of the cellular folding environment that is particularly problematic for protein folding is the level of protein crowding that exists inside the cell (45). Protein crowding increases the risk of newly synthesized peptides adopting improper conformations or increases the potential for improper protein-protein interactions (46). In order to combat these improper protein-protein interactions and to assist with the proper folding of newly synthesized peptides, the cell utilizes a class of proteins called molecular chaperones.

Molecular chaperones perform a variety of functions in the cell, including assisting in the folding of newly synthesized proteins, assisting with refolding of denatured/aggregated proteins, facilitating protein trafficking, and degrading terminally misfolded proteins (47). The basic mechanism of molecular chaperone recognition and binding to proteins is through the exposure of hydrophobic amino acid side chains in the peptide (47). While different molecular chaperone classes may perform varying functions in the cell, molecular chaperones can be split into two general groups: 1) The ATP-dependent chaperones and 2) the ATP-independent chaperones. ATP-dependent molecular chaperones, such as the Hsp70s and chaperonins, initially assist in protein folding by binding exposed hydrophobic stretches and preventing improper protein-protein interactions (47). Upon ATP hydrolysis, these molecular chaperones release the substrates, thereby allowing them to fold. The ATP-independent chaperones, such as the small heat shock proteins (sHSPs), are believed to bind hydrophobic stretches and maintain substrate solubility until the protein can be processed further by other chaperones (48). As mentioned above, some chaperones are also known to play important roles in protein degradation. This is especially true

in the ER where molecular chaperones, such as the ER-luminal Hsp70, Kar2, and the ER lectin, Yos9, bind to misfolded proteins and serve an important role in the selection of proteins to be degraded (49, 50).

Misfolded, aggregation-prone proteins present a distinct challenge to cells. Specifically, they must be destroyed prior to aggregation, as protein aggregation can be toxic to cells (51). In the ER, the mechanism of ERAD is crucial for the clearance of misfolded proteins and to prevent aggregation in the ER (Figures 2 and 3, (1)). Initially, ERAD substrates are recognized as terminally misfolded by a series of factors, including molecular chaperones and components of the UPS (49, 50, 52-56). Once a protein has been selected for ERAD, the components of the UPS append a poly-ubiquitin chain to the terminally misfolded protein (For more, see section 1.1 and 1.3). This ubiquitin chain serves as a recruiting signal for the AAA+ ATPase, Cdc48/p97, at the ER membrane, which is mediated specifically by the Cdc48/p97 cofactors, Ufd1 and Npl4 (20, 23). Once Cdc48/p97 binds to the ERAD substrate, it is removed from the ER and into the cytosol, where it is further processed and degraded by the 26S proteasome (57).

1.3 THE FIRST LINK BETWEEN THE UBIQUITIN PATHWAY AND ERAD

Ubiquitination was first identified as an ATP-dependent process important for protein degradation in the late 1970s/early 1980s (58, 59). However, it was not until the 1990s that a component of the ubiquitination machinery was discovered at the ER (60). This factor is an ER membrane-resident E2 ubiquitin-conjugating enzyme, Ubc6. It was shown that deleting UBC6 leads to the rescue of a sec61 mutant allele that is defective for protein translocation, or entry into the ER. In the absence

of Ubc6, the mutant Sec61 channel has a longer half-life, which allows for partial rescue of protein translocation.

Other early discoveries led to the identification of proteins in the ER that were ubiquitinated. At least initially these were substrates that trafficked through the secretory pathway, but were retained in this compartment due to errors in folding or maturation. One of the most notable substrates identified was the cystic fibrosis transmembrane conductance regulator (CFTR), whose failure to properly fold and mature due to rapid degradation is the cause of cystic fibrosis (CF) (61, 62). Degradation of both immature forms of the wild-type and the ΔF508 mutant form of CFTR, which accounts for the majority of CF cases, was shown to be dependent on both the E1 ubiquitin-activating enzyme and the 26S proteasome for degradation. CFTR and ΔF508 were also directly shown to be ubiquitinated.

Substrates used to identify additional components of the ubiquitination machinery in the yeast ER included a mutated form of a vacuole-targeted protein, carboxypeptidase yscY, which was subsequently termed CPY* (63). Analyses of CPY* degradation uncovered the importance of an E2 ubiquitin-conjugating enzyme, Ubc7, as well as the proteasome in removing this trapped protein from the ER (63-65). In parallel, an enzyme that catalyzes the rate-limiting step in cholesterol synthesis, known as hydroxymethylglutaryl coenzyme A reductase, was known to be metabolically regulated and degraded in the ER (66, 67). By examining the genetic requirements for the degradation of the yeast homolog, Hmg2, three HRD genes that are important for the degradation of Hmg2 at the ER were identified (68). Two of these HRD genes, HRD1 and HRD3,

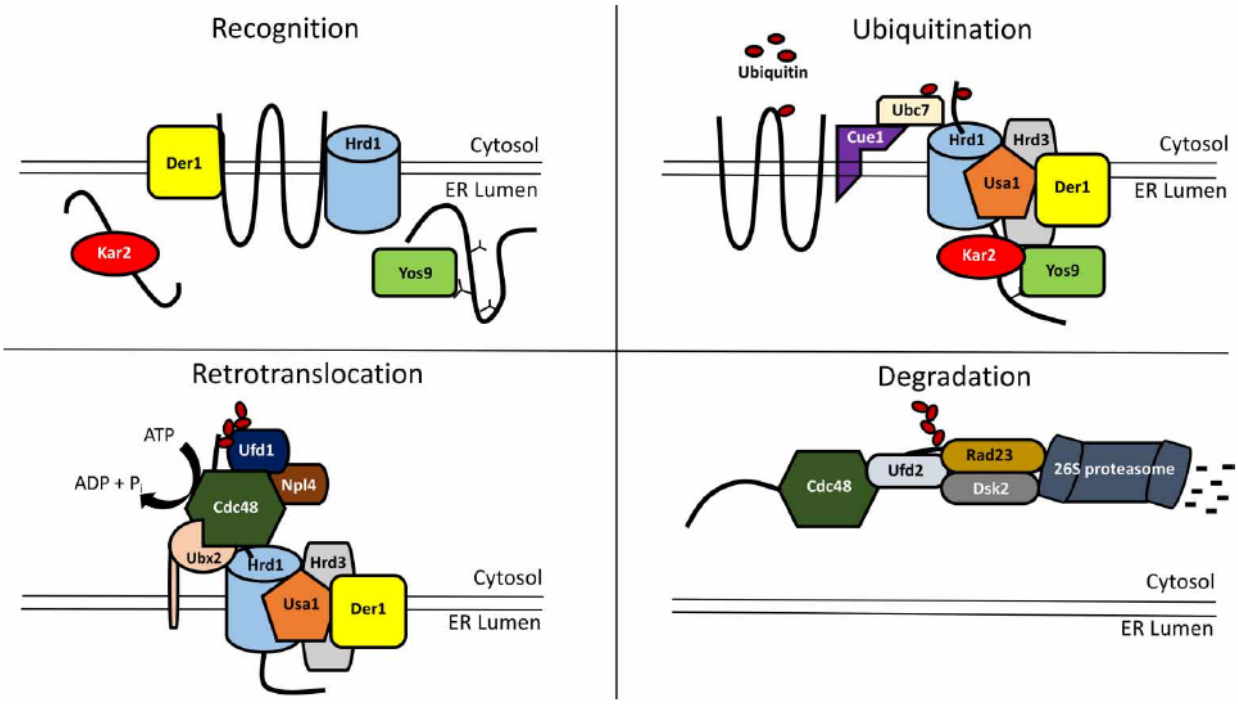

Figure 2. Function of the Hrd1 complex during ERAD in yeast

In the first step during ERAD ('Recognition'), a misfolded substrate is recognized by a subset of factors, namely Kar2 (ER luminal Hsp70 chaperone), Yos9 (ER luminal lectin), Der1 (transmembrane core Hrd1 complex member), or directly by the E3, Hrd1. Once the substrate has been recognized, the substrate is transferred to the Hrd1 complex for polyubiquitination. Kar2 and Yos9 bind to the Hrd1 core complex member, Hrd3, and the substrate is transferred to Hrd1 ('Ubiquitination'). Der1 is bound by Usa1, which helps link Der1 to Hrd1. Cue1 is an ER membrane protein that recruits the E2 ubiquitin-conjugating enzyme, Ubc7, to the Hrd1 complex. After the substrate is polyubiquitinated, the dislocation machinery is linked to the complex. This dislocation complex consists of the membrane protein, Ubx2, which helps recruit the AAA+ ATPase, Cdc48. Cdc48 is stabilized at the Hrd1 complex through an interaction with Hrd1 and through an interaction with the Cdc48 cofactors, Ufd1 and Npl4, with the polyubiquitin chain. Assembly is believed to be due to Ufd1 binding to the polyubiquitin chain, as yeast Npl4

lacks a zinc finger domain. Another class of cofactors that bind Cdc48 and affect retrotranslocation includes DUBS, such as Otu1 (not shown here). Once bound to the substrate, Cdc48 hydrolyzes ATP and liberates the substrate from the ER ('Retrotranslocation'). The Cdc48 cofactor, Ufd2, then extends the polyubiquitin chain and interacts with the ubiquitinated protein shuttles, Rad23 and Dsk2 ('Degradation'). Although not shown in this figure, ubiquitin chains may be trimmed by DUBS prior to substrate passage through Cdc48 and then extended again by Ufd2. Rad23 and Dsk2 can also interact with the 19S cap of the cytosolic 26S proteasome, which leads to substrate degradation. Another DUB associated with the 19S cap of the proteasome, called Rpn11 (not shown), removes the polyubiquitin chain attached to the ERAD substrate, so it efficiently threads into the core of the 26S proteasome for degradation.

are vital for the ubiquitination and degradation of many other ERAD substrates (Table 1) (69-71). Hrd1 is one of the major ER membrane-resident E3s involved in ERAD in yeast and is the central component of the Hrd1 complex, which is conserved between yeast and mammals (see below). Hrd3 is an ER membrane-resident protein that interacts with Hrd1. When HRD3 is deleted, Hrd1 degradation increases, leading to a loss of function of the Hrd1 complex (70, 72, 73). Finally, the major histocompatability complex class I (MHCI) protein was utilized to identify a novel mechanism of immune evasion by human cytomegalovirus (HCMV). A virally encoded, ER-localized protein, US11, triggered nascent MHCI heavy chain transport from the ER into the cytosol, where it is acted upon by a cytosolic N-glycanase, ubiquitinated, and subsequently, degraded by the 26S proteasome (74, 75). Together, these substrates have proved essential for continued analysis of the factors important for ubiquitination and degradation during ERAD.

1.4 EXPANDING THE LINKS BETWEEN UBIQUITINATION AND ERAD

1.4.1 Identification of contributing E3s and their associated complexes

While these initial breakthroughs were crucial to better understand the importance of protein ubiquitination in ERAD, the years that followed led to the identification of additional factors, complexes, and substrates associated with this process (Table 1). In yeast, there are two primary E3s, Hrd1 and Doa10, that are required for ubiquitination and degradation; however, there are currently eight E3s that play some role during the ubiquitination of ERAD substrates in yeast. In mammals, there are four E3s, Hrd1, TEB4, gp78, and CHIP, which are associated with the degradation of several notable ERAD substrates, but ~19 E3s have been linked more generally to ERAD (Table 1). The expanded number of E3s involved in ERAD in mammals when compared with yeast is most probably due to the greater number of potential substrates (e.g. transmembrane proteins) in mammalian cells.

While Hrd1 was the first E3 linked to the ERAD pathway, it was appreciated later that the Hrd1 complex (Figure 2) ubiquitinates substrates that possess misfolded regions in their ER luminal (ERAD-L) or membrane spanning domains (ERAD-M) (68, 69, 71, 76, 77). In yeast, the Hrd1 complex consists of Hrd3, Usa1, Der1, Dfm1, Yos9, Kar2, Ubc7, and Cue1 (73, 78). While these factors are all known to be a part of the Hrd1 complex, not all of them are considered components of the core Hrd1 complex. When the complex was purified, Hrd3, Usa1, Der1, and Yos9 co-purified, thus defining components of the core complex (78). As noted previously, Hrd3 stabilizes the Hrd1 oligomer, but also binds glycosylated misfolded luminal substrates by interacting with a luminal lectin, Yos9, as well as nonglycosylated misfolded substrates via an Hsp70 molecular chaperone, Kar2 (49, 50, 52, 70). Until recently, it was difficult to study the

role of Hrd3 in ERAD due to the increased turnover of Hrd1 when HRD3 is deleted. However, when the ubiquitin-like domain of Usa1 is removed, Hrd1 remains stable and a direct role for Hrd3 in ERAD was established (79). Der1 also binds soluble luminal substrates and interacts with Hrd1 through Usa1 (80, 81). In addition, a Der1 homolog, Dfm1, interacts with Hrd1 and the E3 ligase, Doa10, and helps degrade a Doa10 substrate, Ste6* (21, 82). In a mechanism believed to be independent of ERAD, Dfm1 also interacts with Cdc48 in the absence of Ubx2 (82, 83). As the Hrd1 complex engages substrates, Ubc7 is recruited to the ER membrane by a transmembrane protein, Cue1 (84, 85). In addition to Ubc7, another E2, Ubc1, ubiquitinates select ERAD substrates (69, 86). Hrd1 also recruits the ER membrane protein, Ubx2, to the complex, which anchors Cdc48 to the membrane (21, 22). Ubx2 anchoring facilitates efficient substrate retrotranslocation. Some evidence suggests that Der1 and the mammalian homolog (also see below) may act as the retrotranslocation channel for substrates, or at least are intimately associated with the retrotranslocation process (87-91), while other evidence suggests that Hrd1 could serve as the channel (92, 93). In either case, this would position the ubiquitination machinery near the site of retrotranslocation.

Mammalian homologs for many of the components discussed above were subsequently identified (Figure 3). The mammalian homolog of Hrd1, also called HRD1 or synoviolin (94, 95), is important to ubiquitinate several ERAD substrates (Table 1). Other mammalian homologs of yeast Hrd1 complex members have been identified as well: SEL1L (Hrd3), HERP (Usa1), DERLIN-1, DERLIN-2, DERLIN-3 (Der1), OS-9 and XTP3-B (Yos9), BiP (Kar2), UBE2G2 (Ubc7), and Aup1 (Cue1) (78, 89, 96-102).

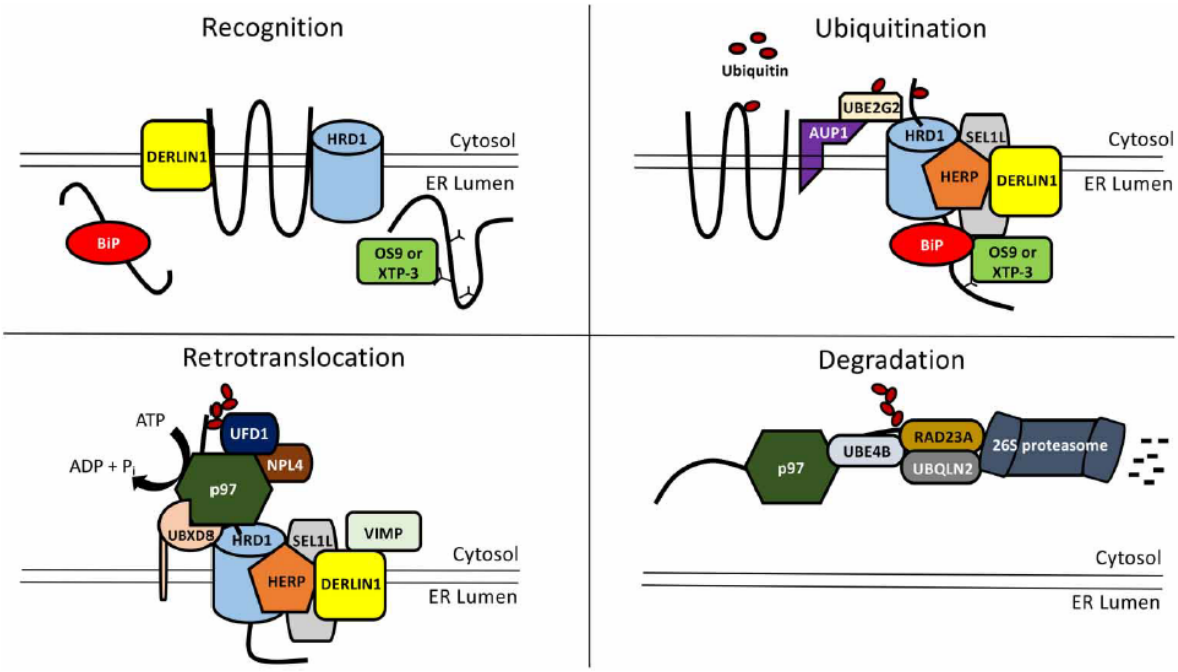

Figure 3. Function of the Hrd1 complex during ERAD in mammalian cells

In the first step during ERAD (‘Recognition’), a substrate is recognized by a group of luminal and membrane-associated factors, namely BiP (Hsp70 chaperone), OS9 and XTP-3 (lectins), Derlin1 (transmembrane core Hrd1 complex member), and/or HRD1. While OS9 and XTP-3 recognize misfolded ER luminal glycosylated substrates, they may also recognize nonglycosylated substrates. The substrate is then transferred to the HRD1 complex and polyubiquitinated. BiP, OS9, and XTP-3 bind the HRD1 core complex member, SEL1L, and the substrate is next transferred to HRD1 (‘Ubiquitination’). DERLIN1 is bound by HERP1, which helps link Derlin1 to HRD1. The mammalian HRD1 complex can utilize DERLIN2 and DERLIN3 as well. AUP1 is a Cue domain-containing ER membrane protein that recruits the E2 ubiquitin-conjugating enzyme, UBE2G2, to the HRD1 complex. Once polyubiquitinated, the dislocation machinery is recruited to the HRD1 complex. This complex includes the membrane protein, UBXD8, which augments p97 recruitment to the HRD1 complex. Along with UBXD8, the HRD1 complex can utilize another protein, called UBXD2, to recruit p97. p97 is further stabilized at the HRD1 complex

through interaction with HRD1 along with the p97 cofactors, UFD1 and NPL4, via the polyubiquitin chain. In an alternative mechanism of p97 recruitment, the cytoplasmic protein, VIMP, binds p97 (not shown) at the HRD1 complex through a VIMP interaction domain in DERLIN1. Another class of cofactors that bind p97 and act during ERAD include DUBS, such as YOD1 (not shown). Once bound to the substrate, p97 hydrolyzes ATP and removes the substrate from the ER ('Retrotranslocation'). After retrotranslocation, the p97 cofactor and a mammalian homolog of Ufd2, UBE4A/B, may extend the polyubiquitin chain and associate with the protein shuttles, RAD23A, and a specific UBIQUILIN, UBQLN2 ('Degradation'). Ubiquitin chains may be trimmed by DUBS prior to substrate transit through p97 and could then be extended again by UBE4A/B. RAD23A and UBIQUILIN also interact with the 19S cap of the cytosolic 26S proteasome, which facilitates substrate degradation. In addition, there is a DUB associated with the 19S cap of the proteasome, RPN11, which removes the polyubiquitin chain attached to the ERAD substrate, which aids efficient entry of the substrate into the 26S proteasome core.

Perhaps not surprisingly, mammalian HRD1 complex members have also been implicated in the ubiquitination of ERAD substrates (Table 1). As in yeast, HRD1 functions in the degradation of both glycosylated (utilizing EDEM1, DERLIN-2, DERLIN-3, OS-9, XTP3-B, and SEL1L) and nonglycosylated substrates (utilizing BiP, HERP, and DERLIN-1) (1, 53-56). While HRD1 activity for glycosylated substrates is generally thought to function in a SEL1L-dependent manner (96, 100), another HRD1 regulator, the ER membrane-resident protein FAM8A1, binds and regulates HRD1 function in an SEL1L-independent manner (103). After substrate association with the HRD1 complex, AUP1, which contains a Cue domain homologous

to that found in the yeast Cue1 protein, binds the complex and recruits UBE2G2 through its G2BR domain (100, 101, 103-106). For some substrates, HRD1 also utilizes the Ubc6 homolog, UBE2J1 (107). Which of these E2 ubiquitin conjugating enzymes is the predominant enzyme for HRD1 is an open question. Mammalian HRD1 also binds to other factors that play a role in ERAD. For example, Hrd1 associates with UBXD2 and UBXD8, which function similarly to yeast Ubx2 in anchoring p97 to the ER membrane. Furthermore, UBXD2 recruits the mammalian Dsk2 homolog, called UBIQUILIN (100, 108-111), to the Hrd1 complex, whereas UBXD8 recruits a cytosolic chaperone, BAG6 (112, 113). Recently, UBIQUILIN and BAG6 were shown to function as chaperones as well, suggesting that they play an important role as holdases for dislocated proteins prior to degradation (112, 114). Yet, another factor that binds the HRD1 complex and recruits p97 is VIMP (VCP-interacting membrane protein) (115). VIMP localizes to the HRD1 complex via association with DERLIN-1 and subsequently binds p97. HRD1 and DERLIN-1 are also capable of binding p97, suggesting that they contribute to the maintenance of p97 residence at the ER membrane (116, 117).

Table 1. List of cellular factors shown to affect the ubiquitination of ERAD substrates

Factors	Select Substrates	Notes	References
E1 Ubiquitin Activating Enzymes[1]			
Yeast			
Uba1			(118)
Mammalian			
E1a, E1b		Isoforms resulting from alternative splicing	(119-121)

E2 Ubiquitin Conjugating Enzymes[2]			
Yeast			
Ubc1	CPY*, Hmg2	Cytosolic E2 that is recruited to the ER membrane by Hrd1	(69, 86)
Ubc6	Sss1, *sec61*, Deg1-Ura3, Pma1-D378N, Ste6*	Integral ER membrane E2	(64, 122-125)
Ubc7	Hmg2, CPY*, SSS1, *sec61*, Deg1-Ura3, Pma1-D378N, Ste6*	Cytosolic E2 that is recruited to ER membrane by Cue1	(63-65, 69, 71, 122-126)
Ubc2	Ste6*	Cytosolic E2 only shown to be important with Ubr1	(127)
Mammalian			
UBE2D1	CFTR, p53, APP	Homolog of yeast Ubc4/5	(121, 128, 129)
UBE2J1	MHCI, CFTR, TCRα, OS-9, EDEM, SEL1L	Homolog of yeast Ubc6	(104, 107, 130, 131)
UBE2K	MHCI	Homolog of yeast Ubc1, used by viral protein US11	(132)
UBE2G2	HERP, gp78, CD3-δ, TCRα, $InsP_3R$	Homolog of yeast Ubc7	(106, 133-135)
E3 Ubiquitin Ligases			
Yeast			
Hrd1	CPY*, sec61-2, Hmg2, pdr5-C1427Y, Huntingtin, unglycosylated PrP,	Integral ER membrane E3	(68, 69, 76, 136-139)
Doa10	Deg1-Ura3, Ubc6, Ste6*, Erg1, α, β, γ subunits of ENaC, Pca1, Zrt1, Sbh2	Integral ER membrane E3	(123, 125, 140-144)
Rsp5	CPY*	Cytosolic E3 required only when substrates are significantly overexpressed and cells are under oxidative stress	(145, 146)
Ubr1	Ste6*, CFTR	Cytoplasmic E3	(127)
Asi1/Asi1/Asi3	Erg11	Integral nuclear membrane-localized E3 complex	(147, 148)

Mammalian			
HRD1[3]	HMGR, TCR-α, CD3-δ, MHCI, NHK, APP, α1AT, gp78, NS1 LC, CD95/Fas, p53, CD147	Homolog of yeast Hrd1	(94, 96, 107, 121, 129, 149-155)
TEB4	Type 2 Iodothyronine Deiodinase (D2), squalene monooxygenase (SM), HMGR	Homolog of yeast Doa10	(142, 156-158)
gp78	CD3-δ, apoB100, CFTR, HMGR, α1AT, Kai1, Cytochrome P450 3A	Homolog of yeast Hrd1	(106, 159-165)
CHIP	CFTR, NCC, Pael-R, Cytochrome P450 3A	Cytoplasmic E3	(128, 165-169)
RMA1/RNF5	CFTR	Integral ER membrane resident E3	(130, 161, 170)
TRC8	MHCI, SREBP-1, SREBP-2, Heme oxygenase-1, XBP1u, α1 integrin, α2 integrin, α4 integrin, β1 integrin, thrombomodulin, PTPRJ and IL12 receptor β1	Integral ER membrane resident E3	(171-175)
SCF^{Fbx2}	Pre-integrin β1, TCR-α, CFTR	Cytoplasmic/ ER membrane-associated E3	(176, 177)
SCF^{Fbx6}	TCR-α	Cytoplasmic/ ER membrane-associated E3	(178)
$SCF^{\beta\text{-}TrCP}$	CD4, Tetherin	Cytoplasmic E3 utilized by HIV protein, Vpu	(179, 180)
RNF4	CFTR	Cytoplasmic/Nuclear E3 that recognizes poly-SUMOylated substrates	(181)
RNF103	Auto-ubiquitination	Integral ER membrane resident E3	(182)
RNF170	Inositol 1,4,5-trisphosphate (IP_3)	Integral ER membrane resident E3	(183)
RNF185	CFTR	Integral ER membrane resident	(184)

		E3 that is homologous to RMA1/RNF5	
PARKIN	Pael-R, mutant glucocerebrosidase	Cytoplasmic E3	(169, 185)
TRIM13	CD3-δ, Cav1.2	Integral ER membrane resident E3 that also plays a role in autophagy	(186, 187)
SMURF1	WFS1	Cytoplasmic/Nuclear-localized E3	(188)
TMEM129	MHCI	Integral ER membrane resident E3 utilized by HCMV	(189)
NIXIN/ZNRF4	calnexin	Integral ER membrane resident E3	(190)
NRDP1	ErbB3	Cytoplasmic E3	(191)
SYVN1	CFTR	ER/Cytoplasmic E3	(177)
Ubiquitination Modifiers			
Yeast			
Cue1	CPY*, Hmg2, KWW	Required for Ubc7 activation and Integral ER membrane protein	(77, 84, 85, 192)
Hrd3	Hmg2, CPY*, sec61-2, Pdr5*, unglycosylated PrP	Integral membrane component of Hrd1 complex	(52, 68, 70, 79, 138)
Ssa1	Ste6*, Pma1-D378S, CFTR	Cytosolic Hsp70	(19, 141, 193, 194)
Ydj1	Ste6*, Pma1-D378S	Cytosolic Hsp40 that can be farnesylated	(19, 141, 193)
Hlj1	Ste6*, CFTR	Homologue of Ydj1	(19, 195)
Otu1[4,5]	CPY*, Spt23	Cytosolic deubiquitinating enzyme	(92, 196, 197)
Ufd3[4]	Spt23	Cytosolic ubiquitin chain length regulator	(197)
Ufd2[4]	Ole1, HMG2, [DEG1]Sec62	Cytosolic ubiquitin extension enzyme (E4)	(17, 20)
Mammalian			

HDJ2	CFTR, Pael-R	Homolog of yeast Ydj1	(128, 169, 198)
SEL1L	NHK, TTR^{D18G}, $RI_{332,}$ tyrosinase	Homolog of yeast Hrd3	(96, 103, 199)
FAM8A1	NHK, TTR^{D18G}	Hrd1 binding partner believed to regulate Hrd1 function	(103)
HSC70	CFTR, Pael-R, ApoB100, ENaC, NCC	Homolog of yeast Ssa1	(128, 169, 200-203)
DNAJB12	CFTR	Integral ER membrane resident Hsp40	(170, 204)
USP13[4]	Ubl4A	Deubiquitinating enzyme	(205, 206)
USP19	CFTR, TCRα	Integral ER membrane resident deubiquitinating enzyme	(207)
USP25	CD3-δ, APP, CFTR	Integral ER membrane resident deubiquitinating enzyme	(208)
AUP1	MHCI, NHK, HMG CoA	Integral ER-membrane cue domain containing protein that recruits Ube2g2 to ER membrane and lipid droplets	(101, 209)
YOD1[4,5,6]	RI_{332}, NHK, TCRα	Homolog of yeast Otu1	(210)
ATAXIN-3[4]	TCRα, CD3-δ, BACE457Δ	Deubiquitinating enzyme	(205, 211, 212)
UBE4B[4]		Homolog of yeast Ufd2	(17, 20)
NEDD8	CFTR	Cytoplasmic Ubiquitin-like protein	(177)

[1] Substrates for the E1 are the E2s
[2] Some ERAD E3s facilitate the degradation of cytosolic proteins (213)
[3] Substrates for the E2s are the E3s
[4] These components can recognize and bind to the Cdc48/p97 complex in the cytosol
[5] May trim ubiquitin chains prior to entry into p97/Cdc48
[6] May also act on ERAD machinery (214)

The other ERAD-associated E3 complex in yeast centers around the nuclear membrane/ER membrane localized E3, Doa10 (140). While Hrd1 functions in collaboration with a variety of other proteins, Doa10 acts predominantly with three different components in a ubiquitination complex: Ubc6, Ubc7, and Cue1 (78, 123, 140). Recent data suggest that Ubc6 initially mono-ubiquitinates the substrate, whereas Ubc7 creates the polyubiquitin chain by adding subsequent ubiquitin moieties (215). In contrast with Hrd1, which ubiquitinates substrates containing misfolded lesions in the ER lumen and ER membrane, Doa10 substrates contain a cytosolic lesion (ERAD-C) (77). As a result, cytosolic chaperones, such as an Hsp70, Ssa1, and the cytosolic Hsp40s, Ydj1 and Hlj1, are also important for the degradation of Doa10-dependent substrates (19, 141, 193-195). Like Hrd1, Doa10 recruits Ubx2 to the complex, allowing for increased efficiency of substrate retrotranslocation by Cdc48 (21, 22). In the mammalian system, TEB4/MARCH-VI (158, 216) is the Doa10 homolog (142, 156-158). TEB4/MARCH-VI acts in a complex with the E2 ubiquitin-conjugating enzyme, UBE2G1 (158). Similar to the situation observed in yeast, cytosolic chaperones, such as HSC70, DNAJB12, and HDJ2 (128, 170, 198, 201, 204), can help degrade some ERAD substrates and UBXD8 can aid in substrate retrotranslocation.

The mammalian E3, gp78 (159), is another major E3 ligase for ERAD substrates in mammalian cells. gp78 is an ER membrane protein that is similar to HRD1 and utilizes UBE2G2. This interaction is through an embedded G2BR domain (106). While gp78 clearly functions as an E3 during ERAD, there is also evidence that it acts as an E4 in co-operation with other E3s (161). Additional evidence suggests that gp78 participates in substrate retrotranslocation downstream of HRD1 (217). The diversity in gp78 function may reflect substrate specificity and partner specificity, which represent an important area of future study. Regardless, similar to HRD1 and TEB4/MARCH-VI, gp78 also recruits UBXD2 or UBXD8 to help cement p97 at the ER

membrane. Alternatively, gp78 can directly interact with p97 through its VIM (VCP-interacting motif) domain (116, 218).

One of the earliest ERAD-requiring E3s identified in mammalian cells was the cytosolic HSC70-interacting protein, CHIP. While several ERAD substrates were identified that require CHIP activity, the best-studied substrate is CFTR (128). Interestingly, CHIP requires HSC70 as a cofactor for function, but CHIP can also act in collaboration with other E3s, such as PARKIN (128, 167, 169). This may reflect the ability of CHIP to act cooperatively, or it may reflect an E4-type activity. For example, while RMA1 and CHIP both facilitate mutant CFTR degradation, the dependence on each E3 was linked to the subdomain in which the mutation resided (130). RMA1 recognizes mutations early in the protein sequence and in the transmembrane domains of CFTR, whereas CHIP is believed to recognize cytoplasmic domains and the C-terminal second nucleotide-binding domain in CFTR.

Several additional E3 ubiquitin ligases have been identified that act on ERAD substrates in both yeast and mammalian cells (Table 1). Many of these enzymes are required for the degradation of only a few substrates, yet this might again reflect the fact that the universe of identified and characterized ERAD substrates is relatively small. In yeast, the cytosolic E3, Ubr1, is required along with Hrd1 and Doa10 during the degradation of Ste6* and CFTR, and employs the cytosolic E2, Ubc2 (127). However, Ubr1 is better known for its role in degrading unstable N-end rule substrates (219). In addition, Rsp5, a cytosolic/Golgi-resident E3, ubiquitinates overexpressed CPY* and other select substrates when cells are exposed to oxidative stress (145, 146). Finally, in yeast, the nuclear membrane E3 complex, consisting of Asi1, Asi2, and Asi3, plays a role in the destruction of Erg11, a sterol synthesis component that resides in the ER (147, 148).

Roles for specialized E3s in ERAD have also been studied in mammalian cells. Some of these enzymes are important only under select conditions. For instance, SCFβ-^{TrCP} and TMEM129 are utilized by viruses to ubiquitinate ER-localized factors associated with the immune system (179, 180, 189). Other ligases recognize specific protein classes: the cytosolic E3s SCFFbx2 and SCFFbx6 target glycosylated ERAD substrates in the cytosol and modify them prior to proteasomal degradation (176, 178). It is unknown if these E3s recognize retrotranslocated, glycosylated ER-resident proteins that have been missed by the cytoplasmic glycosidase, PNGase, which normally removes ER-catalyzed N-glycans prior to ERAD (220, 221). Other E3s connected to the ERAD pathway include TRC8, RNF170, RNF185, TRIM13, SMURF1, NIXIN/ZNRF4, and NRDP1 (Table 1). One E3, RNF103, is an ER-resident ligase that has yet to be linked to substrate degradation. However, the factor regulates protein ubiquitination levels, interacts with p97 and DERLIN-1, and is auto-ubiquitinated (182). Once again, this may reflect the dearth of characterized, potential ERAD substrates that can arise due to errors in secretory pathway folding.

1.4.2 The importance of ubiquitin chain extension (E4) and DUB enzymes during ERAD

For maximal binding to the 26S proteasome, a substrate needs a polyubiquitin chain of at least four ubiquitin molecules, but increasing the length beyond four molecules more modestly increases proteasome affinity (222, 223). Some recent evidence indicates that the addition of multiple single ubiquitin moieties on a proteasomal substrate is sufficient for proteasome targeting (224-226). As a result, varying the ubiquitin chain length could regulate degradation efficiency and modify the speed at which ubiquitinated substrates are degraded (227). In general, however, the effect of chain length on the rate of substrate degradation has not been satisfactorily investigated. But, in order to control ubiquitin chain length, cells possess a multitude of factors that either increase (E4s) or

decrease (DUBs) the length of the chain. While it is possible the extension of the ubiquitin chain is linked to increased degradation, trimming can rescue ubiquitinated substrates or — in some cases — facilitate degradation. For instance, if a substrate is deubiquitinated after p97/Cdc48 activity, it could aggregate in the cytoplasm or might subsequently be re-ubiquitinated by a cytoplasmic E3. Alternatively, if a substrate is deubiquitinated prior to p97/Cdc48 activity, it could remain in the ER membrane and potentially traffic to the Golgi or be re-ubiquitinated by ER-resident E3s. These different fates may be dictated by the timing of DUB activity. However, deubiquitination prior to p97/Cdc48 activity has also been suggested to allow substrate egress through the p97/Cdc48 hexamer (210). Definitive proof of this model awaits the reconstitution and structural analysis of p97/Cdc48-dependent degradation. Regardless, of the ERAD-associated DUBs, several are associated with p97/Cdc48, whereas others reside in the ER membrane/cytoplasm (Table 1). This difference in localization/interaction partners could suggest alternative steps at which these DUBs act, but, to date, this has not been satisfactorily addressed.

The major DUB involved in ERAD in yeast is Otu1. Otu1 was not implicated in ERAD until it was shown to interact with Cdc48, which occurs through its ubiquitin regulatory X (UBX)-like domain (197). Otu1 binding to the N-terminus of Cdc48 does not interfere with binding of the Cdc48 cofactors, Npl4 and Ufd1, which are vital to recognize ubiquitinated substrates (228-230). These data suggest that different members of the Cdc48 hexameric ring bind Otu1 versus Npl4/Ufd1. While Otu1 exhibits deubiquitination activity both in vivo and in vitro, another ubiquitin chain modifier, Ufd3, does not appear to catalyze substrate deubiquitination (197). However, in ufd3Δ cells, the level of free ubiquitin is significantly decreased (231). The effect on free ubiquitin levels may be linked to the Ufd3-binding site on Cdc48, as Cdc48 cannot bind both Ufd3 and the E4, Ufd2, at the same time (197). Interestingly, this site is different from the Otu1-

binding site, as Cdc48 can associate with both the Otu1 and Ufd3 DUBs simultaneously. One view is that the binding of Otu1 and Ufd3 to the Cdc48 complex primes this enzyme to inhibit ubiquitination, and thus degradation, of ERAD substrates. How this critical step might be further regulated is unknown.

As might be anticipated, there are many more ERAD-associated DUBs in mammalian cells than in yeast. YOD1, the mammalian homolog of Otu1, also interacts with p97 through its UBX domain (210). YOD1 deubiquitinates known ERAD substrates and associates with DERLIN-1 and UBXD8, two components of the HRD1 complex (see above). It was suggested that YOD1 co-operates with the p97 complex to efficiently retrotranslocate ubiquitinated substrates, which may be prevented from being threaded through the central p97 pore (also see above); alternatively, YOD1 may act upstream of retrotranslocation by controlling ubiquitin chain length to optimize p97 recruitment (210, 232).

An additional DUB in the mammalian ERAD pathway is ATAXIN-3. ATAXIN-3 aggregates upon extension of its polyglycine domain, which leads to Machado–Joseph Disease (also known as spinocerebellar ataxia type 3) (233). ATAXIN-3 localizes to both the nucleus and the cytoplasm, where it interacts with substrate recognition factors for the 26S proteasome (234). ATAXIN-3 was subsequently shown to bind p97 through an Arg/Lys-rich region (235, 236). Currently, the role that ATAXIN-3 plays in ERAD is not completely clear. Some evidence suggests that ATAXIN-3 removes the ubiquitin chain on ERAD substrates to increase protein half-life, which allows more time for substrate folding (212). An alternative hypothesis is that ATAXIN-3 acts after retrotranslocation to support the degradation of ERAD substrates (211). One reason for this discrepancy may arise due to differences in methodology, which employed either

overexpression studies in vivo or the use of purified complexes in in vitro reactions. Interestingly, ATAXIN-3 itself is modified by ubiquitination, which appears to increase DUB activity (237).

Other mammalian DUBs associated with the ERAD pathway include USP13, USP19, and USP25 (Table 1). USP13 interacts with p97, UFD1, NPL4, and UBXD8, and upon USP13 deletion, cells are more susceptible to ER stress. Moreover, deletion of the gene encoding USP13 leads to the accumulation of an ERAD substrate, TCRαGFP (205). In another study, USP13 was shown to associate with gp78 and deubiquitinate a component of the ERAD complex, keeping the complex from becoming inactivated (206). This result is in line with other studies implicating E3 and DUB activity in regulating the ERAD machinery in addition to or in contrast with the modification of ERAD substrates (also see below). In turn, USP19 has seven isoforms that arise from alternative splicing. Some of these isoforms contain a C-terminal transmembrane domain, which targets them to the ER membrane. The ER membrane-localized population rescues the degradation of two ERAD substrates, TCRα and ΔF508 CFTR (207). Interestingly, expression of a catalytically inactive USP19 mutant partially rescued TCRα, suggesting a DUB-independent role during ERAD. However, Ye and colleagues have provided evidence that the role of USP19 during ERAD is dependent on its overexpression (238). Of note, wild-type levels of USP19 are mostly cytosolic, lack association with ERAD factors, and fail to alter the degradation of ERAD substrates. Finally, USP25, which interacts with p97 as well as HRD1, decreases ubiquitination of the ERAD substrate CD3δ (208).

As mentioned above, a class of E3-like ligases, known as E4s, catalyzes the extension of ubiquitin chains. For ERAD, the best characterized member of this family is the yeast protein Ufd2. In the absence of Ufd2 activity, the length of ubiquitin chains assembled by the E1–E2–E3 complex onto a series of ERAD substrates is insufficient for protein turnover both *in vitro* and *in*

vivo (17). Owing to its interaction with Cdc48, Ufd2 facilitates the degradation of several substrates (20). As noted in the previous section, Ufd2 competes with Ufd3 for binding to Cdc48, which modulates protein turnover (197). Two mammalian Ufd2 homologs, UBE4A and UBE4B, exist, but little is known regarding their role in ERAD. Nevertheless, it has been shown that UBE4B can recognize K48 linkages and interact with p97 (239, 240).

1.5 VARIATIONS ON A THEME

1.5.1 Alternatives to Lys-48 ubiquitin linkage in ERAD

While the Lys-48 polyubiquitin linkage is predominantly used for proteasomal degradation, polyubiquitin chains appended to other lysine residues are recognized by the 26S proteasome. In yeast, ubiquitin chains containing Lys-6, Lys-11, Lys-23, Lys-29, and Lys-33 linkages all accumulate to varying levels when the proteasome is inhibited, whereas Lys-63 ubiquitin chain levels are unaffected (16). Of the non-Lys-48 polyubiquitin chains, Lys-11-based chains are the most affected upon proteasomal inhibition; in addition, only Lys-11 chains increase when Rad23 and Dsk2 were deleted. Interestingly, the yeast E2, Ubc6, is auto-ubiquitinated with Lys-11 isopeptide moieties (16); Doa10 and Ubc6 are responsible for a subpopulation of these cellular Lys-11 chains (16). Lys-11-linked polyubiquitin chains are also induced upon ER stress (16). When similar experiments were performed in mammalian cells, Lys-11, Lys-29, and Lys-48 linkages rose when the proteasome was inhibited (241). Of these, the majority of the identified ubiquitin chain linkages that accumulated were Lys-11 and Lys-48. It is worth noting, however, that the accumulation of polyubiquitin moieties containing chains other than those attached via

Lys-48 may represent mixed linkages. How these are built and assembled is an area of active research (242).

A mechanism for lysine-independent ubiquitination was first identified with viral E3s. For example, the viral E3 ligase, MIR1, promotes the ubiquitination and degradation of a modified MHCI that has an artificial glycine/alanine cytoplasmic domain containing only a single cysteine (243). Since cysteine is the catalytic residue in E1s, E2s, and some E3s, this residue can clearly become ubiquitinated. Alternatively, another viral E3, mK3, can ubiquitinate lysine-less MHCI by conjugating ubiquitin to serine and threonine residues (244). Yet another viral protein, the HIV protein, VPU, utilizes the SCFβ-TrCP E3 ligase to modify two substrates, tetherin and CD4, by utilizing lysine, serine, and threonine (245, 246). Additional evidence obtained investigating the ubiquitination of tetherin by SCFβ-TrCP suggested that tyrosine residues in the cytoplasmic domain, or the free amino group in the N-terminus, might be targeted (247). Since the exact nature of polyubiquitin chains in ERAD substrates is rarely investigated, it is possible that these phenomena are actually quite common. In fact, TCRα, which contains only five cytoplasmic residues (RLWSS), is modified by HRD1 on the serine side chains (248). HRD1 also modifies serines, threonines, and lysines on the immunoglobulin Ns1 LC, which is a trapped ER luminal ERAD substrate (152). Moreover, treatment of mini-HC (γ VH–CH1) and NHK α1-antitrypsin with sodium hydroxide decreased the amount of ubiquitin appendages, suggesting the presence of serine/threonine ubiquitin conjugates on these ERAD substrates. Finally, purified p97 protein complexes from cells treated with an ER stressor and a proteasome inhibitor harbored increased levels of sodium hydroxide-labile species (152). These data suggest that serine/threonine ubiquitination rises during stress, and that this modification plays an important role to mitigate cellular stress in vivo.

ERAD substrates are not only modified with ubiquitin, but also there is evidence that two other protein modifications affect ERAD substrate stability: attachment of NEDD8 and SUMOylation. NEDD8 is a ubiquitin-like protein linked to cullins, which activate select E3 ligases (249). A role for NEDD8 in ERAD has been suggested for the ERAD substrate ΔF508 CFTR (177). During SUMOylation, SUMO (small ubiquitin-like modifier) is conjugated to lysines through the action of dedicated SUMO E1, E2, and E3 enzymes in a reaction analogous to the ubiquitin-conjugation cascade (250, 251). One difference between the SUMO and ubiquitin pathways is that there are three SUMO isoforms in mammals, and only SUMO-2 and SUMO-3 form chains.

While SUMOylation is required to regulate numerous cellular events, SUMO tags can also recruit an E3, RNF4, which leads to mixed SUMO/ubiquitin chains (252-254). One prominent ERAD substrate modified by SUMOylation is CFTR (181). While many E3s facilitate degradation of the disease-associated ΔF508 mutant form of CFTR (Table 1), SUMOylation is also evident. Specifically, ΔF508 is bound by the small heat-shock protein, HSP27, which recruits the E2 SUMO-conjugating enzyme, UBC9. The HSP27/UBC9 complex recognizes a non-native fold in ΔF508 CFTR, which triggers SUMOylation (255). In turn, the poly-SUMO tag recruits RNF4, which poly-ubiquitinates CFTR (181). There is still much more to be explored about this modification — and the coordinated interaction and assembly of ubiquitin and SUMO chains — and it is likely that a growing number of ERAD substrates will be discovered that are similarly SUMOylated.

1.5.2 Post-translational modifications on ERAD complexes

Although this review has focused on protein ubiquitination, Nα-acetylation has also been implicated in ERAD, at least in yeast. The importance of Nα-acetylation in ERAD came from a screen investigating the nature of the Doa10 complex (123). Based on a genetic screen, nat3Δ mutants were found to stabilize a degron, Deg1, which derives from a Doa10-dependent substrate known as Mat2α. Nat3 resides in the NatB complex, which is partially responsible for Nα-acetylation in yeast (256). Importantly, the degradation of this Nα-acetylated population of Deg1 is also Doa10-dependent (257). However, the NatB requirement for Deg1 degradation was absent when wild-type Mat2α was examined (258). Instead, Der1 requires Nα-acetylation and this activity is required for ERAD. Without Nα-acetylation, Der1 itself is ubiquitinated by Hrd1 and subsequently degraded.

As suggested in the preceding section, ERAD activity can also be regulated in response to cellular stress. For example, the ratio of components in the yeast Hrd1 complex is modified when cells are stressed chemically to induce the UPR or by constitutive UPR induction (72). Inactivation of the Cdc48 complex similarly leads to altered ratios of Hrd1 complex components, which may reflect regulated complex assembly and perhaps increased ERAD efficiency (72). In support of this hypothesis, auto-ubiquitination of Hrd1 in vitro is sufficient to recruit the Cdc48 complex, which can then engage and retrotranslocate a substrate into the cytosol (92). Surprisingly, Hrd1 is also retrotranslocated from the ER in a reconstituted system, suggesting that a Hrd1 regulatory factor or a specific modification offsets this destructive event. In mammalian cells, a factor that may regulate the Hrd1 complex is the E2, UBE2J1. UBE2J1 activity decreases the levels of Hrd1 complex members SEL1L, EDEM, and OS-9 (199). Without UBE2J1 activity, ERAD substrates were degraded more rapidly than in wild-type cells, which is believed to be due to greater amounts

and activities of these ERAD-requiring components. Needless to say, numerous other systems probably exist to regulate the activity of the ERAD machinery, which must respond to changes in cellular stress as well as cellular differentiation and growth in vivo.

While the examples cited above suggest mechanisms to augment ERAD, negative ERAD regulators also exist. ERAD inhibition might allow more time for proteins to fold, perhaps after a stress response has been rectified. One negative regulator of ERAD in mammalian cells is the p97 cofactor SAKS1 (259, 260). SAKS1 interacts with p97 through its UBX domain and also requires a functional ubiquitin-associating (UBA) domain to bind polyubiquitin chains (259). When SAKS1 binds to both a polyubiquitinated substrate and p97, the degradation of an ERAD substrate and a misfolded cytosolic quality control (cytoQC) substrate was attenuated. Another negative regulator of ERAD in mammalian cells is the small p97/VCP-interacting protein (SVIP). SVIP localizes to the ER membrane, where it binds p97 and DERLIN-1 (261). By associating with p97 and DERLIN-1, SVIP inhibits the ubiquitination and degradation of select gp78-dependent ERAD substrates. These results support the hypothesis that the p97/Cdc48 complex can be regulated by competition for cofactor binding.

1.5.3 Roles for unexpected factors in ERAD

As a result of the long-term search for factors involved in ERAD through genetic and proteomic approaches, it has become increasingly clear that cytosolic factors play important roles in the degradation of aberrant proteins in the ER. One such protein is the 26S proteasome-interacting E3/E4, Hul5 (30, 262). Hul5 was first shown to be important for the degradation of cytoplasmic substrates (263). However, by utilizing fusions of two known ERAD substrates, CPY* and Sec61-2, to a membrane-tethered product of the LEU2 gene (cytosolic 3-isopropylmalate

dehydrogenase), Hul5 was found to facilitate the retrotranslocation of an ER membrane resident protein (264). Consistent with its activity as an E4, Hul5 was dispensable for the degradation of the CPY* or Sec61-2 portions of the fusion proteins, but instead elongated the ubiquitin chain on the transmembrane anchored LEU2 moieties, which increased interaction with the Cdc48 complex. In the absence of Cdc48 complex interaction, the ER membrane-anchored LEU2 product was stabilized. Furthermore, as discussed earlier in the present study, two E3 ligases that reside in the Golgi and inner nuclear membrane, respectively, Rsp5 and the Asi complex, aid in the degradation of some substrates. Rsp5 degrades CPY* in a pathway known as Hrd1- independent proteolysis, whereas the Asi complex modifies the ER-resident enzyme, Erg11 (145-148). It is unclear if Erg11 degradation represents a unique aspect of the ERAD pathway or if the Asi complex prevents Erg11 activity in the nuclear membrane. Overall, cross-talk between components of different cellular quality control pathways is important for the degradation of proteins, regardless of substrate localization.

Along with alternative E3s, molecular chaperones localized in the ER and the cytosol are implicated in ERAD. However, it is unclear whether these chaperones only serve as recognition factors for E3 binding to substrates or if they also serve to bridge the E3 to the substrate. In addition, evidence indicates that Hrd1 binds soluble ERAD substrates through its transmembrane domains during ubiquitination (92), and the integral membrane ERAD substrate, Hmg2, is recognized by Hrd1 transmembrane domains (265). Some cytosolic chaperones help ubiquitinate transmembrane ERAD substrates. For example, the yeast Hsp70 (Ssa1) and Hsp40 chaperones (Ydj1 and Hlj1) affect the ubiquitination and degradation of several integral membrane substrates that display prominent cytoplasmic domains: Ste6* (19, 125), Pma1–D378S (141), and CFTR (194, 195). Similar requirements for cytosolic chaperones during ubiquitination were seen in

mammalian cells as well (128, 198, 200, 201, 203). Owing to a lack of a requirement for these factors in the degradation of ER luminal substrates, it is believed that they do not function in the retrotranslocation complex, but instead catalyze ubiquitination and/or proteasome targeting.

1.6 THESIS SUMMARY

In this thesis, I aim to address the substrate characteristics that lead to recognition by the ERAD machinery. I also investigate a novel role for a molecular chaperone, the heat shock protein of 104 kDa (Hsp104), in the degradation of a relatively unstable ERAD substrate. To this end, I was able to demonstrate that an ERAD substrate's stability is positively correlated to its insolubility. I was also able to demonstrate that Hsp104 is required for the degradation of an insoluble and unstable ERAD substrate, Q394X. Specifically, I demonstrate that Hsp104 acts downstream of substrate ubiquitination to disaggregate Q394X at the ER membrane prior to retrotranslocation by the Cdc48 complex. While Hsp104 is an AAA+ ATPase, similar to Cdc48, it does not appear to compensate for loss of Cdc48 activity, as over-expressing Hsp104 in a *cdc48* mutant strain did not rescue Q394X degradation. Finally, I establish that the yeast Hsp110 homologue, Sse1, is required for the degradation of Q394X and does not function in the substrate ubiquitination or retrotranslocation. The specific function of Sse1 in the degradation of Q394X will need to be addressed in the future.

2.0 SUBSTRATE INSOLUBILITY DICTATES HSP104-DEPENDENT ENDOPLASMIC RETICULUM ASSOCIATED DEGRADATION

2.1 INTRODUCTION

In eukaryotic cells, approximately one-third of all proteins must enter the secretory pathway at the endoplasmic reticulum (ER). After passing quality control checkpoints, properly folded proteins proceed through the secretory pathway and are delivered to their ultimate location. However, environmental stressors, genetic mutations, or a stochastic decrease in the efficiency or rate of folding leads to the destruction of these nascent proteins via the ER-associated degradation (ERAD) pathway (266-268). To date, numerous factors have been identified that play key roles in the recognition, ubiquitination, retrotranslocation, and proteasome-dependent degradation of ERAD substrates, and a growing number of ERAD substrates are linked to human diseases (269).

In contrast to the many ERAD-requiring factors and disease-associated ERAD substrates, much less is known about the structural characteristics that result in the recognition of misfolded substrates. Evidence suggests that quality control factors recognize the improper exposure of an amphipathic helix (270-272), or other features, such as hydrophobicity (92, 273). There is also evidence that defects in essential post-translational modifications, such as glycosylation, triggers the degradation of misfolded substrates (274, 275). However, due to the limited number and diverse nature of the "degrons" used in these studies, it is not yet possible to delineate the rules underlying substrate selection.

Once an ER-resident protein has been recognized as terminally misfolded, it must be ubiquitinated and retrotranslocated from the ER for degradation. In yeast, ERAD substrates are

primarily ubiquitinated by one of the two ER resident E3 ligases, Hrd1 (69, 76) or Doa10 (123, 140), but more recently the contribution of a cytoplasmic E3, Ubr1, was uncovered (127). Distinct E3 dependencies appear to be due to the localization of the misfolded lesion. If the lesion occurs in the ER membrane (ERAD-M) or in the ER lumen (ERAD-L), the substrate requires the Hrd1 complex (49, 77, 78, 125). However, if the lesion resides in the cytoplasmic portion of the protein (ERAD-C), the Doa10 complex is required. Once substrates are ubiquitinated, the Cdc48/p97 complex is recruited to the substrate, which is then retrotranslocated from the ER and into the cytoplasm for degradation by the 26S proteasome (57, 276, 277). In yeast and most likely in higher eukaryotes, soluble substrates within the ER must be retained in an aggregation-free state prior to retrotranslocation (278), and in turn specific cytosolic chaperones, most notably Hsp70, Ssa1, and Hsp40s, Ydj1 and Hlj1, facilitate the degradation of some ERAD-C substrates (19, 141). Given the diversity of ERAD substrate structures—and the numerous aberrant conformations which they might display—an understanding of the rules that govern which chaperones mediate substrate selection is in its infancy. More generally, it has been assumed, but never directly shown, that the ERAD machinery preferentially selects aggregation-prone substrates.

The handling of integral membrane proteins after retrotranslocation is particularly problematic, especially since these aggregation-prone substrates can be found in the cytoplasm in yeast and mammalian cells (19, 74, 279-281). However, a cytoplasmic protein complex was identified in mammalian cells that acts as a “holdase” for a subset of retrotranslocated membrane substrates. The central component of this complex is Bag6 (112, 282). Bag6 complexes with three other factors, Ubl4A, TRC35, and SGTA, which also interact with an ER-resident E3, gp78 (113, 283). In the absence of SGTA, the ERAD substrate TCRα is stable and the unfolded protein response (UPR) is induced, suggesting that this complex plays a general role in ER homeostasis.

However, the Bag6 dependence has only been investigated for select substrates, most of which are single pass transmembrane proteins. In addition, yeast lack a Bag6 homolog, indicating that other "holdases" for retrotranslocation exist in this organism and that alternate pathways to retain aggregation-prone proteins in solution might be at-play in all eukaryotes.

In this chapter, I have demonstrated that the targeting of a substrate for ERAD is positively correlated to its detergent solubility by utilizing a series of truncations within the same protein. One of the least soluble truncations, which contains the same degron known to cause the degradation of another transmembrane ERAD substrate (284) as well as a cytoplasmic quality control substrate (285), was used for the first time to identify the cytoplasmic chaperone, Hsp104, as a factor required for ERAD. Specifically, Hsp104 was determined to be important for the disaggregation of this insoluble ERAD substrate in the ER membrane, which allows for efficient retrotranslocation by Cdc48. The identification of this previously undiscovered role for Hsp104 in ERAD suggests the potential to identify other novel factors that are important for the ERAD of misfolded proteins, especially in mammalian cells.

2.2 MATERIALS AND METHODS

2.2.1 Yeast strains, plasmids, and plasmid construction

The *S. cerevisiae* strains used in this study are listed in Table 1. Solid and liquid drop-out media were prepared as described previously (286). Yeast strains and cultures utilized for the Ste6 data were grown at 30°C, except for temperature-sensitive strains, which were grown at room temperature (25°C) or then shifted to 37°C, as indicated. Yeast utilized to study the Chimera A

truncations were grown at room temperature (23.5°C). Yeast transformations were performed by the lithium acetate method (287).

A list of the primers and plasmids to create and express the constructs used in this study is presented in Table 2. Plasmids expressing Ste6 truncation mutants were derived from pSM694 (2μ *LEU2 STE6::HA*) and contain the triply iterated hemagglutinin (HA) epitope tag between amino acids 68 and 69 (the ecto position) in Ste6 (288). All of the *STE6* truncation mutations were constructed by homologous recombination in yeast. Briefly, a PCR product containing the desired truncation mutation was generated and co-transformed with a linearized gapped version of the wild-type *STE6* plasmid (pSM694). Plasmids were isolated and sequenced to verify the presence of the mutation.

In order to create the Chimera A truncation series, pCG19 (Guerriero et al, manuscript submitted for peer review), which contains two transmembrane regions annealed to the full length NBD2 of Ste6, was used as the backbone. Primer oMP01 was used in combination with oMP02 through oMP09, resulting in the production of pMP01 through pMP08. Because pCG19 expresses Chimera A with an internal triple HA tag, the resulting pMP01 through pMP08 plasmids are also engineered to express triply HA-tagged proteins. Sequences were verified using DNA sequencing services provided by Genewiz (South Plainfield, NJ).

In order to create pMP13 and pMP14, primers oMP17 and oMP18 were used with oMP19 to create two forms of the *HSP104* over-expression plasmid. pMP13 expresses *HSP104* from the endogenous *HSP104* promoter in the pRS425 vector (289). The endogenous promoter was inserted by including 350 base pairs upstream of the start site for *HSP104* in the insert. pMP14 expresses *HSP104* from the GPD promoter for constitutive expression in the pRS425 vector.

2.2.2 Cycloheximide chase and pulse chase assays

To determine the effects of C-terminal truncations on Ste6 turnover rates, cycloheximide chase analysis was performed as described previously (193) with modifications by Dr. Susan Michaelis and Dr. Meredith Metzger. Briefly, cells were grown to the logarithmic phase in synthetic media and 4 OD_{600} units were harvested, washed, and resuspended to 2 OD_{600} units per ml in synthetic media and incubated at 30°C for 5 min. Cycloheximide was then added to a final concentration of 100 µg/mL to inhibit further protein synthesis. For the 0 min time point, 500 µL of cells were immediately harvested by addition to an equal volume of 2x azide stop mix (20 mM NaN3, 0.5 mg/ml BSA) on ice. Cells were incubated during the chase at 30°C. At each time point after the addition of cycloheximide, 500 µL of cells were harvested as above. The cells were then pelleted, the supernatant was removed, and pellets were frozen at -80°C until preparation of cell extracts. After thawing, the cells were lysed by the addition of a lysis buffer (400mM NaOH, 7% 2-Mercaptoethanol, 20mM Tris pH8, 20mM EDTA, 1mM PMSF, 2mM leupeptin, and 0.7mM pepstatin A) . Proteins were precipitated in 5% trichloroacetic acid (TCA) and protein pellets were resuspended in TCA sample buffer (3.5% SDS, 0.5M DTT, 80mM Tris, 8mM EDTA, 15% glycerol, 0.1mg/ml bromophenol blue). Proteins were analyzed by 8% SDS-PAGE and immunoblotting. HA epitope-tagged proteins were detected using the 12CA5 mouse anti-HA monoclonal antibody (Roche Applied Science, Branford, CT) diluted 1:10,000. Blots were visualized using a Versadoc quantitative digital imaging system. Exposures were adjusted to approximate equal levels of signal at the 0 min time point and blots were quantified using Quantity One software (Bio-Rad Laboratories, Hercules, CA). Half-lives were calculated from exponential curve fits using Excel (Microsoft).

To determine the effects of C-terminal truncations on the rates of turnover of Chimera A and the membrane tethered truncated mutant proteins, cycloheximide chases were performed similarly to previously described methods (290). Briefly, cells were grown to logarithmic phase in SC-ura media until cultures grew to an OD_{600} of 1.0-1.5. The cultures were then incubated at 25°C in a water bath for 15 min, with shaking at 160 RPMs. Cycloheximide was added to a final concentration of 200 µg/mL to each culture, and 1.0-1.5 OD_{600} of cells were harvested at each time point and added to sodium azide (final concentration of 17 mM per sample) on ice. The cells were pelleted as above and flash frozen in liquid nitrogen. After all time points were collected, the samples were thawed on ice and lysed as above. Protein pellets were resuspended in trichloroacetic acid precipitation (TCAP) sample buffer (80 mM Tris, pH 8, 8 mM EDTA, 3.5% SDS, 15% glycerol, 0.08% Tris base, 0.01% bromphenol blue, 5% fresh β-mercaptoethanol) with a mechanical pestle for 20 sec and the samples were incubated at 37°C for 30 min. Next, the resuspsended pellets were centrifuged at 18,000 x g for 1 min and a portion of each sample was loaded onto denaturing 10% SDS-polyacrylamide gels. Total proteins were then transferred to nitrocellulose using the semi-dry Bio-Rad Trans Blot Turbo for immunoblot analysis.

To perform immunoblots, the nitrocellulose blots were incubated with a solution containing a horseradish peroxidase (HRP)- conjugated primary antibody against the HA-tag (Roche Anti-HA-Peroxidase High Affinity (3F10), Rat, 1:5000), and proteins were visualized using the SuperSignal Chemiluminescence (Thermo Scientific, Waltham, MA) and subsequently imaged on a Bio-Rad Universal Hood II. To control for potential variability in loading, the blots were stripped with 0.1 M glycine, pH 2.2, and then incubated with a rabbit primary antibody against the cytoplasmic protein, glucose-6-phosphate-dehydrogenase (G6PDH) (A9521, Sigma-Aldrich) (1:5000). Donkey anti-rabbit secondary antibody conjugated to HRP (1:5000, Cell

Signaling Technology, Danvers, MA) was then used to visualize G6PDH levels. The resulting signals were quantified using the ImageJ program.

To determine the dependence of the designated ERAD substrates on the 26S proteasome for degradation, *BY4742 pdr5Δ* (Table 1) cultures expressing pCG19, pCG12, and pMP01 were grown as described above. The 26S proteasome inhibitor, MG132, was added to half of each culture to a final concentration of 100 µM. To the other half of each culture an equal volume of DMSO was added. Cultures were then incubated for 30 min at 25°C. Next, cycloheximide was added to a final concentration of 200 µg/ml and the chase was performed as described above. To analyze the contribution of specific factors to the degradation of Q394X, the designated strains were temperature shifted to 37°C for 30 min prior to the addition of cycloheximide and remained at 37°C during the chase. The samples were processed essentially as described above.

Pulse chase analyses were performed similarly to previously published methods (291). Briefly, cultures were grown in SC –ura to an OD_{600} of 1.0 at 22.5°C. The cells were then concentrated to 3 OD/ml and were labeled with Express ^{35}S (PerkinElmer Life Sciences, Bridgeville, PA) for 15 min at 26°C. The cells were then harvested at 4,500 x g for 3 min, washed in SC-ura, and finally resuspended in SC-ura containing methionine, cysteine, and cycloheximinde to final concentrations of 13 mM, 40 mM, and 200 µg/ml, respectively. The cells were collected at 0, 15, 30, and 60 min after the addition of cycloheximide and resuspended in 10 mM sodium azide on ice. A total of 1.2 OD_{600} of cells was collected at each time point. The cells were harvested as above and washed in Buffer 88 (20 mM HEPES, pH 6.8, 150 mM KOAc, 250 mM sorbitol, and 5 mM MgOAc) and resuspended in Extract Buffer plus protease inhibitors (50 mM Tris-HCl pH 7.4, 1 mM EDTA, 1% SDS, 3mM PMSF, 6 mM leupeptin, and 2.1 mM pepstatin A). Glass beads were added to half the volume and the mixture was agitated on a Vortex mixer 4 times

for 45 sec with one min on ice between each cycle. Samples were then heated at 37°C for 10 min and centrifuged briefly before 350 µl of immunoprecipitation (IP) wash buffer (50 mM Tris-HCl pH 7.4, 150 mM NaCl, 5 mM EDTA, 1% Triton X-100, and 0.2% SDS) was added to the samples. Next, the mixture were precleared for 3 h at 4°C with 35 µl of a 50/50 slurry of protein A-sepharose beads in Protein-A bead resuspension solution (50 mM Tris–HCl pH 7.4, 150 mM NaCl, 5 mM EDTA, 1 mM azide). Samples were then centrifuged briefly, after which the pre-cleared supernatants were placed in new 1.5mL Epindorf tubes and incubated overnight at 4°C with an anti-HA antibody (Roche, mouse) and 35 µl of the 50/50 slurry of protein A-sepharose beads. The beads were collected by centrifugation and then washed twice each in IP wash buffer and urea IP wash buffer, IP wash buffer supplemented with 2M urea, and then once with TAE (50 mM Tris-HCl pH 7.4, 150 mM NaCl, and 5 mM EDTA). SDS sample buffer (65 mM Tris-HCl pH 6.8, 5 mg/mL bromophenol blue, 2% SDS, 1% β-mercaptoethanol, and 10% glycerol) was added to the precipitated protein, which was resolved by SDS-PAGE as described above. Gels were dried and exposed to a phosphorfilm for 1-2 days, which was then scanned using a GE Typhoon FLA 7000 (Boston, MA). Signals were quantified using ImageJ.

2.2.3 Indirect Immunofluorescence

Samples were prepared similarly to a previously published protocol (292). Briefly, cultures were grown in SC-ura media until reaching an OD_{600} of 0.5-1.0, and then incubated for 10 min at 22.5°C in SC-ura containing 4% formaldehyde. The cells were resuspended in KM (40 mM KPO_4 and 0.5 mM $MgCl_2$) plus 4% formaldehyde and incubated for 1 h at 30°C. After collecting the cells by centrifugation, they were washed in KM and resuspended in KMS (40 mM KPO_4, 0.5 mM $MgCl_2$, and 1.2 M sorbitol). The cell walls were digested with zymolyase 20T (0.5 mg/ml, US

Biological, Salem, MA) at 37°C for 20, 25, or 30 min, and the yeast were centrifuged, resuspended in KMS, and added to poly-lysine treated slides (ThermoFisher). The adhered cells were washed in ice cold methanol and acetone and then blocked using PBS plus 0.5% BSA, 0.5% ovalbumin, 0.66% fish-skin gelatin, and 0.1% Triton X-100. Next, the permeabilized, fixed cells were incubated with primary antibodies against the HA tag in the substrates (1:500, Roche) and Kar2 (1:250) (293). The samples were washed with blocking solution and incubated with DAPI to visualize DNA, along with secondary antibodies Alexa 568 (1:500, goat anti-rabbit, Invitrogen, Carlsbad, CA) and Alexa 488 (1:500, goat anti-mouse, Invitrogen, Carlsbad, CA). Samples were mounted using Prolong Gold Antifade Reagent (Molecular Probes, Eugene, OR) and imaged with an Olympus FV1000 (Shinjuku, Tokoyo), x100 UPlanSApo oil immersion objective, numerical aperture 1.40.

2.2.4 Determination of substrate solubility

For detergent solubility assays, 4000-6000 ODs of yeast grown in selective media and expressing the designated truncations were harvested. To determine the solubilities of the Chimera A truncation series in *BY4742* yeast (Table 1), cultures were incubated at 25°C for 1 h and the cells were harvested by centrifugation. Once harvested, yeast ER-enriched microsomes were purified using a modified version of a previously described large-scale technique (294). Here, the cultures were resuspended in 100 mM Tris-HCl, pH 9.4, plus 10 mM DTT, and the cells were collected and resuspended in lyticase buffer (10 mM Tris-HCl, pH 7.4, 1.5% peptone, 0.75% yeast extract, 0.7 M sorbitol, and 0.5% glucose). Roughly 10-20 units of lyticase was added to each culture and the solution was incubated at 26°C for 1 h. The digested cells were then over-layed on an equal volume of Cushion 1 (20 mM HEPES, pH 7.4, 0.8 M sucrose, and 1.5% Ficoll 400), and the

samples were centrifuged in a Sorvall HB-6 rotor for 10 min at 5800 x g at 4°C. Pellets were resuspended in ice-cold lysis buffer (20 mM HEPES, pH 7.4, 50 mM KOAc, 2 mM EDTA, 0.1 M sorbitol, 1 mM of freshly added DTT, 1 mM PMSF, 2 mM leupeptin, and 0.7 mM pepstatin A), and lysed using a motor driven Potter-Elvehejm homogenizer (Greiner Scientific Corp, Monroe, NC). The samples were then over-layed onto an equal volume of Cushion 2 (20 mM HEPES, pH 7.4, 50 mM KOAC, 1 M sucrose, and 1 mM of freshly added DTT) and centrifuged in the HB-6 rotor for 10 min at 6900 x g at 4°C. The ER-enriched fraction was removed and centrifuged in a Sorvall SS-34 rotor for 10 min at 20,200 x g at 4°C. The pellet was then washed in Buffer 88 and re-centrifuged. The final pellet was resuspended in Buffer 88 to a final concentration of 10 mg/ml as determined spectrophotometrically (A_{280}) in a solution of 1% SDS.

Solubilization assays were performed by adding 30 µl of Buffer 88, the indicated concentration of n-Dodecyl β-D-maltoside, and ER-enriched microsomes to a final concentration of 0.5 mg/ml of protein, so the final volume was 31.5 µl. When designated, these samples also contained 6 M urea. The samples were incubated at room temperature (~22°C) for 30 min and then centrifuged for 10 min at 18,000 x g at 4°C. The supernatant was removed and dispensed into an Eppendorf tube containing 5x SDS sample buffer. In turn, the pellet was resuspended to an equal final volume of 1x sample buffer by pipetting. The samples were then incubated at 37°C for 30 min followed by a brief centrifugation and subjected to SDS-PAGE and immunoblotting with anti-HA as described above. Blots were also incubated in a rabbit polyclonal antisera raised against the ER integral membrane protein Sec61 at a 1:1000 dilution (295). This served as a control for microsome solubilization and protein extraction. The data were analyzed using ImageJ.

2.2.5 Floatation assays

To investigate the state of Q394X in the *HSP104* and *hsp104Δ* strains after heat shock, strains were transformed with pCG12 and pKN31 and grown in selective media. A modified version of a previously published floatation method was utilized (296). Briefly, roughly 30 ODs of cells were temperature shifted to 37°C for 1.5 hrs, 1 hr of which was in the presence of 100 µM copper sulfate, and then collected for 6 min at 4500 rpms in a Thermo Scientific Sorvall ST8 centrifuge. Pellets were resuspended in 200 µL of a lysis buffer (20 mM HEPES, pH 7.4, 50 mM KOAc, 2 mM EDTA, 0.1 M sorbitol, 1 mM of freshly added DTT, 20 µM MG132, 10 mM NEM, and 1 x Roche Complete EDTA-Free PI cocktail). Cultures were bead beat 8 times for 30 sec each with 30 sec on ice in between cycles. Samples were pulled off the beads and placed in a fresh 1.5 mL Epindorff tube. Beads were washed with 200 µL of Buffer 88 and collected into the tubes containing the samples. Samples were centrifuged 5 min at 300 *x g* and 4°C. 170 µL of the supernatant was mixed with 630 µL of a 2.3 M sucrose solution in Floatation Buffer (50 mM HEPES pH 7.4, 150 mM NaCl, 5 mM EDTA, freshly added 1 mM DTT, 1mM PMSF, and 1 x Roche Complete EDTA-Free PI cocktail). Gradients were layered from bottom to top with 600 µL of 2.3 M sucrose in Floatation Buffer, 800 µL sample (~1.8M sucrose), 1.2 mL of 1.5 M sucrose in Floatation Buffer, and 1 mL of 0.25 M Sucrose in Floatation Buffer. Gradients were centrifuged at 100,000 *x g* in a SW55 TI for 16 hrs at 4°C. 300 µL fractions were taken from the top of the fraction and put in fresh 1.5 mL Epindorff tubes. 160 µL of fractions were added to an equal volume of Denaturing Buffer (2x TBS pH 7.4, 2% SDS, 8M urea, 20 mM NEM, and 2x Roche Complete EDTA-Free PI cocktail) and heated for 30 min at 42°C. Samples were centrifuged for 5 min at 15,000 *x g*. 250 µL of samples were diluted into 1125 µL of Dilution Buffer (1 x TBS pH 7.4, 2% Triton, 10 mM EDTA, 0.5% deoxycholate, 10 mM NEM, and 1x Roche Complete EDTA-Free PI cocktail). 40

µL of HA-conjugated beads were added to the samples and incubated overnight at 4°C on a rotator. TCA was added to the remaining fractions to a final volume of 20% TCA and incubated on ice for 30 min. Samples were centrifuged for 20 min at 4°C and 18,000 *x g*. Pellets were washed with ice old Acetone and centrifuged again. Supernatants were aspirated and pellets allowed to dry briefly. Pellets were resuspended in 1 x SDS sample buffer by mechanical disruption. IPs were washed 3 x in IP wash buffer, followed by resuspension and brief agitation of the beads in 40 µL of TCAP. IPs and TCA samples were incubated at 37°C for 30 min and centrifuged for 1 min. IP samples were resolved on 7.5% polyacrylamide gels while TCA samples were resolved on 10% gels. Gels were transferred to nitrocellulose as previously described. TCA samples were blocked in TBST + 5% milk at room temperature for 30 min, then incubated with anti-HA antiserum. IP blots were boiled in water for 1 hr, blocked in TBST + 5% milk for 30 min at room temperature, then incubated with 1° anti-ubiquitin serum (Sant Cruz, P4D1, Mouse 1:1000) for 1.5 hrs at room temperature. IP blots were washed 3 x 5 min, and then incubated for 1.5 hrs at room temperature with 2° anti-mouse HRP-conjugated antiserum (1:5000, Cell Signaling). Both blots were washed 3 x 5 min in TBST and processed for visualization and quantification as described above.

2.2.6 in vivo Ubiquitination Assays

To investigate the role of select factors on the ubiquitination of Q394X, designated strains were transformed with pCG12 and pKN31 and grown in selective media. Briefly, 15 ODs of cells were temperature-shifted to 37°C for 1.5 hrs, of which 1 h was in the presence of 100 µM copper sulfate, and collected as described above. Cells were resuspended in 1 mL of RIPA Buffer (10 mM Tris-Cl pH 8.0, 140 mM NaCl, 1 mM EDTA, 1 % Triton-X100, 0.1% Sodium Deoxycholate, 0.1% SDS, 1mM PMSF, 2mM leupeptin, and 0.7mM pepstatin A) and lysed by bead beating 4 times for

45 sec each with 1 min on ice between each cycle. Supernatants were removed and placed in fresh 1.5 mL Epindorff tubes. Beads were washed with 500 µL of RIPA buffer, removed, and pooled with supernatants. Samples were centrifuged 3 min at 13,000 rpm and protein levels were determined by measuring Abs_{280nm} in 2% SDS. Equal amounts of total protein were added to be immunoprecipated in a final volume of 1 mL. 40 µL of HA-conjugated beads were added to each IP sample and incubated over-night at 4°C on a rotator. IPs were washed, then IP and protein samples were resolved and quantified as described above.

2.2.7 in vitro Ubiquitination Assays

in vitro ubiquitination conjugation reactions were performed using a variation of a previously described method (19) and consisted of 1 mg/ml microsomes purified from the designated strains expressing Q394X, 1 mg/mL cytosol, and an ATP regenerating system (1 mM ATP, 40 mM creatine phosphate, 0.2 mg/mL creatine phosphokinase in Buffer 88) in a final volume of 40 µl. Purified yeast cytosol was prepared using liquid nitrogen via a modified version of a previously published technique (294). After cells were grown at 37°C for 1 h, they were harvested, washed in Buffer 88, and flash frozen in liquid nitrogen. The frozen cells were then lysed using a cold mortar and pestle for 1 min in the presence of liquid nitrogen for a total of 6 rounds of grinding. Addition of apyrase (0.02 units/reaction) instead of the ATP regenerating system served as a negative control. Samples were pre-incubated at room temperature for 10 min and were next incubated at room temperature, after ^{125}I-ubiquitin (2.4×10^6 cpm/rxn) was added to a final concentration of 1.5 mg/ml ubiquitin. The samples were then incubated at 37°C for 45 min before 125 µl of a 1.25% SDS Stop solution (50 mM Tris–Cl, pH 7.4, 150 mM NaCl, 5 mM EDTA, 1.25% sodium dodecyl sulfate (SDS), 1 mM PMSF, 2 mM leupeptin, 0.7 mM pepstatin A, and 10

mM N-ethylmaleimide (NEM)) was added to the reactions and incubated at 37°C for 30 min. A total of 400 µl of a Triton solution (50 mM Tris–Cl, pH 7.4, 150 mM NaCl, 5 mM EDTA, 2% Triton X-100, 1 mM PMSF, 2 mM leupeptin, 0.7 mM pepstatin A, and 10 mM NEM), 35 µl of a 50/50 protein A-sepharose slurry in Protein A bead resuspension solution, and anti-HA antibody were then added to each reaction and samples were immunoprecipitated overnight at 4°C on a rotator. After centrifugation, the pellets were washed 3 times in an IP wash buffer, and after all fluid was removed from the beads, TCAP sample buffer was added, the samples were briefly agitated, and incubated at 37°C for 30 min. The precipitated chimeras were then resolved on duplicate 10% SDS-polyacrylamide gels. One gel was transferred to nitrocellulose and incubated with anti-HA-HRP antibody to control for IP levels. The second gel was washed in ddH_2O, placed on filter paper, and dried. Dried gels were then exposed to a phosphorfilm for 2-3 d. Imaging and quantification were performed as described above.

2.2.8 Live cell imaging

Yeast strains lacking the *PDR5* gene and expressing an integrated, C-terminal GFP-tagged copy of Hsp104 were transformed with either the Q394X or an empty expression vector control. Overnight cultures were grown in SC –ura media and diluted to early log phase the next day. At that time, MatTek (Ashland, MA) glass bottom microwell dishes were treated with 1 mg/mL concanavalin A (ConA) and allowed to dry at 22°C for 1.5 hrs. After the cells doubled twice, the cultures were treated with either DMSO or a final concentration of 10 µM of MG132 and immediately placed in wells in the MatTek dishes. The dishes were then placed on a temperature controlled stage set to 45.7°C, which was required to shift the cells to 37°C. Cells were imaged from multiple sections of the plate every 5 min for 1 hr. Images were taken on a point scanning

Nikon A1 confocal (Chiyoda, Japan). The objective was a 1.40 NA 100x and images were taken at a half frame per second, averaging two frames per image.

2.3 RESULTS

2.3.1 Select Truncations in an NBD Lead to Decreased Protein Stability

A C-terminal 42 amino acid truncation in the yeast ATP-binding cassette (ABC) transporter, Ste6, leads to the selection of this yeast plasma membrane protein for ERAD (284). The destabilizing truncation resides in the cytoplasmic second nucleotide binding domain (NBD2) of Ste6 (black arrow, Figure 4A). This ERAD substrate is known as Ste6*, and many of the requirements for the degradation of this protein, referred to here as "Q1249X", have been characterized (19, 125, 284). Because the truncation in Ste6* was identified in a genetic screen, Drs. Meredith Metzger and Susan Michaelis from the Johns Hopkins School of Medicine wished to determine why this mutation destabilizes Ste6. To this end, they introduced a series of truncations into NBD2 both N- and C-terminal of Q1249. In cycloheximide chase analyses, most of the truncated proteins immediately N-terminal and C-terminal to Q1249 were similarly unstable. In contrast, a modest C-terminal truncation (R1268X) and, surprisingly, a more severe truncation upstream of Q1249 (L1240X) were as stable as the wild type protein (Figure 4B-C).

To investigate the mechanism underlying the recognition and degradation of these truncated species in a more simplified system—one in which the potential contribution of Ste6's

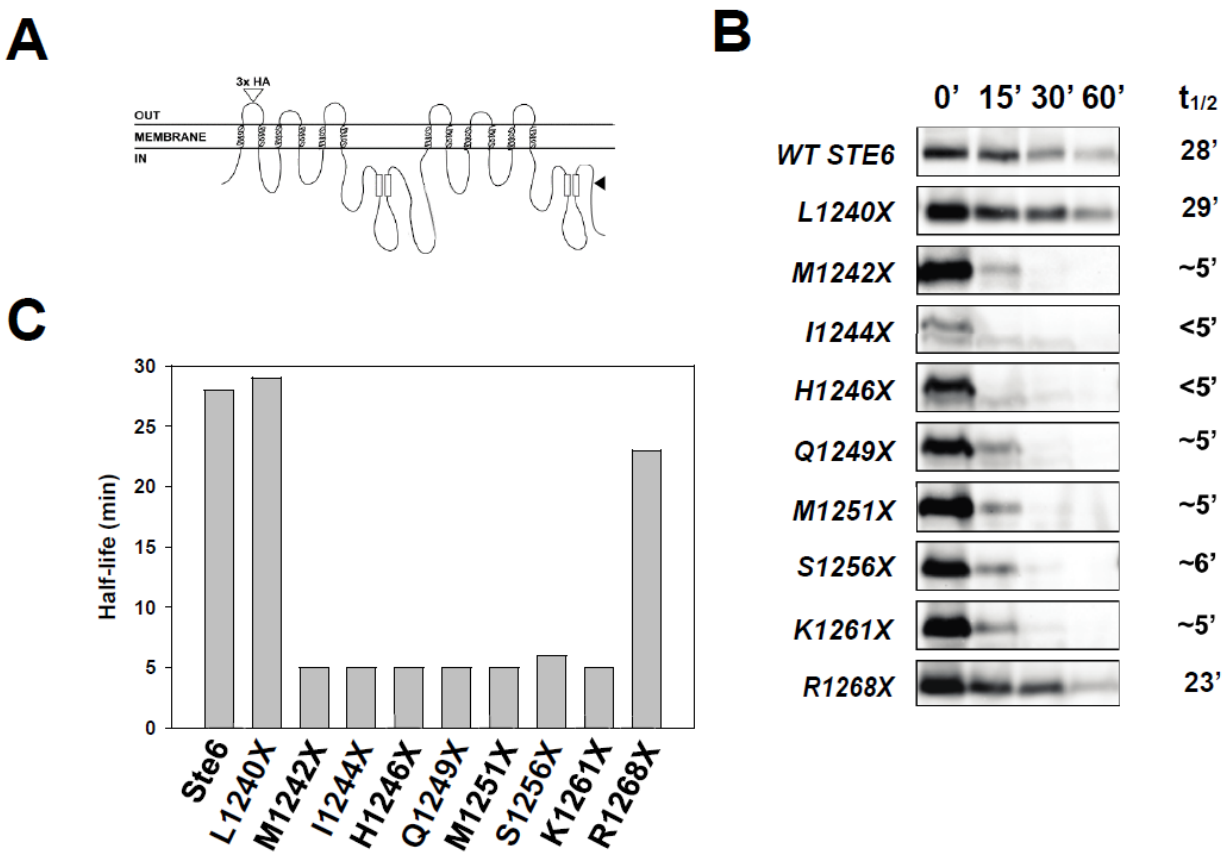

Figure 4. The metabolic stability of Ste6 containing truncations in the second nucleotide binding domain is highly variable

(A) Schematic of the yeast 12-transmembrane a-factor transporter, Ste6, with the relative site of the Q1249 truncation ("Ste6*") marked by an arrow. (B) Metabolic stabilities were determined by Drs. Meredith Metzger and Susan Michaelis from the Johns Hopkins School of Medicine by cycloheximide chase analysis and proteins were visualized by immunoblotting with an anti-HA antibody; $t_{1/2}$ indicates approximate half-life of each protein. (C) A bar graph depicting the relative half-lives of the Ste6 truncations.

12 transmembrane domains during ERAD might be lessened—NBD2 was tethered to the ER by introducing a hydrophobic hairpin at the N-terminus. Into the resulting chimera, "Chimera A", I

then introduced the analogous Ste6 truncations. As anticipated, the truncation analogous to Q1249X/Ste6* (Q394X) was unstable, as were substrates truncated near this site. Similar to the results with the most severe and shortest truncations in Ste6, the L385X and R413X truncations in Chimera A were as stable as the wild type protein (Figure 5B-C). To ensure that differences in the half-lives were not an artifact of the method, I also determined the half-life of Chimera A and Q394X by pulse chase analysis, and the turnover rates of these substrates were similar to what was observed in the cycloheximide chase assays (Figure 5D). These data indicate that the Chimera A truncation series provides a unique opportunity to investigate how the ERAD machinery distinguishes between a stable and an unstable substrate that are identical but differ only by the presence/absence of 2 amino acids (i.e., L385X and M387X).

To offer a glimpse of the potential structures adopted by these truncation mutants, Dr. Chris Guerriero from the University of Pittsburgh Department of Biological Sciences created a homology model for NBD2 from Ste6 based on the structure of murine P- glycoprotein, from which his analysis suggested was the ideal model protein to create a homology model (Figure 6). Subsequent homology models from Phyre2 (297) and Uniprot (www.uniprot.org) produced homology models similar to Dr. Guerriero's model from the murine P-glycoprotein. Each of the destabilizing truncations occur within a βαβ turn, while the stable mutated proteins have truncations at either the beginning (L1240X/L385X) or end (R1268X/R413X) of this structural motif. These results suggest that disrupting, but not deleting this secondary structure increases protein turnover. I further predict the destabilizing mutations give rise to unaccommodated β strands, which might be aggregation-prone.

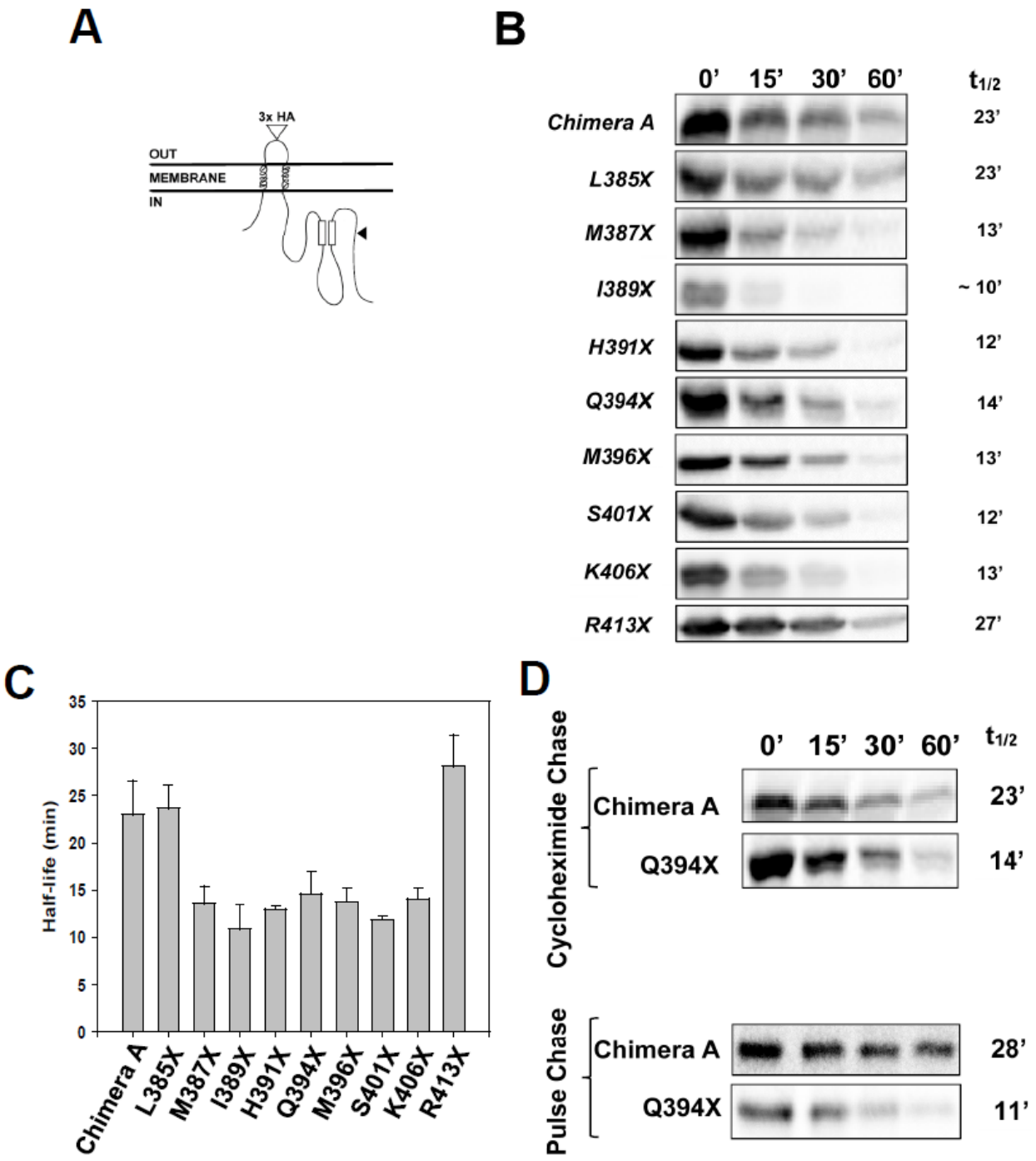

Figure 5. The metabolic stabilities of Chimera A truncation mutants reflects the half-lives of the analogous Ste6 truncation mutants

(A) Schematic of the yeast dual pass transmembrane protein, Chimera A, with the relative site of the Q394 truncation marked by an arrow. Chimera A consists of the first transmembrane domain

of Ste6 followed by a second poly Ala/Leu transmembrane domain annealed to NBD2 from Ste6. (B) Metabolic stabilities were determined by cycloheximide chase analyses and proteins were visualized by immunoblotting with an anti-HA antibody. (C) A bar graph depicts the relative half-lives of the Chimera A truncations. (D) The relative half-lives of Chimera A and Q394X by cycloheximide chase analysis were compared to the Chimera A and Q394X half-lives by pulse-chase analysis. For pulse chase analyses, cells were pulsed for 15 min with ^{35}S-Met, then chased for 1 hr. Cells were lysed and the substrates were immunoprecipitated with an anti-HA antibody and Protein A-Sepharose. Representative images from each condition are shown, but a total of 6 (for cycloheximide chase analyses) and 7 (for pulse chase analyses) independent experiments were performed and the data were averaged for $t_{1/2}$ calculations.

2.3.2 The Rate of Degradation for the ER-Membrane Resident Chimera A Truncation Series by ERAD Correlates with their Solubility

To ensure that the Chimera A truncated mutants are ERAD substrates, I confirmed that two of the more stable (Chimera A and L385X) and the less stable (Q394X) substrates localize to the ER (Figure 7A), and their degradation is proteasome-dependent since treatment with the 26S proteasome inhibitor, MG132, slows their turnover by ~2-3-fold (Chimera A and L385X) or ~7 fold (Q394X) (Figure 7B). In contrast, there appears to be no dependence on the vacuole for degradation (Guerriero et al, manuscript submitted for peer review). These results, along with degradation being Hrd1 and Doa10-dependent (Figure 7C), demonstrates that the Chimera A derivatives are ERAD substrates.. It is important to note that I failed to observe complete substrate stabilization with either proteasome inhibition or the deletion of *HRD1* and *DOA10*. The lack of

complete dependence on the proteasome may arise because MG132 is known to only inhibit the chymotrypsin activity of the 26S proteasome, leaving two 26S proteasome activities intact (298). It is also possible that the drug had decreasing stability over time, leading to varying levels of proteasome inhibition throughout the chase. For the incomplete dependence of Q394X degradation on Hrd1 and Doa10, work in our lab has shown that Q394X is not degraded by the vacuole (Guerriero et al, submitted for peer review). However, other labs have identified alternative E3 ligases that act during ERAD, such as the cytosolic E3, Ubr1 (127), as well as several other known E3s (see Table 1). Therefore, compensation by other E3s could also be responsible for the lack of complete stabilization of Q394X in the absence of Hrd1 and Doa10.

I next asked why the truncation mutants fit into two groups: those that are more vs. less stable. Based on a previous analysis of individual ERAD substrates, there is some evidence that substrate insolubility is associated with protein recognition and degradation by ERAD (92, 273). To address whether members of the Chimera A truncation series exhibit different solubilities, I prepared ER-enriched microsomes from strains expressing each protein and then measured their solubilities after treatment with dodecyl maltoside (DDM) and centrifugation. DDM was initially chosen for two reasons: 1) the hydrophilic-lipophilic balance (HLB) for DDM is in the optimal range of a surfactant for membrane protein solubilization (299, 300) and 2) DDM was determined to be an optimal non-ionic detergent to solubilize membrane proteins over others, such as Triton-X-100 (301). To confirm that DDM was the detergent I would use in my solubility assays, I tested the solubility of Q394X in the presence of a variety of other non-ionic detergents, including octyl glucoside, digitonin, and Triton-X100. I determined that none of these were able to improve the solubility of Q394X over what I observed with DDM (data not shown).

Utilizing this assay, I was able to determine that the Chimera A truncations exhibit varying solubilities in DDM (Figure 8). Strikingly, there is a positive correlation between substrate stability and detergent solubility (Figure 9A). As a control for this experiment, I also examined the solubility of the ER-membrane protein, Sec61, in the samples (Figure 8). I consistently see similar levels of solubilization of Sec61 in our assays, suggesting that the difference in insolubility between the mutants is not likely to be due to varying levels of membrane disruption. I also found that Q394X solubility in the presence of DDM is significantly increased by urea, such that the amount of Q394X in the supernatant ("S") now equals the amount seen when the solubility of the more stable Chimera A species is examined under identical conditions (Figure 9B). These combined results strongly suggest that ERAD substrate selection can depend on a measureable biochemical parameter, one that takes into account the protein's aggregation-propensity *in vitro*. Moreover, the ability of urea to augment the solubility of an ERAD substrate so it becomes more "wild type" suggests a potential role for chaperones to prevent aggregation of the substrate.

2.3.3 Hsp104 is Required to Degrade a Poorly Soluble ERAD Substrate

Cytosolic molecular chaperones play important roles in the ERAD of integral membrane proteins (141, 194), including Ste6*(125). To define whether the same cytosolic chaperones are required to facilitate Q394X degradation, I utilized strains expressing Q394X in which the genes corresponding to each chaperone were either deleted or mutated. Similar to what was observed with Ste6* (125), both the cytosolic Hsp70, Ssa1 (Figure 10A), and the cytosolic Hsp40, Ydj1 (Figure 10B) contribute to Q394X degradation. These chaperones were previously shown to augment Ste6* ubiquitination (19), but based on the relative insolubility of this substrate, as well as the fact that Ssa1 and Ydj1 function with Sse1 in a disaggregation complex (302, 303), I

measured Q394X turnover in a strain lacking Sse1. As shown in Figure 10C, Q394X was stabilized in *sse1Δ* yeast. Based on the fact that these chaperones act as disaggregases, and can work in conjunction with a dedicated protein disaggregase in yeast, Hsp104 (48, 304, 305), I next investigated the role of Hsp104 in the degradation of Q394X. Although significant stabilization of an ERAD substrate has never been observed in an hsp104Δ mutant, I observed strong stabilization of Q394X in the hsp104Δ strain. Moreover, when a multicopy plasmid was introduced into a strain containing HSP104 driven from its native promoter, Q394X degradation was accelerated (Figure 10D, solid triangles). I did not observe a similar dependence on Hsp104 for the degradation of Ste6* (Figure 11), suggesting that there are some potential differences in the recognition and clearance of Ste6* vs Q394X by ERAD (for more details, see Discussion). Similar to our observations for E3 dependence, we also did not see 100% stabilization of Q394X degradation in our mutant yeast. This could be explained by compensation by other chaperones/incomplete inactivation of the temperature sensitive mutants.

Because some chaperones are required for substrate ubiquitination during ERAD, such as Ssa1 and Ydj1 (19, 141), I next asked if Hsp104 and Sse1 also facilitate Q394X ubiquitination. To measure substrate ubiquitination, I expressed Q394X in *HSP104*, *hsp104Δ*, *SSE1*, and *sse1Δ* strains that also expressed myc-tagged ubiquitin. After the substrate was immunoprecipitated, I found that Q394X ubiquitination was not affected by the loss of Hsp104 function (Figure 12). As a control, I found that Q394X ubiquitination—like Ste6* ubiquitination (19)—was blunted when Ssa1 was inactivated at the non-permissive temperature in the *ssa1-45* yeast strain. Together, these data indicate that Hsp104 plays a previously unknown role during ERAD, one that functions downstream of substrate ubiquitination.

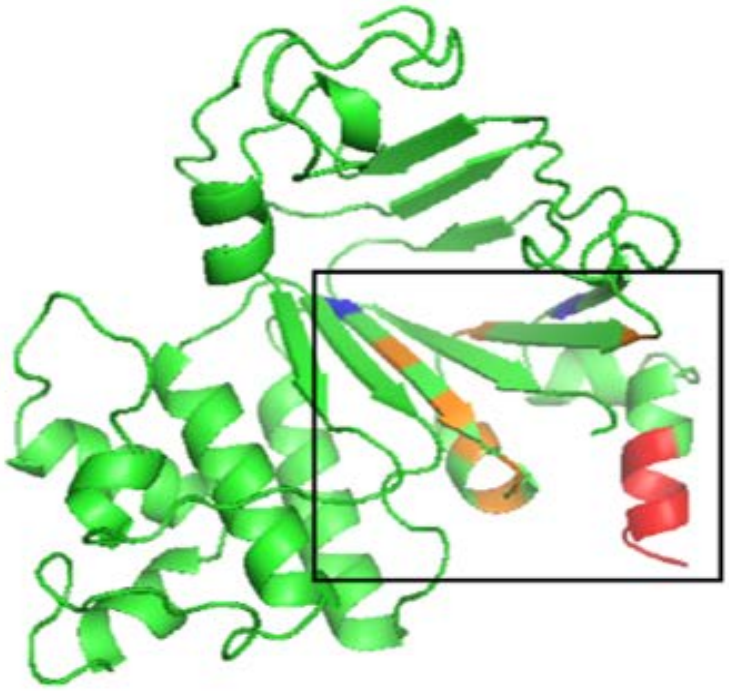

b

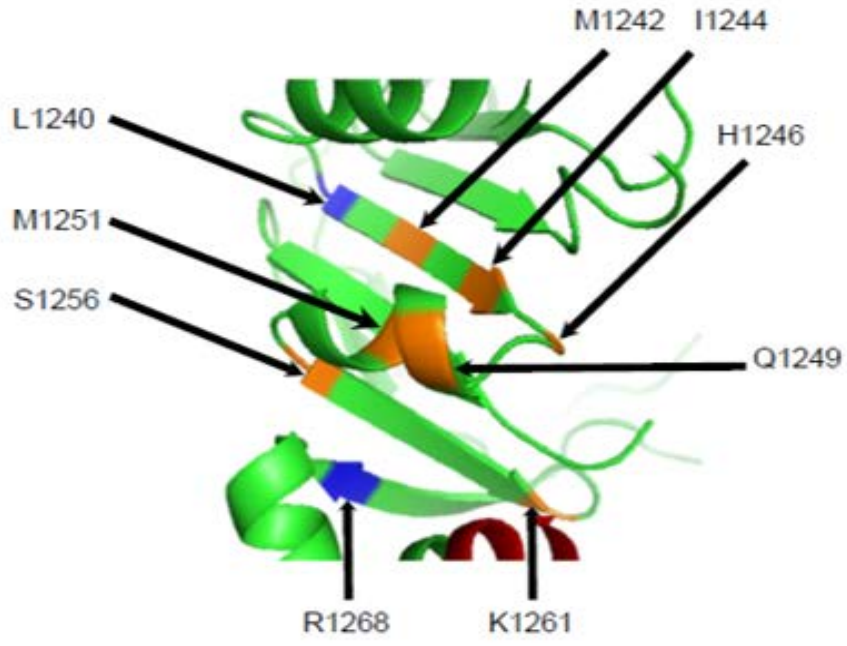

Figure 6. The truncation sites in the second nucleotide binding domain (NBD2) reside within a predicted β-sheet

A structure for the closest homologous domain was selected by querying the Research Collaboratory for Structural Bioinformatics Protein Data Bank, www.rcsb.org (306). The mouse P-glycoprotein (PDB ID: 4M1M, (307)) was chosen based on 35% sequence identity in the NBD2 sequence. Homology models were then constructed with Moddeller 9v13 (308). Shown here is the predicted model of the cytosolic NBD in the absence of its TM domains. A magnified view of the region containing the truncations in the Ste6 and Chimera A NBD2 is shown (amino acids 1240-1268 in Ste6). The structure and predicted sites of each truncation were visualized using PyMOL (The PyMOL Molecular Graphics System, Version 1.7.4.5 Schrödinger, LLC.). Shown in red is the C-terminus of the NBD2. Sites labeled in blue demonstrate similar half-lives to the wildtype protein while those labeled in orange are degraded more quickly.

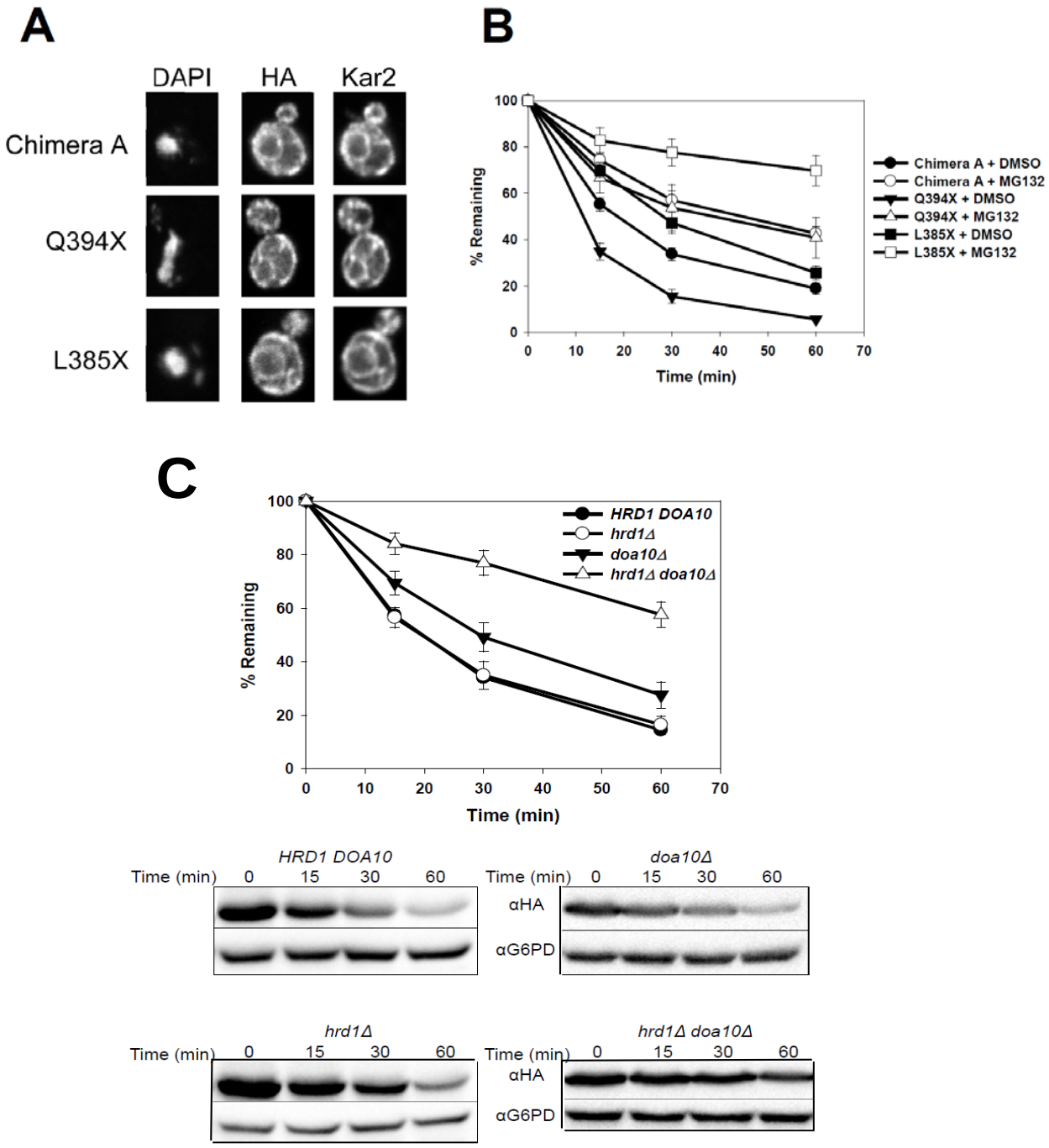

Figure 7. Chimera A truncations are localized to the ER and are degraded by ERAD

(A) The cellular localization of Chimera A, Q394X, and L385X were determined by indirect immunofluorescence microscopy. Each truncation was detected with anti-HA antibody, anti-Kar2 antiserum was used to mark the ER, and the nucleus was visualized with DAPI. (B) Yeast strains lacking *PDR5* and expressing either Chimera A, Q394X, or L385X were treated with DMSO

(closed circles) or 100 µM MG132 (open circles) for 30 min prior to a cycloheximide chase analysis performed at 26°C. Data represent the means of N = 9 (L385X) or N = 12 (Chimera A and Q394X) independent experiments, +/- SEM; Chimera A, $P < 0.001$ for all time points, Q394X, $P < 0.01$ for all time points, L385X, $P < 0.001$ at the 30 and 60 min time points, for data ±MG132. (C) Cycloheximide chase analyses were performed at 26C for Q394X to determine the requirement for two canonical ERAD E3s, Hrd1 and Doa10. N = 3-6 independent experiments, +/- SEM.

In addition to Hsp104, other chaperones are known to prevent protein aggregation, and some of these also function with Hsp104. Therefore, I measured Q394X degradation in yeast lacking the small heat shock proteins (sHSP), as they help to facilitate substrate disaggregation by Hsp104 (48, 309), as well as in strains containing a temperature-sensitive mutation in the TriC complex or in yeast deleted for *SGT2*, which encodes the yeast homolog of a "holdase" that functions during the retrotranslocation of ERAD substrates in mammals (48, 283, 310, 311). In addition, the yeast homologue of UBIQUILLIN, called Dsk2, was investigated for a role in Q394X degradation, as UBIQUILLIN plays an important role in the degradation of known ERAD substrates (110). As shown in Figure 13, the degradation of Q394X was unaffected in any of these strains, suggesting that Hsp104 is a dedicated chaperone during the ERAD of this new model substrate.

2.3.4 Q394X aggregates in the ER membrane in the absence of Hsp104 function

Because Hsp104 is important for the degradation of Q394X (Figure 10D) and acts at some point downstream of Q394X ubiquitination (Figure 12), I hypothesized that Hsp104 plays a role in the

disaggregation of Q394X prior to degradation. In order to test this hypothesis, I utilized a modified flotation assay (296). In the absence of Hsp104 at high temperatures, a population of Q394X shifts to a heavier fraction (Figure 14B, Fraction 7, HSP104 vs hsp104Δ). This population of Q394X that shifts to a heavier fraction in the absence of Hsp104 is also poly-ubiquitinated, suggesting it has been selected for ERAD (Figure 14C, Fraction 7, HSP104 vs hsp104Δ). To control for any variation in fraction removal and to determine if this heavier population of Q394X in the hsp104Δ samples is still localized to the ER, I compared the location of Sec61 between the HSP104 and hsp104Δ (Figure 14D). Indeed, there appears to be no significant difference in the location of Sec61 between the HSP104 and hsp104Δ samples (Fractions 3-7), suggesting this shift in Q394X density is due to the absence of Hsp104 function. While a majority of the Sec61 appears to be present in fractions 3-6, there is roughly 5-10% of the Sec61 in fraction 7, where I see the increase of Q394X residence in the *hsp104Δ* samples. These results, along with the localization of Hsp104-GFP to puncta when temperature-shifted cells express Q394X (Figure14), suggest that Hsp104 acts to reduce Q394X aggregation, potentially at the ER-membrane.

Since I know that Hsp104 acts downstream of Q394X ubiquitination (Figure 12), I next investigated the role of Hsp104 in Q394X retrotranslocation from the ER. Using a previously established *in vitro* retrotranslocation assay from our lab (19), I discovered that ubiquitinated

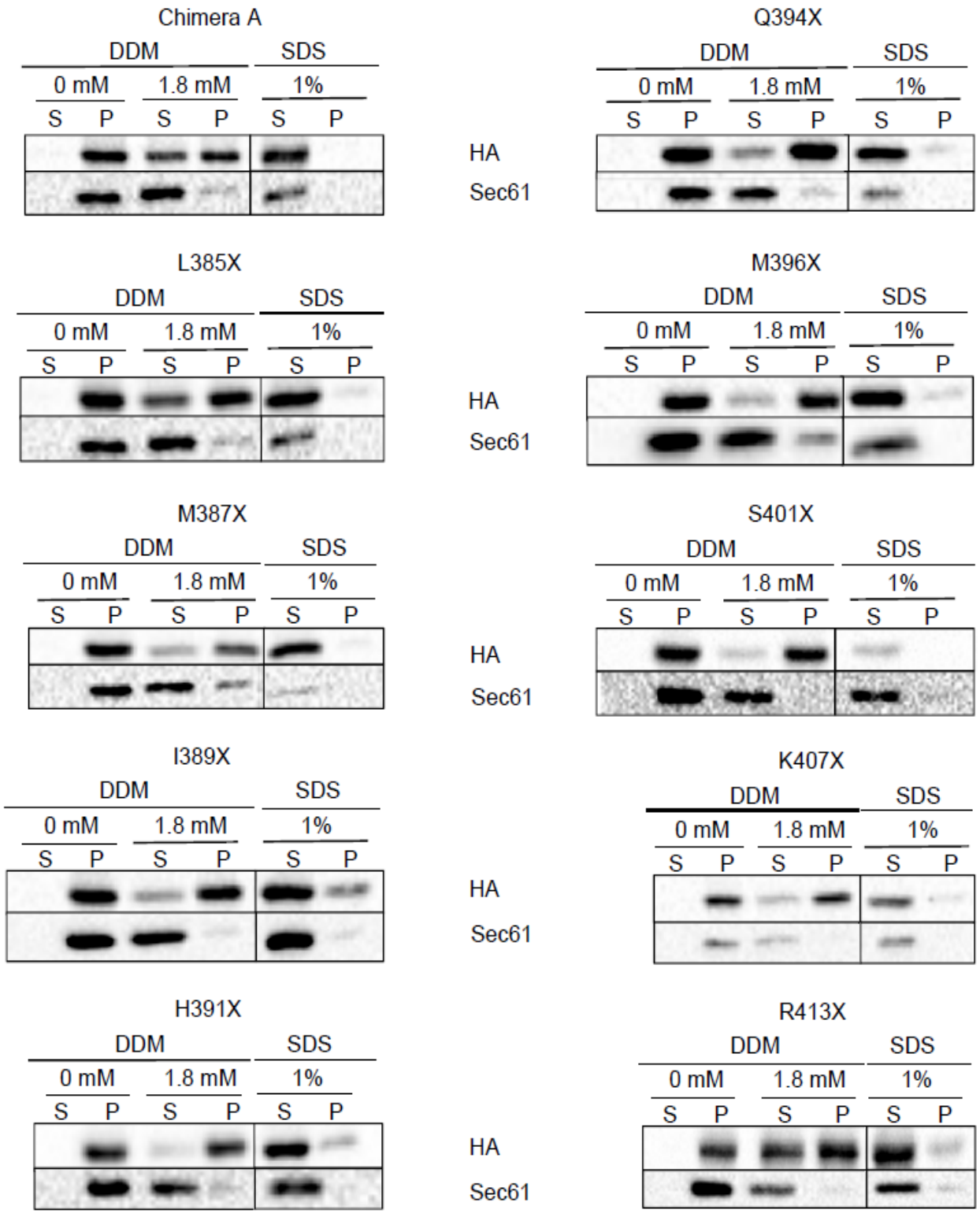
Chimera A
DDM
SDS
0 mM
1.8 mM
1%
S P S P S P
HA
Sec61
Q394X
L385X
M396X
M387X
S401X
I389X
K407X
H391X
R413X

Figure 8. The Chimera A truncation mutants display varying levels of detergent solubility

BY4742 (wild type) yeast expressing the indicated truncations were harvested and ER-enriched microsomes were prepared as described in the Experimental Procedures. The microsomes were then treated with 1.8 mM DDM to solubilize the substrates. As controls, reactions were conducted in the absence of detergent ("0 mM") or in the presence of the strong, ionic detergent sodium dodecyl sulfate (SDS). Samples were centrifuged at 18,000 *x g* and the percent of solubilized (S) and membrane-retained (P) protein was determined by immunoblotting with an anti-HA antibody. These values are reported in Figure 3C. Sec61 solubilization was also monitored by use of an anti-Sec61 antibody to control for variations in membrane solubilization between samples. The images are representative for N = 4 independent experiments.

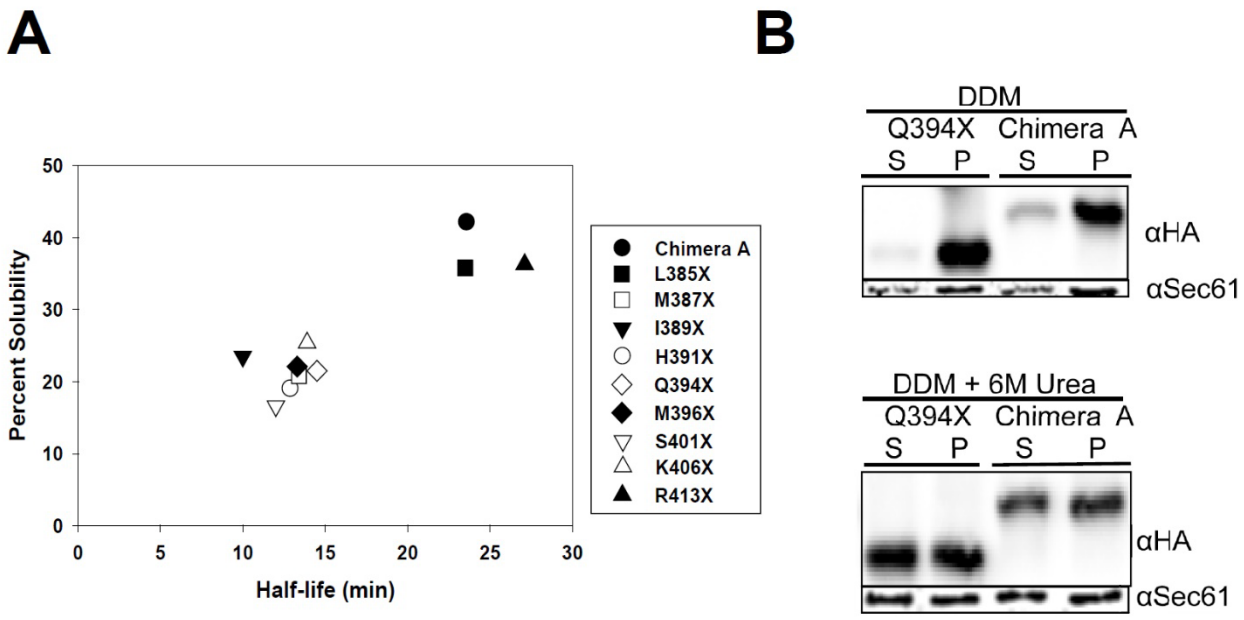

Figure 9. The half-lives of the Chimera A truncations correlates with detergent solubility

(A) The metabolic stabilities of the truncation mutants were determined by cycloheximide chase analyses at 26°C and protein solubilities were determined by the percent of soluble substrate after ER-derived microsomes were treated with 1.8 mM of the non-ionic detergent, dodecyl-maltoside (DDM) and the mixture was centrifuged at 18,000 *x g*. Data represent the means of N = 4-6 independent experiments for stability measurements and N = 4 independent determinations for protein solubility. (B) Wild type (BY4742) microsomes containing Q394X were treated with 0.6 mM DDM alone or 0.6 mM DDM in the presence of 6 M urea and protein residence in the supernatant (S) and pellet (P) fractions was analyzed after centrifugation and immunoblotting. Sec61 was used as a control for membrane solubilization.

Q394X is less efficiently retrotranslocated in the absence of Hsp104 function (Figure16B, Supernatant ("S") lanes as a percentage of the total ubiquitinated signal for *HSP104* vs *hsp104Δ*).

In this experiment, the supernatant was defined as the soluble fraction after an 18,000 *x g* centrifugation step. I observed the same ratios of retrotranslocated, ubiquitinated Q394X in both the *HSP104* and *hsp104Δ* reactions after a 100,000 *x g* centrifugation step, suggesting the retrotranslocated protein is soluble and not in a partially aggregated state (Figure 16C). Interestingly, there is a high molecular weight population of ubiquitinated Q394X that is present when using components purified from *hsp104Δ* cells, but not from the *HSP104* cells (Figure 16 B-C, asterisk). Components purified from strains lacking the sHsps, which do not play a role in Q394X degradation (Figure 13A), did not significantly alter the retrotranslocation of ubiquitinated Q394X (Figure 17). Interestingly, while Sse1 does play an important role in Q394X degradation, it does not appear to play a significant role in the retrotranslocation of Q394X (Figure17). This result, along with a minimal change in Q394X ubiquitination when Sse1 is absent (Figure 12), suggests that Sse1 may act at some point after Q394X is retrotranslocated from the ER. The decrease in the efficiency of Q394X retrotranslocation in the absence of Hsp104 function, along with the shift of Q394X in the *hsp104Δ* strain to a denser, ER-localized (Sec61-containing) fraction led me to ask whether Hsp104 acts on aggregated Q394X in the ER membrane prior to retrotranslocation or on aggregated Q394X that has already been retrotranslocated. To address this question, the Q394X-containing pellets were washed in urea and recollected at 18,000 *x g*. I found that negligible amounts of ubiquitinated Q394X were solubilized by urea in reactions both

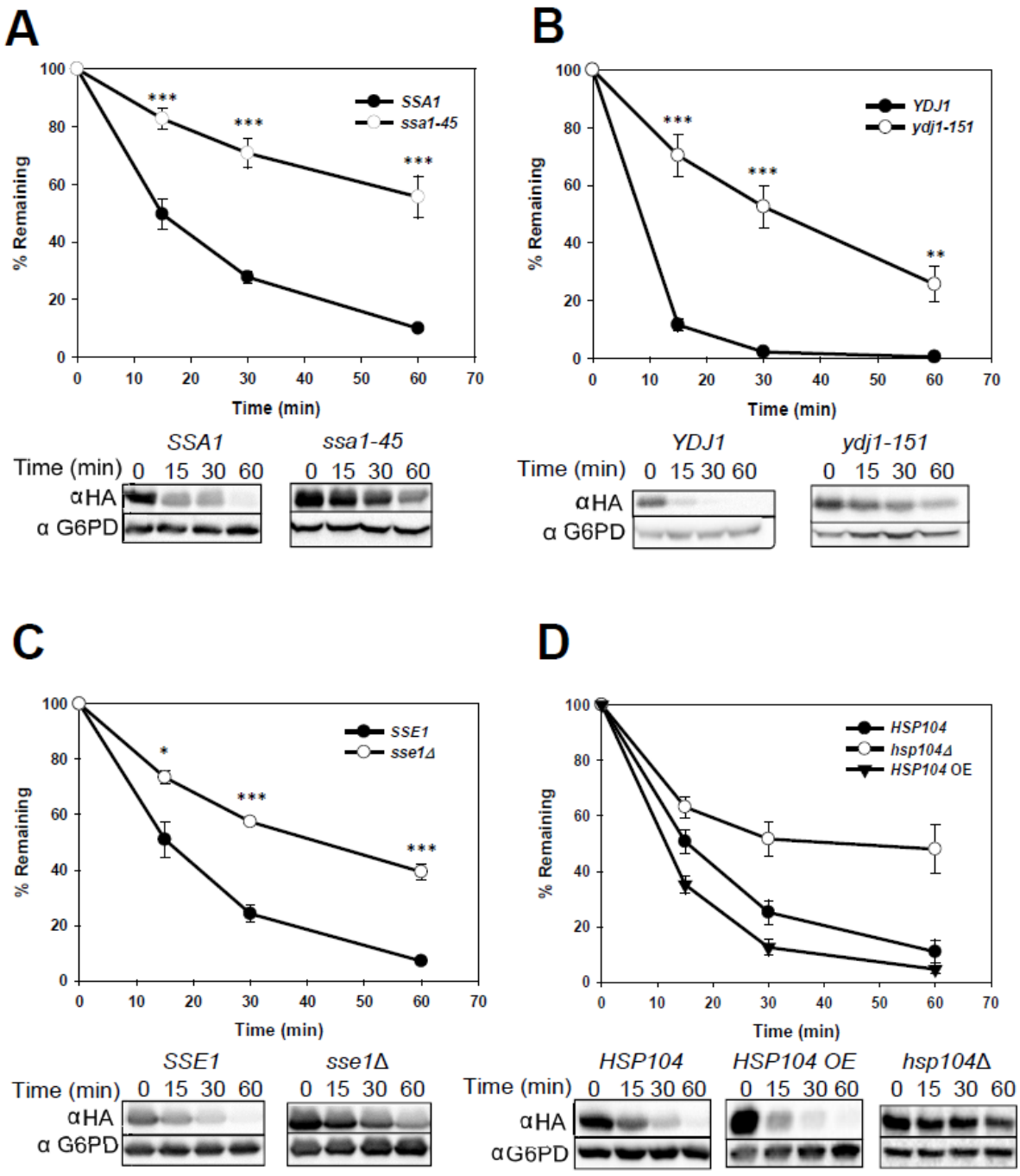

Figure 10. The degradation of an unstable/poorly soluble substrate, Q394X, requires select cytoplasmic chaperones

The stabilities of Q394X in the indicated wildtype and mutant strains were determined by cycloheximide chase analyses at 37°C. (A) The yeast cytosolic Hsp70, Ssa1; N = 6 independent experiments, +/- SEM. (B) The yeast cytosolic Hsp40, Ydj1; N = 6 independent experiments, +/-

SEM. (C) The yeast cytosolic Hsp110, Sse1; N = 3 independent experiments, +/- SEM. (D) The yeast cytosolic disaggregase, Hsp104; N = 3-6 independent experiments, +/- SEM, P < 0.01 for time points 15 min and 30 min for *hsp104Δ* vs *HSP104*. For *HSP104 OE*, P < 0.05 at time point 15 min for *HSP104* vs *HSP104 OE* is an Hsp104 overexpression strain. In all panels, *P < 0.05, **P < 0.01, ***P < 0.001.

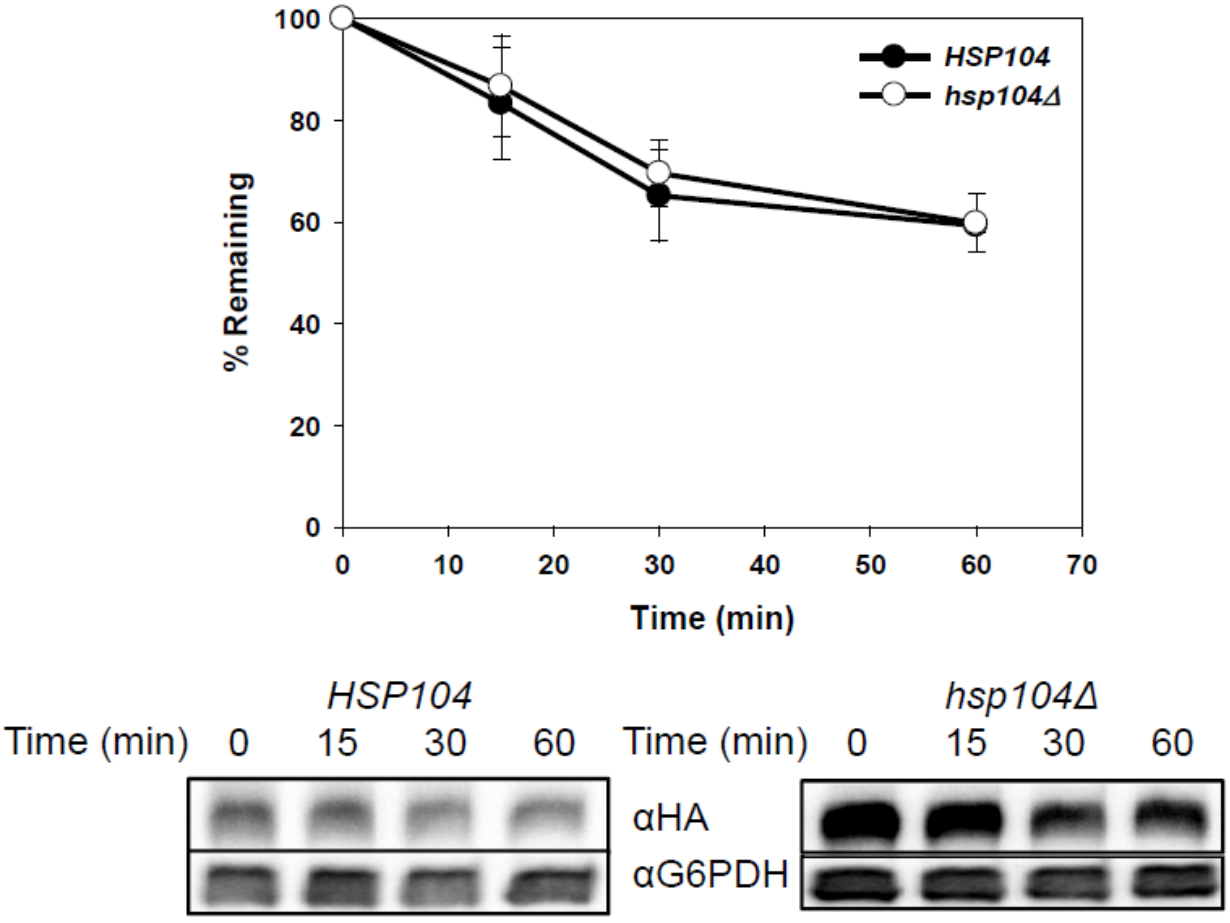

Figure 11. Hsp104 is not required for the degradation of Ste6*

The stability of Ste6* in the absence of Hsp104 function was determined by cycloheximide chase analyses at 37°C. N = 3 independent experiments, +/- SEM.

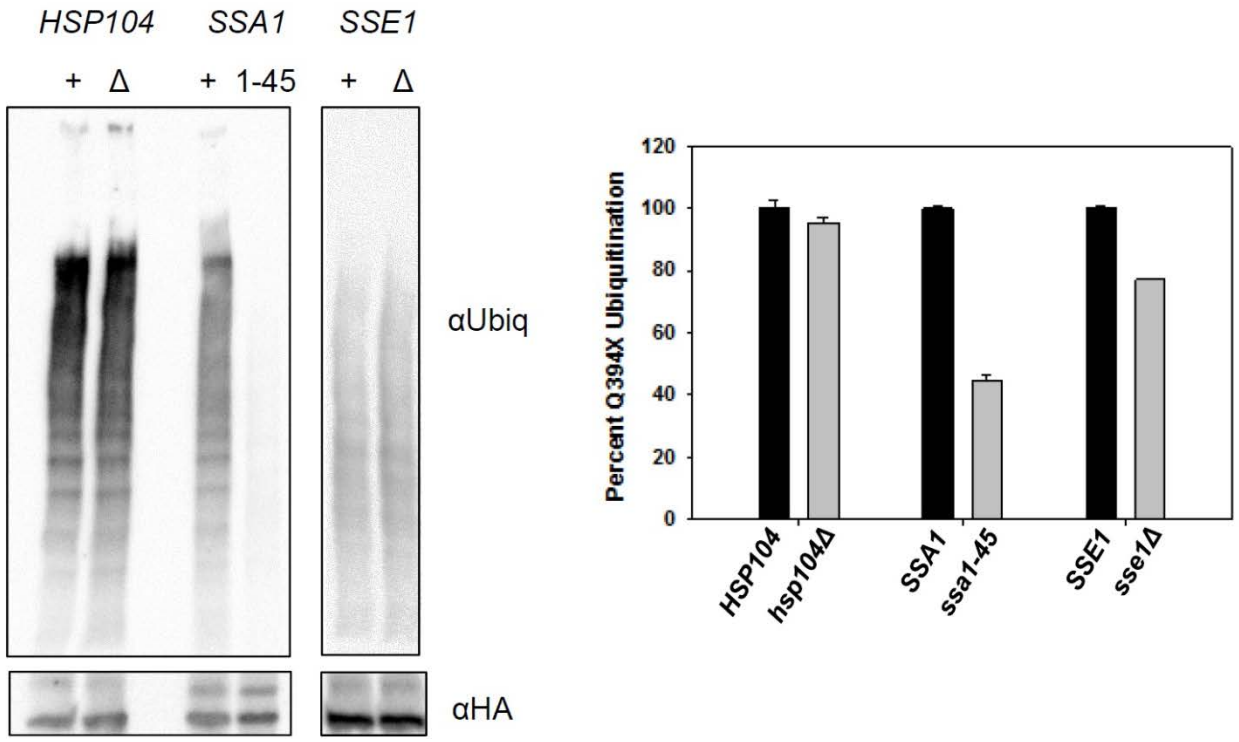

Figure 12. Hsp104 acts downstream of Q394X ubiquitination

Q394X ubiquitination was examined in the indicated yeast strains after cells were shifted to 37°C for 1.5 hrs, lysed, and the substrate was immunoprecipitated using anti-HA-conjugated agarose beads. Q394X was detected (HA) as well as total ubiquitin. The percent of *in vivo* ubiquitination was calculated after ubiquitination levels were first normalized against Q394X protein levels (Ubiquitin/HA), with the signal in the wild type strains set to 100%. Data represent the means of N = 3 (*SSE1* and *sse1Δ*), N = 4 (*HSP104*, *SSA1*, and *ssa1-45*), and N = 5 (*hsp104Δ*) independent experiments, +/- SEM; ***P < 0.001.

in the presence and absence of Hsp104 (Figure 19A, "US" lanes). As a control for this experiment, we found that Cdc48 and Hsp104 were completely released from the microsome membrane after treatment with urea, while a population of Sec61 and Q394X remained in the ER membrane (Figure 19B). This result suggests that Q394X residing in the pellet has not already been retrotranslocated. Based on these results, one could hypothesize that Hsp104 acts to retrotranslocate ubiquitinated Q394X into the cytosol. However, over-expression of Hsp104 in a *cdc48* mutant strain did not rescue Q394X degradation (Figure 20). Therefore, I believe that Hsp104 acts on aggregated, ubiquitinated Q394X in the ER membrane prior to retrotranslocation by Cdc48 (Figure 21).

2.4 DISCUSSION

The process of ERAD has been linked to multiple human diseases and, as a result, has been heavily studied (269). While much has been discovered about the process of ERAD, one area that has been difficult to address is why substrates are recognized as being misfolded and degraded by ERAD. Interestingly, Dr. Meredith Metzger and Dr. Susan Michaelis (Johns Hopkins University, Baltimore, MD) found that truncations in the yeast ABC transporter, Ste6, starting at the C-terminus were not sufficient to increase the extent of the degradation of the mutant Ste6 protein. This effect is the opposite of what has been demonstrated for another plasma membrane ATPase, Pma1, where truncating further from the C-terminus led to increased protein degradation (312). Utilizing a homology model of the Ste6 NBD2 made by Dr. Christopher Guerriero against the

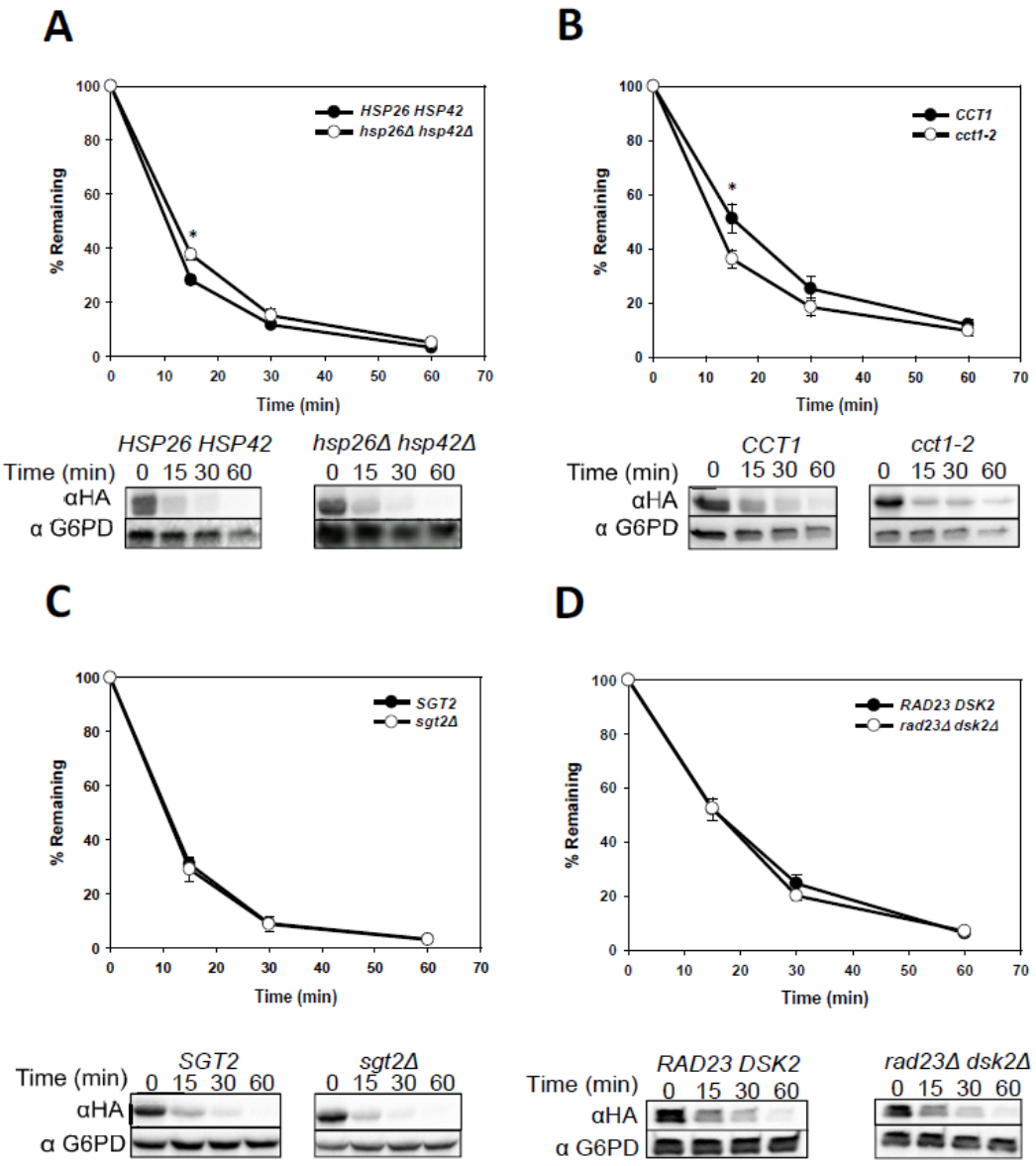

Figure 13. The ERAD of Q394X is unaffected by the small heat shock proteins, the TriC complex, a component of the Tail-Anchor insertion complex, or the Rad23-Dsk2 Ubl/Uba-domain containing proteins

All cycloheximide chases were performed at 37°C with a 30 min pre-shift at 37°C. The stability of Q394X was investigated in the absence of (A) the small heat shock proteins, Hsp26 and Hsp42 (N = 3), (B) the activity of a chaperonin subunit, Cct1 (N = 16), (C) the Tail-Anchor insertion

pathway component, Sgt2 (N = 6), and (D) the 26S proteasome-associated factors, Rad23 and Dsk2 (N = 6). All data represent the means of the indicated number of independent experiments, +/- SEM.

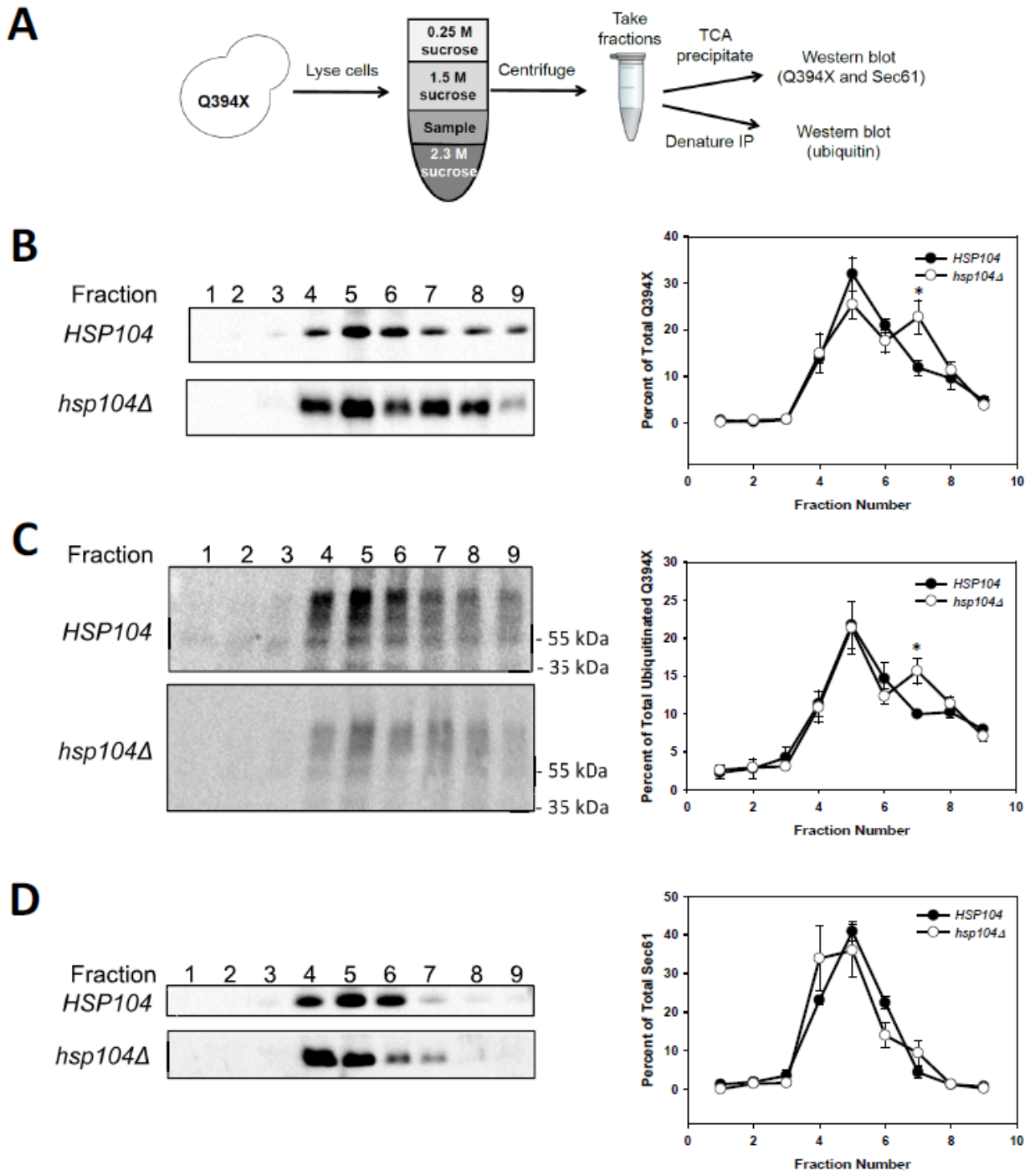

Figure 14. Hsp104 is required to disaggregate ubiquitinated Q394X

(A) A schematic of the flotation assay used to determine substrate oligomerization. Cell lysates from *HSP104* or *hsp104Δ* cells expressing the Q394X mutant treated at 37°C for 1.5 hrs were prepared and analyzed by equilibrium sucrose density centrifugation. Proteins in each fraction

were TCA precipitated and immunoblotted with anti-HA antibody to detect (B) Q394X, or (C) were denatured and immunoprecipitated to detect ubiquitinated Q394X. (D) The migration of Sec61 was used to identify the migration of the ER. Data represent the means of N = 4-5 independent experiments +/- SEM; * $P < 0.05$.

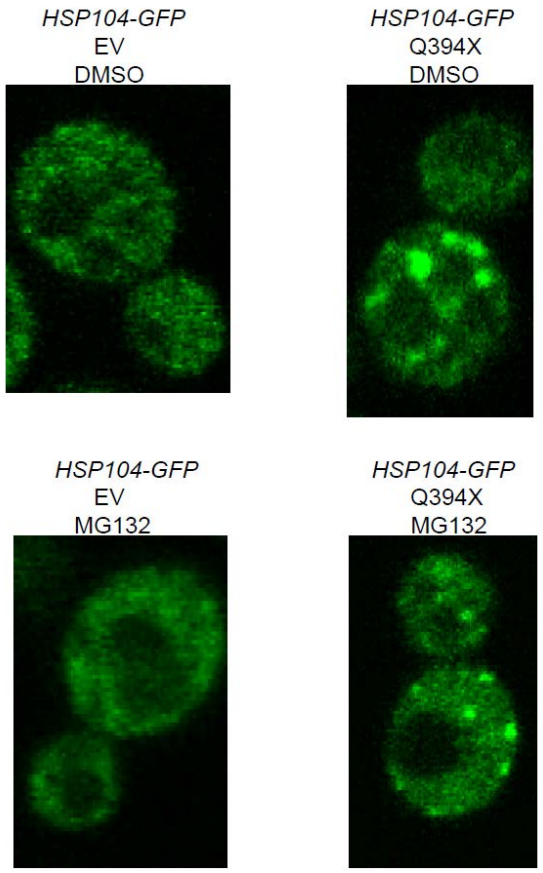

Figure 15. GFP-tagged Hsp104 localizes to puncta when temperature-shifted cells express Q394X

Yeast strains lacking *PDR5* and containing an integrated *HSP104-GFP* were utilized to monitor Hsp104 localization under conditions where Hsp104 is required for Q394X degradation. Specifically, cells expressing either an empty expression vector (EV) or the insoluble mutant, Q394X, were incubated at 37°C and treated with DMSO or the proteasome inhibitor, MG132.

published structure of the murine P-glycoprotein, another ABC transporter, I hypothesize that these truncations disrupt a predicted β-sheet. In fact, alterations and improper folding of β-sheet

rich proteins is well known to cause a multitude of human diseases linked to protein aggregation (51, 313). Therefore, further investigation into why these truncation mutants are processed differently could contribute important information to better understand ERAD substrate selection.

To simplify our system, I then introduced the analogous Ste6 truncations in a model ERAD substrate, called Chimera A. I demonstrated that the analogous truncations in Chimera A have similar trends in the measured metabolic stabilities as their Ste6 counterparts. This new system allowed me to investigate the characteristics responsible for substrate selection by ERAD without complications due to complex intradomain interactions.

Next, I utilized the Chimera A truncations to address why select members of my truncation series exhibited shorter metabolic stabilities than others. It is important to point out that the NBD2 of Ste6 has a predicted amphipathic helix (123). However, this predicted amphipathic helix is over 100 amino acids away from the region where the truncations reside. Based on Dr. Christopher Guerriero's homology model, it does not seem likely that these two regions interact. Therefore, I chose to investigate whether the Chimera A truncation mutants exhibit varying solubilities, which is another substrate characteristic hypothesized to lead to selection for ERAD (92, 273). For example, Gilon et al. (1998) found that fusing the C-terminus of two proteins to specific peptides led to decreased protein stability. Furthermore, these proteins developed a dependence on two E2s known to be important in ERAD: Ubc6 and Ubc7 (60, 122). It was determined that these peptides were highly hydrophobic. However, this finding was discovered by fusing synthetic peptides to the C-termini of a protein. The peptides are not a native part of the proteins and could disrupt overall secondary structure and induce alternative interactions with cellular components. In addition, Stein et al. (2014) showed that a more aggregation-prone version of the ERAD substrate, CPY*, had a higher binding affinity than CPY* to Hrd1, which plays a role in ERAD.

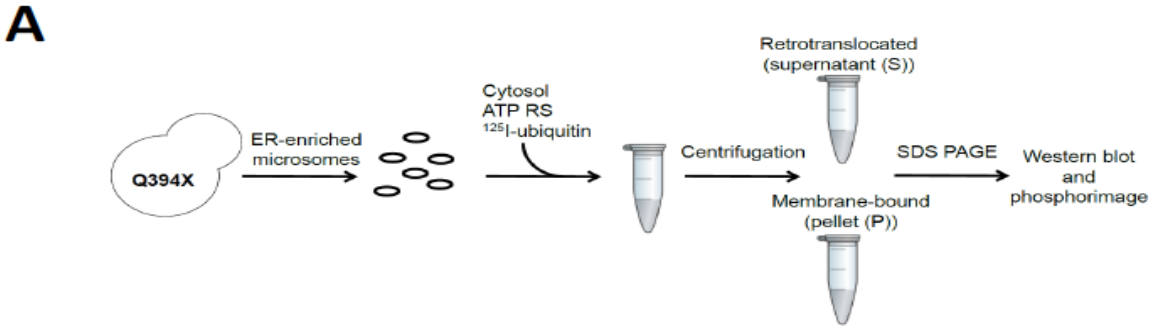
A
Q394X
ER-enriched microsomes
Cytosol
ATP RS
125I-ubiquitin
Centrifugation
Retrotranslocated (supernatant (S))
Membrane-bound (pellet (P))
SDS PAGE
Western blot and phosphorimage

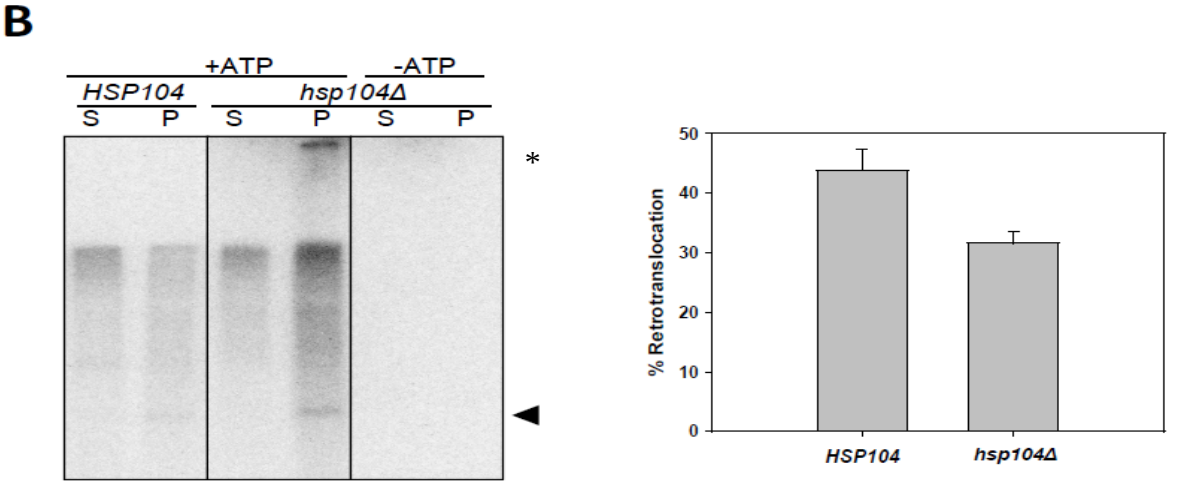
B
+ATP
-ATP
HSP104
hsp104Δ
S
P
S
P
S
P
*
% Retrotranslocation
50
40
30
20
10
0
HSP104
hsp104Δ

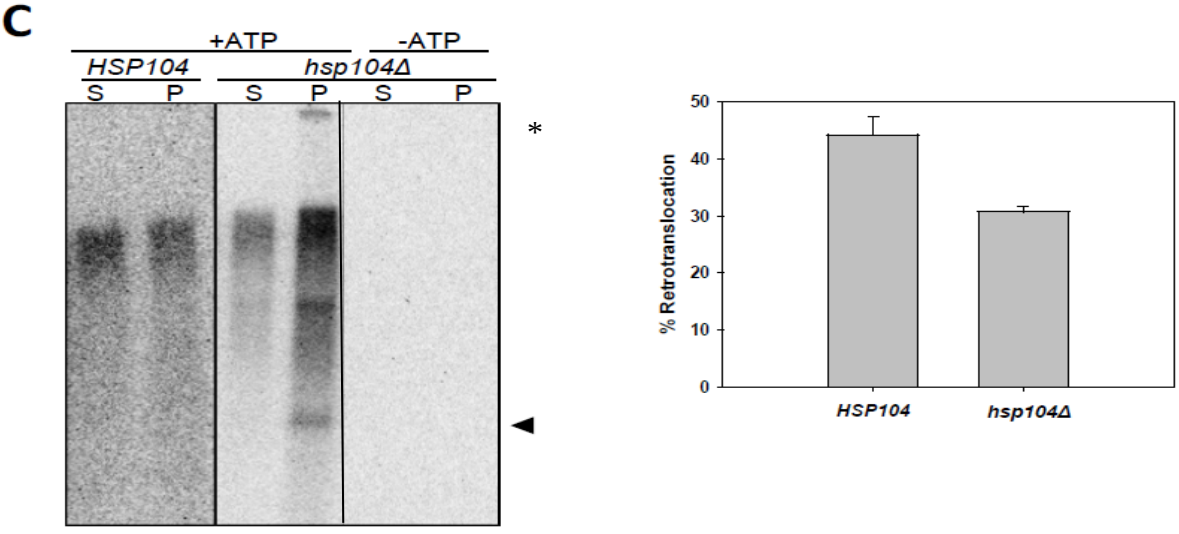
C
+ATP
-ATP
HSP104
hsp104Δ
S
P
S
P
S
P
*
% Retrotranslocation
50
40
30
20
10
0
HSP104
hsp104Δ

Figure 16. Loss of Hsp104 function leads to a decrease in the amount of soluble, ubiquitinated Q394X

(A) A schematic of the *in vitro* ubiquitination/retrotranslocation assay. (B,C) *in vitro* ubiquitination assays utilizing an 18,000 *x g* (B) or 100,000 *x g* (C) centrifugation step were utilized to collect retrotranslocated Q394X. Ubiquitinated Q394X was immunoprecipitated from the retrotranslocated supernatant (S) fractions and the membrane bound pellet (P) fractions after immunoprecipitation. Reactions were run in the presence of either wild type (*HSP104*) or *hsp104Δ* cytosol, and in the presence or absence of ATP, as indicated. The native molecular weight (arrow) and high molecular weight species (asterisk) of Q394X are marked.

While important, this was shown using purified components in reactions in which Hrd1 had been immobilized and used at high concentrations.

Utilizing my Chimera A truncation series, I demonstrated a positive correlation between substrate solubility and substrate stability. Importantly, I was able to show that this difference in solubility within the Chimera A truncation series is not due to variations in membrane extraction; the solubility of a less soluble Chimera A mutant is able to be rescued by the addition of urea. For the first time, by using a series of mutations within the same protein, I was able to positively correlate the stability and solubility of an ERAD substrate. This correlation between solubility and stability is further supported by evidence from Arteaga and colleagues (271). While the authors concluded that the exposure of an amphipathic helix was the deciding factor for ERAD substrate selection, they also determined that the hydrophobicity of a predicted amphipathic helix was crucial for substrate selection and degradation. Because they never determined the solubilities of their substrates, it is possible that the exposure of the hydrophobic residues within

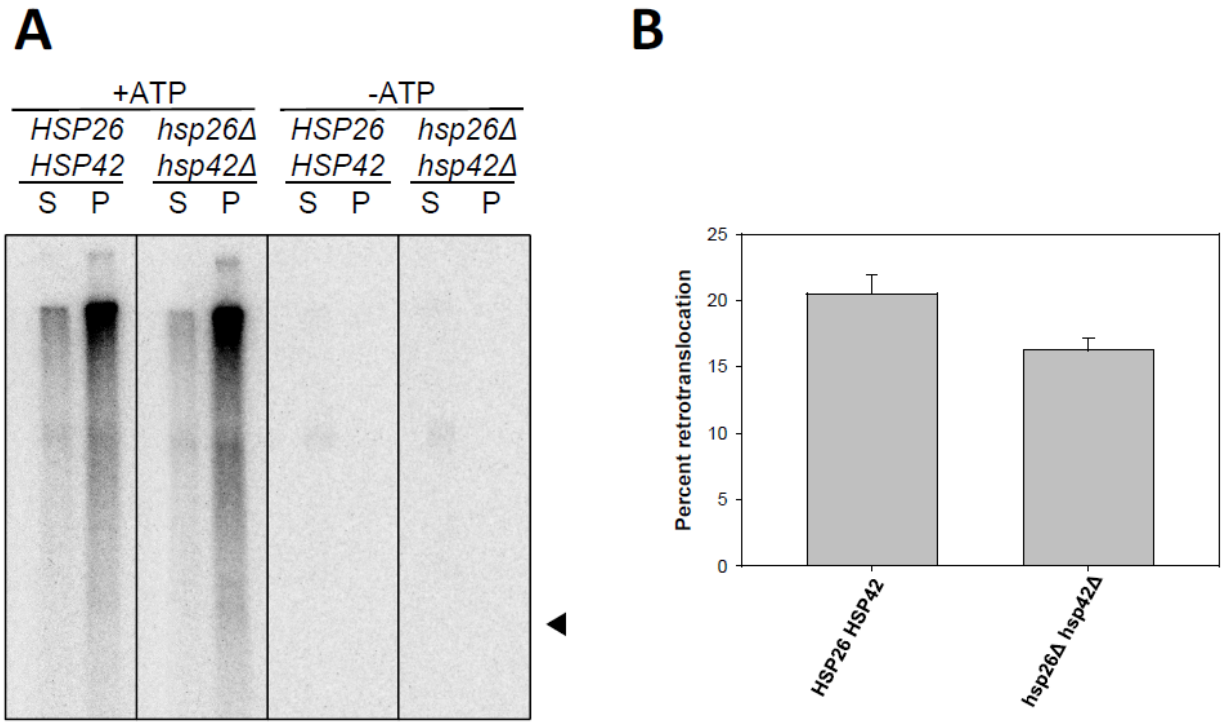

Figure 17. The retrotranslocation of ubiquitinated Q394X is unaffected by the small heat shock proteins

(A) *In vitro* ubiquitination assays were performed with cytosol and microsomes isolated from *HSP26 HSP42* and *hsp26Δ hsp42Δ* strains. (B) Quantification of the percentage of retrotranslocated, ubiquitinated Q394X is present. After centrifugation, the retrotranslocated (S) and membrane integrated (P) populations of ubiquitinated Q394X were immunoprecipitated with an anti-HA antibody and visualized by SDS PAGE and phosphorimage analysis. The native molecular weight of Q394X is marked by an arrow. N = 3 independent experiments, +/- SEM.

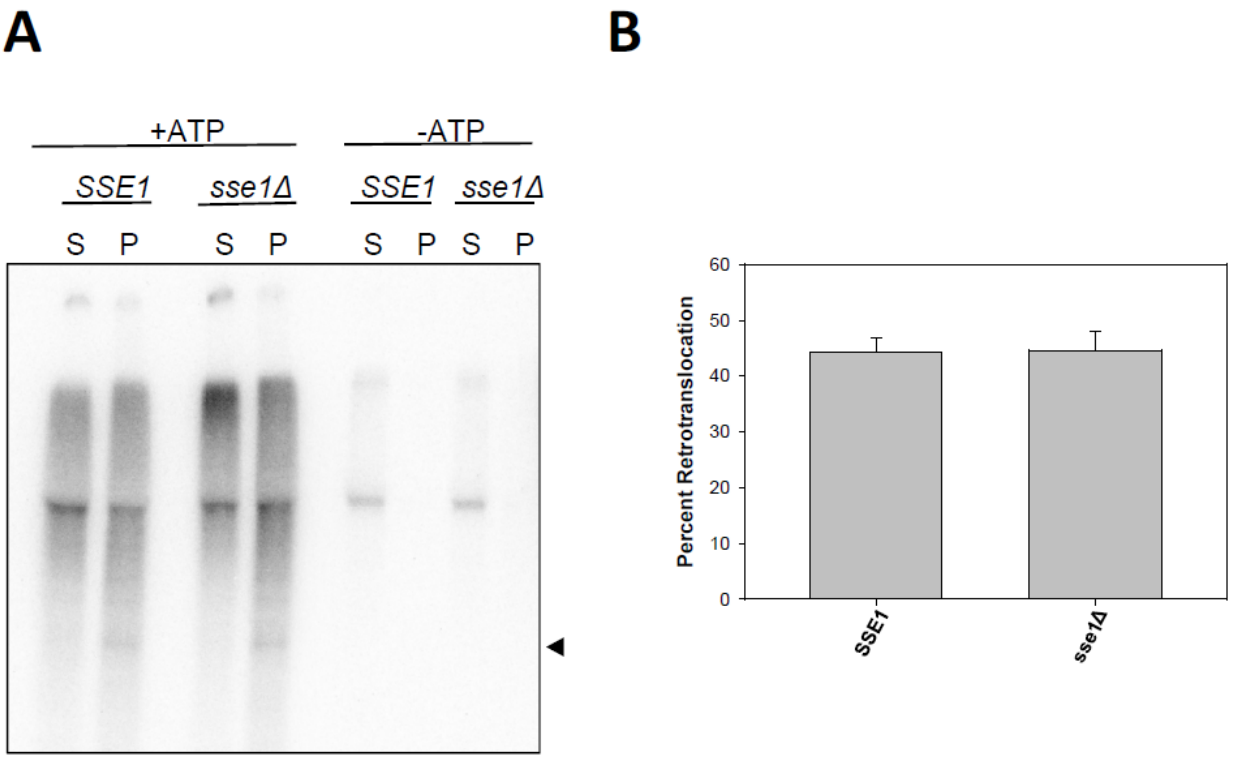

Figure 18. Sse1 does not affect the retrotranslocation of ubiquitinated Q394X.

(A) *In vitro* ubiquitination assays were performed with cytosol and microsomes isolated from *SSE1* and *sse1Δ* strains. (B) Quantification of the percentage of retrotranslocated, ubiquitinated Q394X is present. After centrifugation, the retrotranslocated (S) and membrane integrated (P) populations of ubiquitinated Q394X were immunoprecipitated with an anti-HA antibody and visualized by SDS PAGE and phosphorimage analysis. The native molecular weight of Q394X is marked by an arrow. N = 6 independent experiments, +/- SEM.

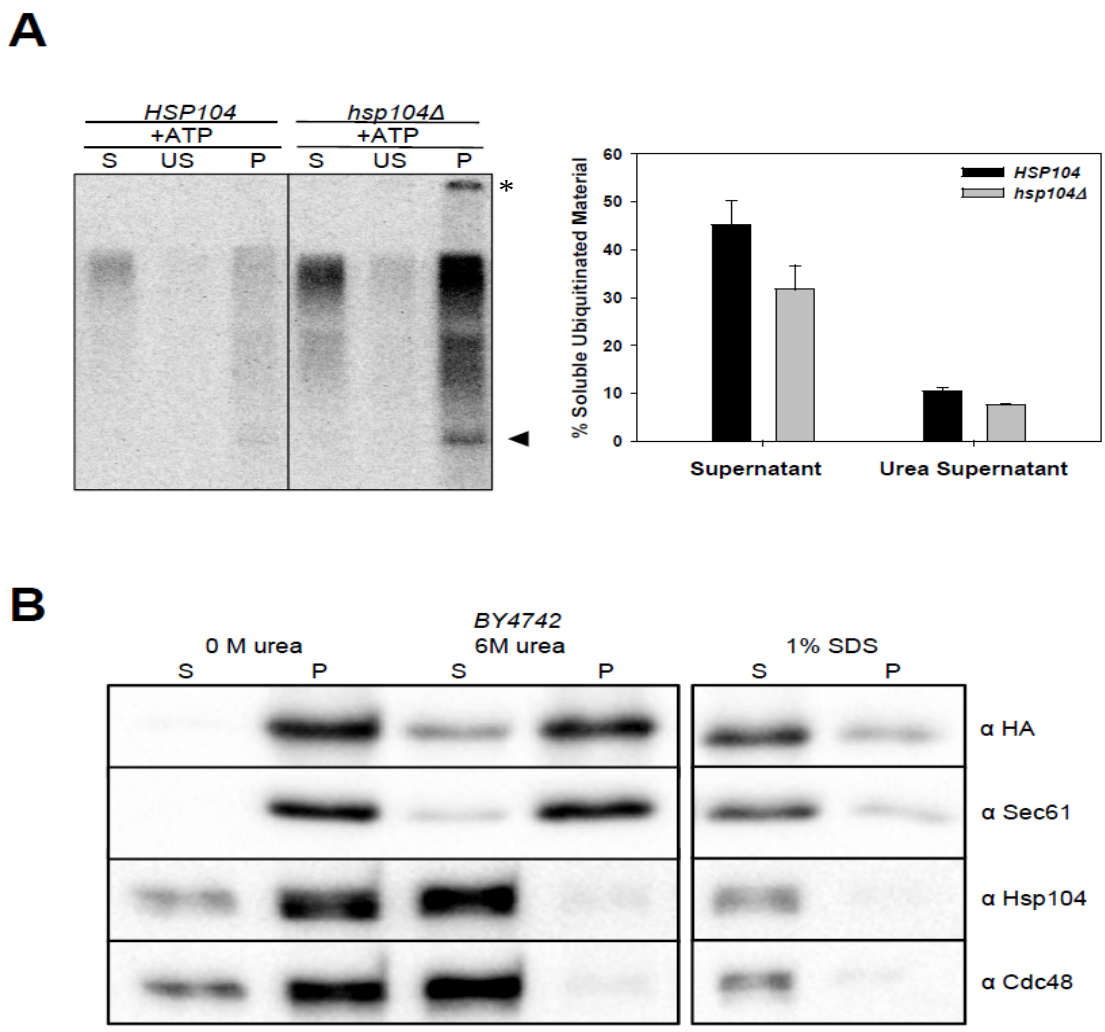

Figure 19. Hsp104 acts on ubiquitinated Q394X in the ER membrane to increase retrotranslocation efficiency

(A) The membrane bound (P) fraction in a ubiquitination/retrotranslocation assay was collected and washed in 6 M urea to differentiate between membrane-integrated (P) and retrotranslocated, membrane-associated Q394X (US). Quantification of the percentage of retrotranslocated, ubiquitinated Q394X is present. After centrifugation, the retrotranslocated (S), urea solubilized (US), and membrane integrated (P) populations of ubiquitinated Q394X were immunoprecipitated with an anti-HA antibody and visualized by SDS PAGE and phosphorimage analysis. N = 3 independent experiments, +/- SEM. The native molecular weight (arrow) and

high molecular weight species (asterisk) of Q394X are marked. N = 4. (B) ER-enriched microsomes were washed with 6 M urea and collected by centrifugation. As controls, samples were either diluted in buffer or incubated with the strong ionic detergent, SDS. The solubilized fractions (S) and the re-suspended pelleted fractions (P) were TCA precipitated and resolved by SDS-PAGE. Blots were incubated with antibodies against the HA tag in Q394X, the ER-localized integral membrane protein, Sec61, and the cytosolic proteins, Cdc48 and Hsp104.

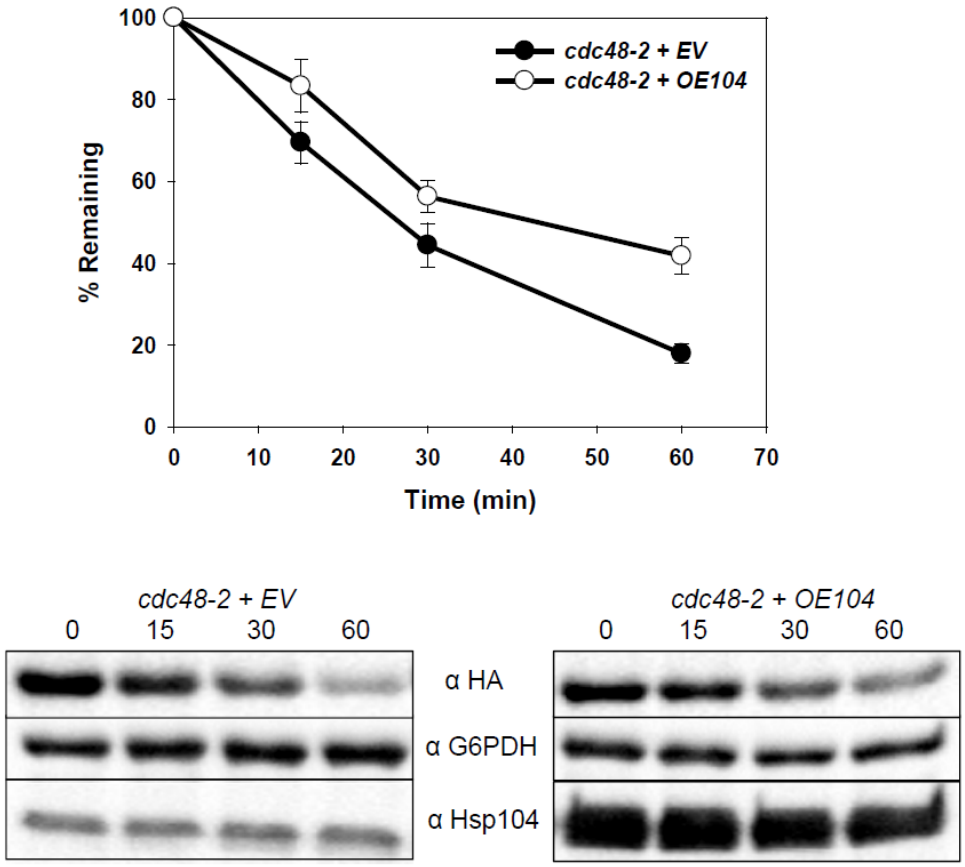

Figure 20. Degradation of Q394X in a cdc48 mutant is not rescued by over-expressing Hsp104.

Mutant *cdc48-3* yeast expressing Q394X and either a high copy number plasmid containing *HSP104* (OE104) or an empty expression vector (EV) were pre-treated at 39C for 2.5 hrs and remained at 39C for the duration of the cycloheximide chase. Lysates were blotted for Q394X levels (αHA), a loading control (αG6PDH), and Hsp104 levels (αHsp104). N = 6-7 independent experiments, +/- SEM.

the predicted amphipathic helix could instead lead to substrate recognition by ERAD targeting factors. Once an ERAD substrate is selected for degradation, various components of the cellular machinery are required to process the substrate for degradation (Chapter 1). The cell possesses a

network of factors that are important for the ubiquitination and subsequent degradation of an ERAD substrate, including molecular chaperones. Previous studies utilizing Ste6* (Q1249X) have determined many of the factors required for its degradation by ERAD (125, 296). Two factors that are important for Q1249X degradation are the cytoplasmic Hsp40, Ydj1, and Hsp70, Ssa1. Similar to Q1249X, I demonstrated a requirement for both Ydj1 and Ssa1 in the degradation of the Q1249X analogous, less soluble Chimera A mutant, Q394X. In addition to Ydj1 and Ssa1, I identified two novel cytosolic factors that are required for Q394X degradation: 1) the yeast Hsp70 Nucleotide Exchange Factor (NEF), Sse1, and 2) the yeast cytosolic disaggregase, Hsp104. This is the first example of Hsp104 being strongly linked to the degradation of an ERAD substrate. While Hsp104, Sse1, Ssa1, and Ydj1 are required for efficient Q394X degradation, I did not see a universal requirement of cytosolic chaperones for Q394X degradation. Some of these dispensable factors are known to interact with, and often act in similar folding pathways, as the chaperones discussed above (48, 310, 311). Therefore, I believe that the requirement for Hsp104, Sse1, Ssa1, and Ydj1 in Q394X degradation is specific and not due to a general stress response in the cell.

While Ssa1 and Ydj1 are required for the degradation of both Q1249X (Ste6*) and Q394X, the degradation of these substrates exhibited different Hsp104 dependencies. I observed a strong stabilization of Q394X degradation in the absence of Hsp104 function while Q1249X degradation was unaffected. There are two potential explanations for this result: 1) the two NBDs present in Q1249X are able to interact, which reduces the insolubility and aggregation propensity of the truncated NBD of Q1249X or 2) the NBDs in Q1249X may interact with the transmembrane domains (TMDs) not present in Q394X, which helps to mask the insolubility and aggregation propensity of the truncated NBD. Evidence from solved structures and ATP hydrolysis assays of

A

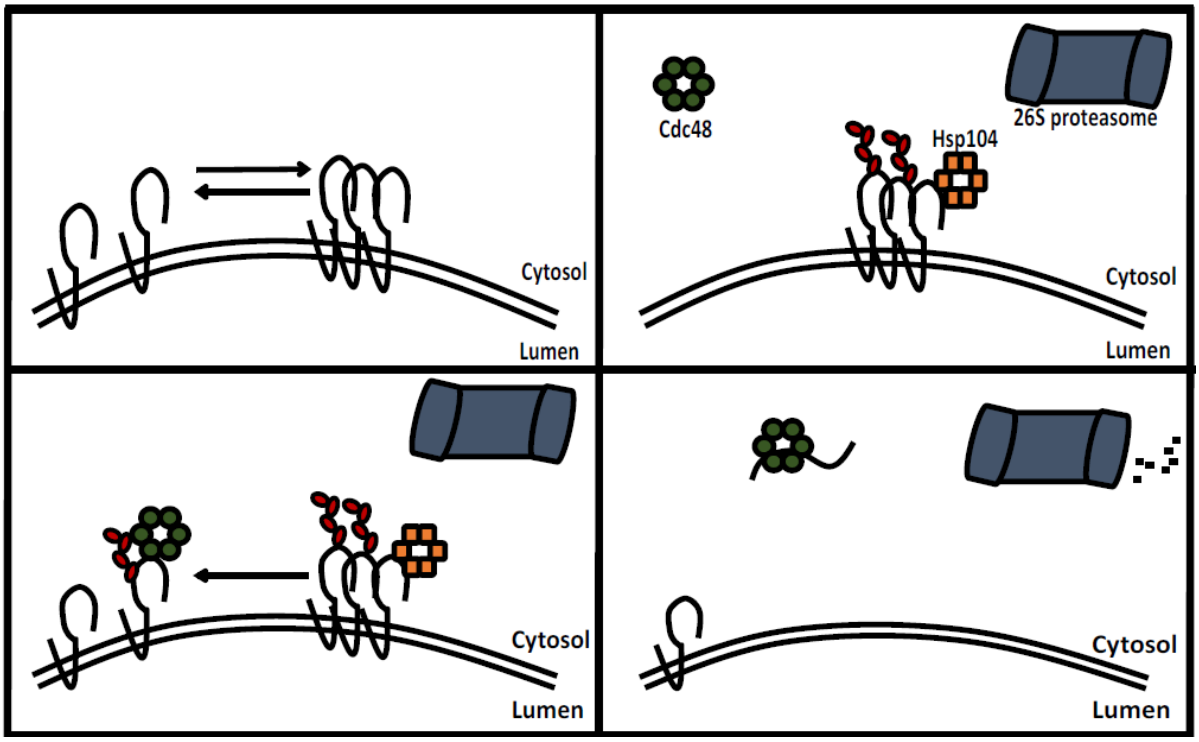
Cytosol
Lumen
Cdc48
26S proteasome
Hsp104
Cytosol
Lumen
Cytosol
Lumen
Cytosol
Lumen

B

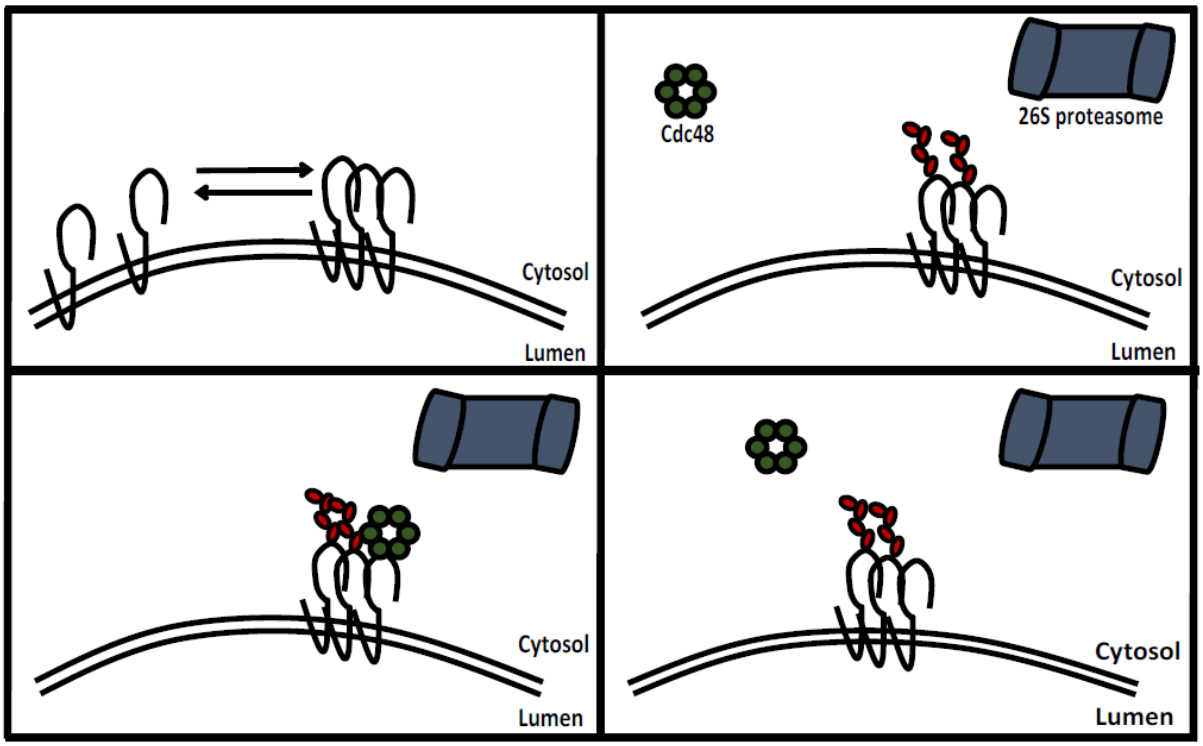
Cytosol
Lumen
Cdc48
26S proteasome
Cytosol
Lumen
Cytosol
Lumen
Cytosol
Lumen

Figure 21. Model for role of Hsp104 in the ERAD of Q394X.

In yeast, there exists two populations of Q394X in the ER-membrane: 1) aggregated and 2) non-aggregated in the ER-membrane. Cellular stress, in this case heat shock, can lead to an increase in the aggregated population of Q394X. This aggregated population of Q394X is ubiquitinated by cellular components and (A) disaggregated in the ER membrane by Hsp104. This disaggregated population is then able to be retrotranslocated by Cdc48 into the cytosol where it is degraded by the 26S proteasome. (B) However, loss of Hsp104 leads the increased presence of aggregates. These aggregates are still ubiquitinated but can no longer be retrotranslocated by Cdc48, leading to the decreased degradation of Q394X.

other ABC transporters strongly suggest that the NBDs of ABC transporters dimerize for efficient function (314, 315). Similarly, there is evidence that suggests the interactions between NBDs and TMDs are required for efficient protein folding and transport (316-318). While interactions between the NBDs and NBDs/TMDs has not been thoroughly studied in Ste6, it has been demonstrated that the ectopic expression of the two halves of Ste6 results in rescue of mating in a *ste6Δ* mutant (319). This result suggests that the two halves of Ste6 are able to associate in some way that allows for proper channel function.

There are several potential roles for how these cytosolic chaperones could facilitate the degradation of Q394X. Both Ssa1 and Ydj1 have been demonstrated to be required for the efficient ubiquitination of multiple ERAD substrates (19, 141). Similar to the Ssa1 role for ubiquitination of other ERAD substrates, I demonstrated that Ssa1 is required for efficient Q394X ubiquitination. Unlike Ssa1, it does not appear that Hsp104 is required for Q394X ubiquitination. Therefore, I

hypothesized that Hsp104 is playing a role in Q394X degradation downstream of substrate ubiquitination.

One potential post-ubiquitination step in ERAD that Hsp104 facilitate is substrate retrotranslocation. Currently, it is understood that after substrate ubiquitination, substrates are retrotranslocated from the ER into the cytosol by the AAA+ ATPase, p97/Cdc48 (57). To this end, it appears that Hsp104 localizes to puncta under heat shock only when we express Q394X. One caveat to that is a lack of co-localization of these puncta to the ER, which will need to be done in the future. Furthermore, I observed a shift of Q394X to a denser fraction in a sucrose gradient in *hsp104Δ* cells, suggesting that Q394X is aggregating in the absence of Hsp104. The ubiquitination of this population of Q394X suggests it has been selected for ERAD. The more dense population of Q394X that appears in the absence of Hsp104 co-localizes to a fraction where the ER-resident protein, Sec61, is present. Therefore, this result can be interpreted in one of three ways: 1) Hsp104 is important for the efficient retrotranslocation of Q394X from the ER to the cytosol, 2) Hsp104 acts to maintain Q394X solubility or disaggregates Q394X post-retrotranslocation, or 3) Hsp104 acts to actively retrotranslocate Q394X into the cytosol. In mammalian cells, the Bag6 complex binds retrotranslocated substrates in the cytosol to maintain their solubility prior to degradation by the 26S proteasome (112). However, in yeast, there is no Bag6 homolog, meaning that other cytosolic proteins may be performing this function in yeast. Recently, Cdc48 was identified to maintain the solubility of a retrotranslocated ERAD substrate prior to degradation (320). Based on our results, it is possible that Hsp104 is performing a similar function as Cdc48 for the Q394X protein.

By further addressing the specific role of Hsp104, I was able to show a lower amount of retrotranslocated, ubiquitinated Q394X in the *in vitro* ubiquitination assays when Hsp104 function

is lost. This effect appears to be due to a decreased efficiency of retrotranslocation and is not due to the aggregation of ubiquitinated Q394X after it has been retrotranslocated into the cytosol, as urea is not able to rescue the solubility of ubiquitinated material. Therefore, what is pelleted is still integrated in the ER membrane. Furthermore, the decreased efficiency of Q394X retrotranslocation is also not due to Hsp104 actively retrotranslocating Q394X, as over-expression of Hsp104 in a *cdc48* mutant was unable to rescue Q394X degradation. Additionally, overexpression of Hsp104 was unable to rescue the growth phenotype of the *cdc48* mutant at 39°C (data not shown). Together, these results suggest that while they are both AAA+ ATPases, Hsp104 and Cdc48 function differently in cells and Hsp104 is unable to compensate for the loss of Cdc48 function. Based on these results, I hypothesize that Hsp104 is responsible for disaggregating Q394X in the ER membrane, which allows for more efficient retrotranslocation of ubiquitinated Q394X by Cdc48.

Due to the nature of cytosolic aggregates, such as aggresomes, and the known function of Hsp104, it is reasonable to hypothesize that Hsp104 localizes to Q394X aggregates in the ER membrane. Disease-linked aggresomes contain a variety of heat shock proteins, such as Hsp70, Hsp40, Hsp90, and others (321). Because Q394X appears to remain in the ER membrane prior to Hsp104 activity, it is also possible that ER-resident proteins associate with these aggregates. Q1249X and CFTR were previously shown to reside in sub-compartments of the ER, called ER associated compartments (ERACs), where they remain prior to degradation by ERAD (322). These compartments contain wild type ER-resident proteins as well, such as Kar2, Ste14, and Sec63. However, normal trafficking of secretory proteins was not disturbed by the presence of ERACs.

In terms of the predicted model for Hsp104 activity in the degradation of ubiquitinated Q394X, I hypothesize that Hsp104 recruitment to the aggregated Q394X is not driven by interaction with ubiquitin. Instead, I hypothesize that Hsp104 recognizes the aggregated population directly and acts to hand off the disaggregated, ubiquitinated Q394X to Cdc48 for retrotranslocation. This could explain the presence of a high molecular weight species of ubiquitinated Q394X that is present in the *hsp104Δ* reactions and not the *HSP104* reactions. Moreover, this hypothesis fits with current results from our lab, showing a negative correlation between the hydrophobicity of a membrane protein and the ability of Cdc48 to retrotranslocate a membrane substrate (Guerriero et al., manuscript submitted for peer review). Also, Li and colleagues (323) recently discovered a role for Hsp104 in the disaggregation of proteins that were bound to the mitochondrial membrane after a heat shock. They determined that Hsp104 function was important to transport proteins into the mitochondria prior to degradation. Because Q394X contains a cytoplasmic degron, it is possible that Hsp104 acts similarly at the ER membrane as it does at the mitochondrial membrane, except to allow for export into the cytosol where substrates are degraded by the proteasome.

I identified only a small decrease in Q394X ubiquitination when Sse1 function was lost. However, unlike Hsp104, Sse1 does not appear to play a role in Q394X retrotranslocation. Work from Bukau and colleagues (324) has shown that partial disaggregation of luciferase by the Ssa1/Ydj1 complex occurs upon the addition of Sse1, but addition of Hsp104 and Sse1 is required for fast, optimal disaggregation. These authors also identified that the NEF activity of Sse1, and not its ATPase chaperone-like activity, is required for protein disaggregation. The specific activity of Sse1 required for Q394X degradation will be defined in the future.

In summary, by using a series of truncation mutants in a single protein, I have demonstrated that substrate selection for ERAD is positively correlated with substrate solubility. Furthermore, I have identified several cytosolic chaperones that are important for the degradation of a relatively insoluble protein. One of these chaperones, Hsp104, has never before been shown to be important for ERAD. I also provide data that Hsp104 acts to disaggregate a relatively insoluble protein, which is important for the efficient retrotranslocation of the substrate by Cdc48. In the future, it will be interesting to identify how mammalian cells deal with this insoluble protein to maintain homeostasis in the cell.

3.0 CONCLUSIONS

In this thesis, I set out to address the mechanism by which cells recognize an ERAD substrate. To do this, I utilized a novel truncation series in a domain, NBD2 of Ste6, that has previously been used to characterize the degradation of a 12 transmembrane ERAD substrate, Ste6* (125, 284, 296), as well as the cytoplasmic quality control (cytoQC) system required to degrade the cytoplasmic form of this domain, called NBD2* (285). Prior to my work, Drs. Meredith Metzger and Susan Michaelis from Johns Hopkins University School of Medicine created a series of truncations in the Ste6 NBD2 that reside both N-terminal and C-terminal to the site of truncation in Ste6* (Q1249X). Utilizing this Ste6 truncation series, they identified a subset of these truncations that were degraded as efficiently as Ste6*. However, not all of the truncations were similarly degraded. Two truncations were identified that had similar metabolic stabilities to that of the wildtype Ste6: one truncation was more N-terminal (L1240X) and one truncation was more C-terminal (R1268X) to the Q1249X truncation. Therefore, I aimed to address why the difference of only a few amino acids can cause a protein to exhibit drastically different stabilities. To determine the effects these truncations have on the NBD2 domain, I utilized a novel protein, called Chimera A. Chimera A consists of two transmembrane domains annealed to the NBD2 of Ste6. Utilizing this protein should reduce intramolecular interactions that can alter the properties that are important for substrate recognition and degradation by ERAD. Importantly, we were able to show that the analogous truncations in Chimera A appear to have similar trends in their metabolic stabilities as their Ste6 counter parts.

The observation that truncating the C-terminus of Ste6 and Chimera A is not sufficient to lead to a decrease in metabolic stability is different than what was observed for another ERAD

substrate (312). Therefore, we hypothesized that a difference in the metabolic stabilities of the C-terminal truncations is likely caused by a change in the properties of the substrates. To date, there are several models to explain which substrate properties lead to ERAD substrate selection. These models suggest different alterations to the protein: 1) the exposure of an amphipathic helix (270-272), 2) increased substrate hydrophobicity (92, 273), and 3) loss of essential post-translational modifications (274, 275).

I also set out to characterize which cellular factors are required for the degradation of a retrotranslocated, membrane spanning ERAD substrate. Utilizing the Q1249X (Ste6*) analogous truncation in Chimera A, called Q394X, I selected a series of cytoplasmic factors to begin investigating their potential roles in Q394X degradation. I first sought to show a similar dependence on cytoplasmic chaperones known to be important for Q1249X degradation. Once I was able to identify commonly required factors, I next intended to identify novel cytoplasmic chaperones required for Q394X degradation. Interestingly, I identified one novel factor, the cytoplasmic disaggregase, Hsp104. Because Hsp104 has never before been linked to ERAD, I set out to better characterize its role in the degradation of Q394X.

Previous investigations into the cellular components required for the ERAD of Ste6* have identified multiple factors (125, 296). Of these, two were of particular interest to me: 1) the cytoplasmic Hsp40 (Ydj1) and 2) the cytoplasmic Hsp70 (Ssa1). One important role for these molecular chaperones in Ste6* degradation is in substrate ubiquitination (19). The importance of cytoplasmic factors for the ubiquitination and degradation of ERAD substrates has long been established (See Chapter 1). However, there has not been a definitive requirement in ERAD for the cytoplasmic disaggregase, Hsp104. Hsp104 functions in a complex to disaggregate proteins with Ssa1, Ydj1, the yeast small heat shock proteins, Hsp26 and Hsp42, and the yeast nucleotide

exchange factor, Sse1 (48, 303, 305, 309). Based on the known cellular role for Hsp104, there could be several potential functions for Hsp104 in ERAD: 1) disaggregating the substrate in the membrane, 2) disaggregating the substrate once it is retrotranslocated into the cytoplasm, or 3) assisting Cdc48 in the retrotranslocation of Q394X.

Cdc48 is the cytoplasmic AAA+ ATPase that is responsible for retrotranslocating substrates from the ER to the cytoplasm, where they are subsequently degraded by the proteasome (57, 116). However, Cdc48 has recently been shown to play another role in ERAD. Specifically, Cdc48 is responsible for maintaining the solubility of a retrotranslocated ERAD substrate, serving as a holdase in the cytoplasm prior to degradation (320). Interestingly, Ste6* was previously shown to be completely retrotranslocated from the ER prior to degradation, likely making it a candidate to require a cytoplasmic holdase (19). To date, Cdc48 is the first holdase for retrotranslocated ERAD substrates identified in yeast. However, in mammalian cells, other complexes have been identified to serve as a holdase for retrotranslocated ERAD substrates. Most notable is the Bag6 complex, which consists of Bag6 and the components of the tail-anchored protein insertion complex, UBL4A, TRC35, and SGTA (283). In yeast, there is no homolog for the key component of this complex, Bag6. Therefore, it is possible that other factors, such as Hsp104, may also serve as holdases in the yeast cytoplasm.

In this thesis I report new discoveries about the process of ERAD and novel factors that play a role in this pathway. These findings are as follows:

3.1 TRUNCATIONS WITHIN THE NBD2 IN CHIMERA A LEAD TO HIGHLY VARIABLE EFFECTS ON PROTEIN METABOLIC STABILITY

As mentioned above, I have shown that a series of truncations in an ER-tethered form of the NBD2 behave similarly to what was observed by Drs. Meredith Metzger and Susan Michaelis for the analogous truncations in Ste6. Specifically, I determined that the Chimera A truncations separate into two groups. One group has a significantly reduced metabolic stability when compared Chimera A. The second group has a similar metabolic stability to that of Chimera A. Importantly, these differences in metabolic stability do not simply correlate with how far into the domain I truncate, as the mutant with the largest truncation I tested (L385X) was equally as stable as Chimera A. Meanwhile, the mutant with a truncation two amino acids more C-terminal (M387X) was significantly less stable. Use of a homology model suggests that the more stable truncations appear to occur at the beginning or end of a β-sheet in the NBD2 structure while those that are less stable appear to disrupt the β-sheet. Therefore, I hypothesize that disrupting this β-sheet leads to a significant change in the properties of the substrates, leading to enhanced degradation. I also demonstrated that the Chimera A truncation series is degraded via ERAD, as several of the truncations localize to the ER, require Doa10 and Hrd1 for degradation, and are significantly stabilized when the proteasome is inhibited.

To address the predicted structural changes to the NBD of Ste6/Chimera A when truncated at the different sites, I used Phyre2 to predict the resulting structures for several of the truncations. Results from these predictions did not suggest any drastic alterations to the overall predicted NBD structure when compared amongst the modelled truncations. For example, when I compared the models for the L385X vs the M387X truncations, it appears that the major change is to the predicted secondary structure of the C-terminus. In the case of L385X, Phyre2 suggests that the

C-terminus ends in an α-helix that bundles with other predicted α-helices in the protein. For M387X, Phyre2 instead predicts the C-terminus to partially interact with a core β-sheet preceded by a long unstructured region. It is possible that this change in predicted secondary structure helps components of ERAD to recognize M387X as being more misfolded. However, these are only homology models and it is possible that disrupting the C-terminus through truncation has greater effects on the NBD structure, potentially as the proteins are being synthesized and attempt to fold co-translationally. Therefore, I am unable to definitively state the exact effect these truncations have on the NBD structure that leads to selection for ERAD. It is possible that there is a level of protein unfolding that represents a threshold: Crossing over this threshold could then result in select misfolded substrates being more efficiently selected for ERAD than others.

3.2 THE METABOLIC STABILITY OF THE CHIMERA A TRUNCATION SERIES POSITIVELY CORRELATES WITH SUBSTRATE SOLUBILITY

To determine which substrate properties may be altered by these truncations, leading to increased turnover, I investigated substrate solubility. Specifically, I identified that the less stable truncations also exhibited reduced detergent solubility. I demonstrated that this reduced detergent solubility is not due to differences in substrate extraction from the membrane, as the solubility of the less stable construct, Q394X, was rescued to similar levels as those of Chimera A with the addition of urea. I hypothesize that the destabilizing truncations lead to decreased solubility, which increases their recognition and degradation by ERAD. While this hypothesis favors the model where hydrophobicity is responsible for driving substrate selection for ERAD, it is interesting to apply these findings to a model that instead suggests the exposure of an amphipathic helix leads

to substrate recognition for ERAD. In one of the findings supporting the second hypothesis, an amphipathic helix that becomes exposed in an ERAD substrate is a very hydrophobic (271). It is possible then that it is not necessarily the exposure of the secondary structure, but instead, the exposure of the hydrophobic regions within the unstable amphipathic helix that lead to increased ERAD. Importantly, investigators never studied the solubility of the unstable construct that contained an exposed amphipathic helix. Therefore, it could be that insolubility is also responsible for increased degradation of their substrate by ERAD.

3.3 HSP104 IS IMPORTANT FOR THE DISAGGREGATION OF Q394X IN THE MEMBRANE, WHICH ALLOWS FOR THE EFFICIENT RETROTRANSLOCATION AND DEGRADATION OF THE ERAD SUBSTRATE

I demonstrated a requirement for Hsp104 in Q394X degradation, as the loss of Hsp104 activity leads to increased Q394X metabolic stability. I further determined that Hsp104 acts downstream of substrate ubiquitination, unlike two other factors I identified as being important for Q394X degradation, Ssa1 and Ydj1. To define the role played by Hsp104 downstream of substrate ubiquitination, I utilized a density floatation assay to show that Q394X shifts to a denser fraction in the absence of Hsp104 function. This shift in Q394X density is interesting, as Hsp104 was shown to localize to the puncta under conditions where Hsp104 is required for Q394X degradation. This more dense population of Q394X was still ubiquitinated and co-localized with the ER, which was identified by monitoring the density at which Sec61 resides.

Based on these results, it is possible that Hsp104 helps retrotranslocate Q394X. I next demonstrated that in the absence of Hsp104 activity, Q394X is less efficiently retrotranslocated,

as the altered ratio of ubiquitinated Q394X in the soluble fraction is not caused by aggregation of Q394X after release from the membrane. However, Hsp104 does not appear to actively retrotranslocate Q394X, as over-expression of Hsp104 was unable to rescue a *cdc48* mutant. Therefore, I hypothesize that Hsp104 acts to disaggregate Q394X at the membrane, which allows for its increased efficiency of retrotranslocation by Cdc48.

3.4 THE YEAST NUCLEOTIDE EXCHANGE FACTOR, SSE1, ALSO ACTS DOWNSTREAM OF Q394X RETROTRANSLOCATION

Along with Hsp104, I found that Sse1 is important for the degradation of Q394X. However, unlike Hsp104, I demonstrated that Sse1 is not required for Q394X retrotranslocation. Since loss of Sse1 activity only mildly affects Q394X ubiquitination, I hypothesize that Sse1 instead acts downstream of substrate retrotranslocation. Previously, Sse1 was demonstrated to maximize Hsp40/Hsp70/Hsp104 disaggregation activity (324). Also, *in vitro*, Hsp110, the mammalian homolog of Sse1, acts with Hsp70 to disaggregate proteins (302). Therefore, further investigation into the role of Sse1 in the degradation of Q394X is warranted.

3.5 IMPLICATIONS OF MY WORK ON PROTEIN FOLDING AND DISEASE

Protein aggregation has long been identified as a hallmark for multiple human neurodegenerative diseases, including Parkinson's Disease, Alzheimer's Disease, and Huntingtin's Disease. For some of these disease, problematic proteins improperly fold, leading to increased intermolecular

interactions, such as amyloid formations (51). The formation of these amyloid structures results from the packing of β-sheets into highly structured, low free energy conformations (325). At the protein folding level, β-sheets require partner amino acids that reside in more distant regions of the protein. These distant interactions are believed to lead to an increase in the amount of time required to complete folding compared to α-helices (326). This propensity for β-sheet-rich proteins to form improper intermolecular interactions, along with the increased time required for folding, leads to my hypothesis that disrupting β-sheets in select chimeras leads to decreased protein stabilization.

While the exact population of aggregated proteins responsible for neurotoxicity in diseases has yet to be definitively identified, it is understood that aggregated proteins can be responsible for cell toxicity. These aggregates can sequester other proteins, and can be transmitted between cells (327-329). As a result, there is a benefit that could be gained by identifying mechanisms for clearing these problematic aggregates. While there is no current homologue of Hsp104 in mammalian cells, work from Dr. James Shorter's lab at the University of Pennsylvania has demonstrated the ability of purified Hsp104 to break-up mammalian aggregated proteins that are linked to disease (330). In fact, upon introducing a single point mutation into the regulatory M-domain of Hsp104 (A503V), Hsp104 was more efficiently able to resolve aggregates containing the neurodegenerative-linked proteins, FUSE, TDP-43, and α-synuclein. This finding suggests a potential therapeutic role for Hsp104 in multiple neurodegenerative diseases. To this end, two potential functional orthologues for Hsp104, called RuvbL1 and RuvbL2, have recently been identified (331). Further characterization of these proteins could allow for a native mammalian protein to be targeted to treat neurodegenerative diseases.

3.6 FUTURE WORK

Future work on this project can be split into two groups: 1) Short term investigations and 2) Long term investigations. I will now discuss what would be done next if I had more time to work on this project or what I would suggest for the person who takes over my project:

3.6.1 Short Term

I would first address two important points regarding the data presented here in my thesis. First, I would better attempt to link a dependence on Hsp104 for the degradation of the less soluble and less stable Chimera A truncations. While I have tried doing metabolic stability studies at multiple elevated temperatures in the *hsp104Δ* strains expressing Chimera A, Q394X, L385X, and I389X, which consist of both stable and unstable proteins, the substrates consistently seem to acquire Hsp104 dependence. This is likely because they are chimeric proteins, most of which contain altered domains. Because we only see an Hsp104 dependence for Q394X degradation at higher temperatures, this presents a problem. Hsp104 is expressed at low levels at 25°C (332). Instead, Hsp104 was shown to be upregulated after heat shock at 39°C. Therefore, minimal Hsp104 levels in wildtype cells could be why we see no effect on Q394X degradation in the *hsp104Δ* strain at 26°C. To address this, I would over-express Hsp104 in the wild type (*BY4742*) strains expressing the four substrates listed above. I would then determine if any of their metabolic stabilities are further decreased when Hsp104 is over-expressed at 25°C. I hypothesize that the metabolic stabilities of Q394X and I389X will be even further decreased when Hsp104 is over-expressed compared to Chimera A and L385X. Finally, I would demonstrate that Hsp104-GFP co-localizes to the ER through the expression of Sec63-mCherry. Cells containing an empty vector or Q394X

along with DMSO or MG132 to inhibit the proteasome would be temperature shifted. I will measure the number of cells with Hsp104-GFP puncta that co-localize to Sec63-mCherry. I hypothesize that only when we express Q394X will we see co-localization of Hsp104-GFP and Sec63-mCherry, demonstrating that Hsp104 localizes to the ER membrane under conditions where Hsp104 is required for the degradation of Q394X.

Next, I would continue to investigate the role of Sse1 in the degradation of Q394X. To start, I would utilize the floatation assay with the *SSE1* and *sse1Δ* strains the same way I did for the *HSP104* and *hsp104Δ* strains. Because I hypothesize that Sse1 acts after Q394X retrotranslocation, I anticipate that Q394X will shift to even denser fractions, most likely localizing to the cytoplasm. Next, I would utilize a series of Sse1 constructs that contain point mutations in the ATPase domains of Sse1 (333). These constructs were shown to rescue the *sse1Δ* growth defect under stress conditions. Therefore, we may be able to determine the ability of Sse1 to act as a holdase for retrotranslocated Q394X.

Another important next step would be to identify other substrates that exhibit a positive correlation between stability and solubility. I have begun to work with three synthetic constructs (αS824, β4, and β23) that were previously shown to aggregate and cause cell death at different rates when expressed in the cytoplasm (334). The next step would be to successfully clone these proteins and anneal them to tm1-2 of Chimera A to anchor them in the ER membrane. I would characterize their localization and dependence on ERAD for degradation, followed by correlating their degradation rate with their solubility. I would further determine chaperone dependence for the degradation of these transmembrane proteins, specifically focusing on correlating them with those identified to be important for the degradation of Q394X. This would allow me to begin to

potentially identify a specific group of chaperones that are required for the clearance of insoluble transmembrane proteins within cells.

In our lab, we have also begun to investigate the correlation between stability and solubility for two Cystic Fibrosis Transmembrane Conductance Regulator (CFTR) mutants that have been linked to Cystic Fibrosis (CF). These mutants consist of a point mutation in the second NBD of CFTR (N1303K) and a truncation in the second NBD of CFTR (W1282X). We currently have a set of model substrates, consisting of tm1-2 of Chimera A annealed to these mutant NBDs of CFTR, along with a construct consisting of tm1-2 annealed to the full-length NBD2 of CFTR. Preliminary stability assays have determined that the W1282X mutation significantly decreases substrate expression and substrate stability compared to the wild type CFTR NBD2 chimera. The N1303K mutation on the other hand appears to make the CFTR chimera more stable. I would further characterize the localization of these proteins, their dependence on ERAD and molecular chaperones for degradation, and determine their solubilities via the detergent solubility assay. These chimeras are of particular interest as they would help to characterize the effects these mutations have on the properties of CFTR and contribute important information to the field of CFTR research.

3.6.2 Long Term

The major project to be continued in the long term would be shifting this work into mammalian cells. I would first clone the Chimera A truncation series into a mammalian expression vector and transform them into HEK293T cells, which were previously used to identify cytoplasmic factors that associate with transmembrane ERAD substrates (112). I would then determine if stability and solubility once again positively correlate, through cycloheximide chases and detergent solubility

assays. If stability and solubility are positively correlated, I would utilize Q394X for two separate approaches. First, I would specifically investigate the role of Bag6 and the Hsp104 functional orthologues, RuvbL1 and RuvbL2 (331), for a role in Q394X stability in mammalian cells. Second, I would perform pull downs with cells expressing Q394X vs Chimera A and submit samples for mass spec analyses to determine what factors associate with Q394X. With hits from the mass spec results, I would determine potential mechanisms for their role in Q394X degradation in mammalian cells. It would be interesting to compare what I learn through both the targeted (Bag6, RuvbL1, and Ruvbl2) and non-biased (mass spec) research directions to that which I learned in yeast that is reported in this thesis. This research direction presents a potential to identify new factors in mammalian cells that are important for the processing of transmembrane ERAD substrates.

APPENDIX A

YEAST STRAINS, PLASMIDS, AND OLIGONUCLEOTIDES USED IN THIS STUDY

Table 2. Yeast Strains Used in This Study

Strain	Relevant Genotype	Reference/Source
SM2721	*MAT*a *trp1 leu2 ura3 his4 can1 ste6-Δ5(8-1290)*	(288)
BY4742	*MATα his3Δ1, leu2Δ0, lys2Δ0, ura3Δ0*	Invitrogen
pdr5Δ	*MATα his3Δ1, leu2Δ0, lys2Δ0, ura3Δ0 pdr5Δ::KAN*	Open Bio Systems
sgt2Δ	*MATα his3Δ1, leu2Δ0, lys2Δ0, ura3Δ0 sgt2::KAN*	Open Bio Systems
HSP104	*MAT*a *ura3-52 lys2-801 ade2-101 trp1-Δ63 his3-Δ200 leu2-Δ1*	(335)
hsp104Δ	*MAT*a *ura3-52 lys2-801 ade2-101 trp1-Δ63 his3-Δ200 leu2-Δ1 hsp104::LEU2*	(305)
SSA1	*MATα his3-11,15 leu2-3,112 ura3-52 trp1-Δ1 lys2 SSA1 ssa2- 1::LEU2 ssa3-1::TRP1 ssa4-1::LYS2*	(336)

ssa1-45	*MATα his3-11,15 leu2-3,112 ura3-52 trp1-Δ1 lys2 ssa1-45 ssa2-1::LEU2 ssa3-1::TRP1 ssa4-1::LYS2*	(336)
W303-1B	*MATα ade2-1 his3-11,15 leu2-3,112 ura3-1 trp1-1 can1-100*	(337)
ydj1-151	*MATα ade2-1 his3-11,15 leu2-3,112 ura3-1 trp1-1 can1-100 ydj1-2::HIS3 ydj1-151::LEU2*	(337)
sse1Δ	*MATα ade2-1 his3-11,15 leu2-3,112 ura3-1 trp1-1 can1-100 sse1::KAN*	(338)
CCT1	*MATα leu2-3,112 ura3-52 trp1-7 tcp::LEU2 (YCpMS38; TCP1::TRP1)*	(339)
cct1-2	*MATα leu2-3,112 ura3-52 trp1-7 tcp::LEU2 (YCpMS38; tcp1-2::TRP1)*	(339)
HSP26 HSP42	*MAT*a *ura3-52 leu2-3,112 his3-Δ200 trp1-Δ901 ade2-101 suc2-Δ9 GAL*	(340)
hsp26Δ hsp42Δ	*MAT*a *ura3-52 leu2-3,112 his3-Δ200 trp1-Δ901 ade2-101 suc2-Δ9 GAL hsp26::HIS3 hsp42::LEU2*	(340)
rad23Δ dsk2Δ	*MATa, his3*Δ*1, leu2*Δ*0, ura3*Δ*0, rad23*Δ*::KanMX, dsk2*Δ*::KanMX*	(125)
HSP104-GFP	MATa, *pdr5Δ::kanMX4 can1Δ::STE2pr-Sp_his5, lyp1Δ, ura3Δ0, met15Δ0, HSP104-GFP-LEU2*	Nystrom lab

Table 3. Yeast Plasmids and primers used in this study

Name	Relevant Genotype/Sequence	Reference
Plasmid		
pSM694	*2μ LEU2 STE6::HA*	(288)
pSM1175	*2μ LEU2 ste6-L1240X::HA*	This study
pSM1176	*2μ LEU2 ste6-M1242X::HA*	This study
pSM1177	*2μ LEU2 ste6-I1244X::HA*	This study
pSM1178	*2μ LEU2 ste6-H1246X::HA*	This study
pSM1179	*2μ LEU2 ste6-M1251X::HA*	This study
pSM1180	*2μ LEU2 ste6-S1256X::HA*	This study
pSM1264	*2μ LEU2 ste6-R1268X::HA*	This study
pSM1400	*2μ LEU2 ste6-K1261X::HA*	This study
pSM2319	*2μ LEU2 ste6-Q1249X::HA*	This study
pCG19	*2μ URA3 Chimera A::HA*	This study
pCG12	*2μ URA3 chimera A-Q394X::HA*	This study
pKN31	*2μ HIS3 Pcup1-mycUb-Tcyc1*	(19)
pMP01	*2μ URA3 chimera A-L385X::HA*	This study
pMP02	*2μ URA3 chimera A-M387X::HA*	This study
pMP03	*2μ URA3 chimera A-I389X::HA*	This study
pMP04	*2μ URA3 chimera A-H391X::HA*	This study
pMP05	*2μ URA3 chimera A-M396X::HA*	This study
pMP06	*2μ URA3 chimera A-S401X::HA*	This study
pMP07	*2μ URA3 chimera A-K406X::HA*	This study
pMP08	*2μ URA3 chimera A-R413X::HA*	This study
pMP09	*2μ LEU2 HSP104*	This study
pMP10	*2μ LEU2 P-GPD HSP104*	This study
Primers		
oMP01	*5'*-GCGCCCGGGATGAACTTTTTAAGTTTTAAGAC-*3'*	This study
oMP02	*5'*-CGCCCGCGGTTATAGAGCAGGTGGACCTTTTTTGACC-*3'*	This study

oMP03	*5'*-CGCCCGCGGTTATGTTAGTAGAGCAGGTGGACC-*3'*	This study
oMP04	*5'*-CGCCCGCGGTTAAACCATTGTTAGTAGAGCAGGTGGACC-*3'*	This study
oMP05	*5'*-CGCCCGCGGTTACGTTATAACCATTGTTAGTAGAGCAGG-*3'*	This study
oMP06	*5'*-CGCCCGCGGTTACATTTGTTCACTATGCGTTATAACC-*3'*	This study
oMP07	*5'*-CGCCCGCGGTTAGTTACAAGACCTCATCATTTGTTCAC-*3'*	This study
oMP08	*5'*-CGCCCGCGGTTAAAGAACTGCAATCGAGTTACAAGACC-*3'*	This study
oMP09	*5'*-CGCCCGCGGTTACTCAACCACTTTACCATCTTTAAG-*3'*	This study
oMP10	5'GAAGTAATTATCTACTTTTTACAACA	This study
oMP11	5'CGCGGATCCATGAACGACCAAA-3'	This study
oMP12	5'CGCCTGCAGTTAATCTAGGTCATCATCAATTTCC-3'	This study

APPENDIX B

INTERACTIONS BETWEEN INTERSUBUNIT TRANSMEMBRANE DOMAINS REGULATE THE CHAPERONE DEPENDENT DEGRADATION OF AN OLIGOMERIC MEMBRANE PROTEIN (341)

B.1 INTRODUCTION

In eukaryotic cells, approximately one-third of all proteins enter the secretory pathway at the Endoplasmic Reticulum (ER). Once in the ER, proteins may fold into their native states, and if successful continue along the secretory pathway. However, upon cellular stress or mutations within the protein sequence, these secretory pathway substrates are instead degraded by a process called Endoplasmic Reticulum-Associated Degradation (ERAD). ERAD is an important area of research for several reasons, including the connection between substrate clearance/aggregation and human disease (269).

One such ERAD substrate that is linked to human disease is the epithelial sodium channel, ENaC. ENaC is a heterotrimeric membrane protein consisting of an alpha, beta, and gamma subunit that are assembled in the ER and function at the plasma membrane in the kidney to transport sodium (342). Altered function of the ENaC channel can lead to several diseases, including Liddle's syndrome and pseudohypoaldosteronism type I (343, 344). It was shown previously that ERAD of the non-glycosylated population of the alpha subunit of ENaC requires the function of the ER-luminal Hsp70 cochaperone, called Lhs1 in yeast and GRP170 in

mammalian cells (345). However, the role of Lhs1 in the degradation of αENaC, along with the mechanism of recognition of αENaC by Lhs1, had not yet been identified. To address these questions, I collaborated with Dr. Teresa Buck in the Brodsky lab to test the hypothesis that non-glycosylated αENaC is recognized by Lhs1 due to decreased solubility and that Lhs1 subsequently plays a role in non-glycosylated αENaC retrotranslocation prior to degradation.

B.2 MATERIALS AND METHODS

B.2.1 Detergent Solubility Assay

BY4742 and *lhs1Δ* strains constitutively expressing αENAC or the mutant αENaC containing no glycosylation sites, called ΔG αENAC, were grown to a final OD_{600} of 1.5 in 4 liters of culture. Cultures were shifted to 37°C for 1 hr, shaking at ~160 rpm in a water bath. Cells were harvested by centrifugation for 5 min at 5000 rpm and 4°C in a Piramoon F7S-4x1000Y rotor. Once harvested, ER-enriched microsomes were isolated using a previously described large scale technique (294). The microsomes were incubated with Buffer 88 (20 mM HEPES–NaOH, pH 6.8, 150 mM potassium acetate, 5 mM magnesium acetate, 250 mM sorbitol), and the indicated concentration of the non-ionic detergent, n-Dodecyl β-D-maltoside. Each sample contained a final concentration of roughly 0.5 mg/mL of protein. For controls, one sample was resuspended in Buffer 88 alone to monitor for microsome integrity and to monitor aggregation, and one sample was treated with the ionic detergent, sodium dodecyl sulfate (SDS). After the addition of microsomes, the samples were incubated at room temperature (~21.5°C) for 30 min. The samples were then centrifuged for 10 min at 18,000 *x g* and 4°C in a Beckman Coulter Microfuge 22R

Centrifuge. The supernatant was removed and dispensed into a new 1.5 mL Eppendorf tube, which contained 1:4 volume of 5x SDS sample buffer (0.325 M Tris pH 6.8, 10% SDS, 5% β-mercaptoethanol, and 0.25 mg/mL Bromophenol Blue), and the pellet was resuspended in an equal volume of 1 x SDS sample buffer by pipetting. All samples were incubated at 37°C for 30 min and centrifuged for 1 min at 15,000 rpm at room temperature in an Eppendorf centrifuge 5424 microcentrifuge. Proteins were separated on denaturing 10% polyacrylamide gels and transferred to nitrocellulose using the semi-dry Bio-Rad Trans Blot Turbo. Blots were blocked in a TBST plus 5% milk solution for 30 min at room temperature on a rocker. The blots were incubated for 1.5 hrs at room temperature in a primary antibody solution against the HA tag found in both αENaC and ΔG αENaC (Roche Anti-HA-Peroxidase High Affinity (3F10), Rat, 1:5000). The nitrocellulose blots were washed 3 times for 5 min in TBST at room temperature on a rocker. Bound antibodies were visualized after incubation in the SuperSignal Chemiluminescence (Thermo Scientific) reagent for 5 min at room temperature on a rocker, and imaged on a Bio-Rad Universal Hood II. Nitrocellulose blots were stripped using 0.1 M glycine, pH 2.2 for 30 minutes, blocked in TBST plus milk as above, and then incubated in a rabbit primary antibody against the ER integral membrane protein, Sec61 (1:5000), for 1.5 hrs at room temperature. This served as a control for microsome solubilization and protein extraction. Nitrocellulose blots were again washed 3 times for 5 min in TBST at room temperature and incubated 1.5 hrs in a donkey anti-rabbit secondary antibody conjugated to HRP (1:5000, Cell Signaling Technology). Nitrocellulose blots were washed 3 times for 5 min in TBST and bound antibodies were again visualized using SuperSignal Chemiluminescence. Quantification was done using the ImageJ program.

B.2.2 In vitro Ubiquitination and Retrotranslocation Assay

In vitro ubiquitination reactions were set-up to quantify the level of ubiquitination of ΔG αENAC in *BY4742* vs *lhs1Δ*. Yeast purified cytosol was harvested according to a previously published technique (294) from *BY4742* cells lacking any expression vectors and that were treated at 39°C for 2 hours, but with one small modification. Instead of breaking cells with a blender, cells were lysed using a cold mortar and pestle for 1 min, followed by the addition of liquid nitrogen. A total of 6 rounds of grinding for 1 min each round was done to sufficiently break the cells. *In vitro* reactions consisted of ER-enriched microsomes purified from either *BY4742* or *lhs1Δ* strains expressing ΔG αENAC, yeast purified cytosol, and the appropriate amount of a 10x ATP regenerating system (10mM ATP, 400 M creatine phosphate, 2 mg/mL creatine phosphokinase in Buffer 88). A negative control was set up as well for both the *BY4742* and the *lhs1Δ* reactions, utilizing apyrase (0.02 units/reaction) instead of the ATP regenerating system. Reactions contained final concentrations of 1 mg/mL microsomes, 1mg/mL cytosol (ΔG αENaC ubiqutination assays) or 5mg/mL (αENaC and ΔG αENaC retrotranslocation assays), the ATP regeneration system or apyrase, and Buffer 88. These *in vitro* reactions were then pre-incubated at room temperature for 10 min. After the incubation at room temperature, ^{125}I-ubiquitin was added to each reaction to a final concentration of 1.5 mg/mL. Samples were then incubated at 37°C for 45 min. For the retrotranslocation assays, samples were centrifuged at 18,000 *x g* for 10 min at 4°C. Supernatants were removed and put in a fresh 1.5mL epindorf followed by resuspension of the pellets in an equal volume of Buffer 88. For both assays, 125 µL of a 1.25% SDS stop solution (50 mM Tris–Cl, pH 7.4, 150 mM NaCl, 5 mM EDTA, 1.25% SDS, 1 mM PMSF, 1 µg/mL leupeptin, 0.5 µg/mL pepstatin A, and 10 mM N-ethylmaleimide (NEM)) was added to the reactions and incubated at 37°C for 30 min. A total of 400 µL of a Triton solution (50 mM Tris–Cl, pH 7.4, 150 mM NaCl,

5 mM EDTA, 2% Triton X-100, 1 mM PMSF, 1 µg/mL leupeptin, 0.5 µg/mL pepstatin A, and 10 mM NEM.), 30 µL of a 50/50 protein A-sepharose slurry, and 2.5 µL of anti-HA (Roche, mouse) antibody were added to each reaction. The HA-tagged protein was then immunoprecipitated overnight at 4°C on a rotator. After centrifugation, the beads were washed 3 times in an IP wash buffer (50 mM Tris–Cl, pH 7.4, 150 mM NaCl, 5 mM EDTA, 1% Triton X-100, 0.2% SDS, 10 mM NEM). After all wash fluid was removed from the beads, 40 µL of TCA sample buffer (80 mM Tris–Cl, pH 8.0, 8 mM EDTA, 0.25 M DTT, 3.5% SDS, 15% glycerol, 0.08% Tris-base, 0.01% bromophenol blue) was added and the samples were agitated on a Vortex and incubated at 37°C for 30 min. Proteins were then resolved on duplicate denaturing 10% polyacrylamide gels. One gel was used to determine IP efficiency, and was processed for a Western blot as explained above. The second duplicated gel was washed in ddH_2O for 5 min, placed on filter paper, and dried using a Fisher Scientific Gel Dryer for 1.5 hrs. Dried gels were then exposed to phosphorfilm for 2-3 days. The phosphorfilm was scanned using a Typhoon FLA 7000.

B.3 RESULTS

B.3.1 The Lhs1-dependent non-glycosylated population of αENaC is less soluble than the glycosylated population of αENaC, independent of Lhs1 function

Previous work from Buck et al. (345) first identified Lhs1 as an important factor in the ERAD of αENaC, but the role and mechanism of substrate recognition by Lhs1 was not addressed. To address why Lhs1 selectively recognizes the non-glycosylated population of αENaC, I utilized a detergent solubility assay to determine the relative solubility of the glycosylated and

unglycosylated populations of αENaC in the *lhs1Δ* strain. ER-enriched microsomes containing αENaC were purified from *lhs1Δ* yeast and treated with varying levels of DDM. As shown in the figure, below (part A), the glycosylated population appears to be more soluble when compared to the non-glycosylated population of αENaC across all DDM concentrations. Importantly, there is no difference between the two populations of αENaC when we treat microsomes in the absence of detergent (the material remained in the pellet fraction) or when we use the ionic detergent, SDS, which liberated nearly all of the protein. These results suggest that the two populations of αENaC are still in the membrane after microsome purification and are both able to be solubilized by a strong detergent.

To address whether Lhs1 activity alters the solubility of the non-glycosylated population of αENaC, I purified ER-enriched microsomes from both a wildtype strain (*BY4742*) and an *lhs1Δ* strain expressing ΔG αENaC. These microsomes were once again treated with DDM and their relative solubilities were determined by western blot. Regardless of whether Lhs1 is present in cells, ΔG αENaC is equally soluble at the various DDM concentrations (part B). In contrast, as above, ΔG αENaC was insoluble and remained in the pellet fraction when detergent was absent and was readily solubilized by SDS. These results suggest that while the non-glycosylated population of αENaC is less soluble than the glycosylated population, Lhs1 has no effect on maintaining substrate solubility.

B.3.2 Deletion of LHS1 leads to increased ubiquitination of non-glycosylated αENaC but decreased retrotranslocation of ubiquitinated αENaC

Because Lhs1 is required for non-glycosylated αENaC degradation, we wanted to address what role Lhs1 plays in the ubiquitination of αENaC. Therefore, to enhance the signal corresponding

to ubiquitinated protein, I used the ΔG αENaC construct. I then used an established ubiquitination assay from the lab to determine what role Lhs1 plays in the ubiquitination of αENaC (294). In this assay, we incubate ER-enriched microsomes containing our substrate with purified yeast cytosol and radioactively labeled ubiquitin. With the addition of ATP, our substrate is ubiquitinated and retrotranslocated, which we can monitor through the radioactivity. Surprisingly, unlike other Hsp70 cochaperones, such as the cytoplasmic Hsp40, Ydj1 (19, 141), Lhs1 deletion did not decrease ΔG αENaC ubiquitination (part C). Instead, there appears to be a 3-4 fold increase in ΔG αENaC ubiquitination when using membranes prepared from the *lhs1Δ* strain compared to membranes from the wildtype (*BY4742*) strain.

Since Lhs1 appears to play a role in the ubiquitination of non-glycosylated αENaC, I also investigated the role of Lhs1 during αENaC and ΔG αENaC retrotranslocation, which is downstream of ubiquitination in the process of protein degradation from the ER. By exposing our SDS-PAGE separated samples to phosphorfilm, we can determine the percentage of ubiquitinated material that is retrotranslocated. After quantifying the amount of ubiquitinated protein in the supernatant, I found that the level of ubiquitinated αENaC and ΔG αENaC that is extracted out of the ER-enriched microsomes is roughly half as much in the *lhs1Δ* reactions compared to the wildtype (*BY4742*) reactions (part D). This result suggests that Lhs1 plays an important role in the efficient retrotranslocation of αENaC prior to degradation.

A

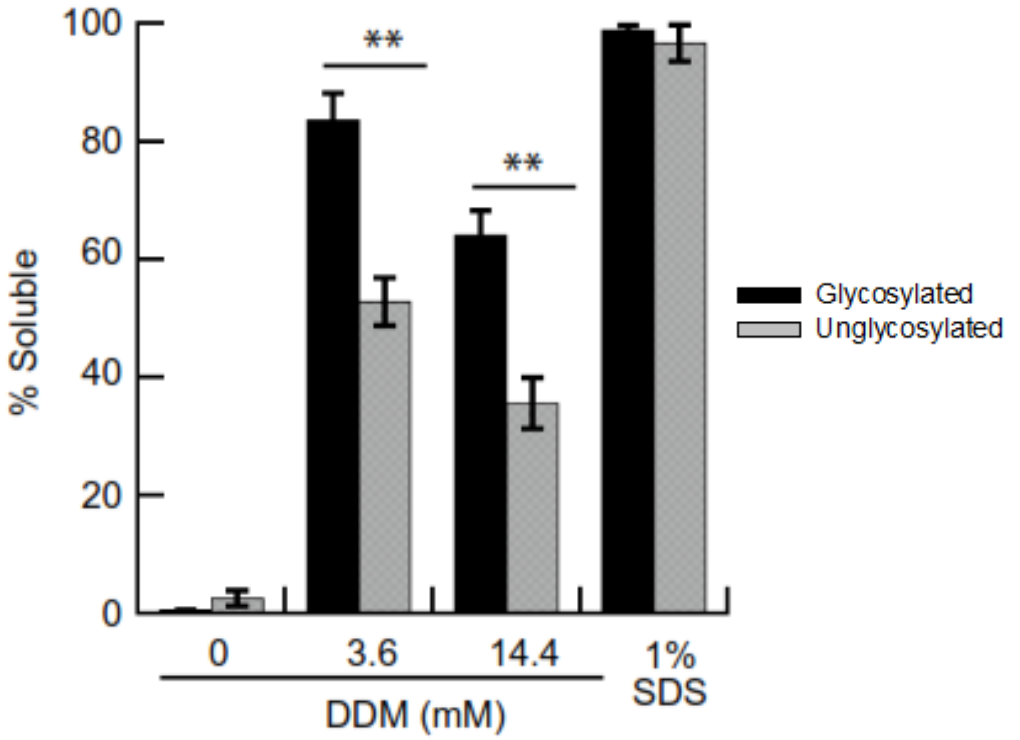
100
80
60
40
20
0
% Soluble
**
**
Glycosylated
Unglycosylated
0
3.6
14.4
1%
SDS
DDM (mM)

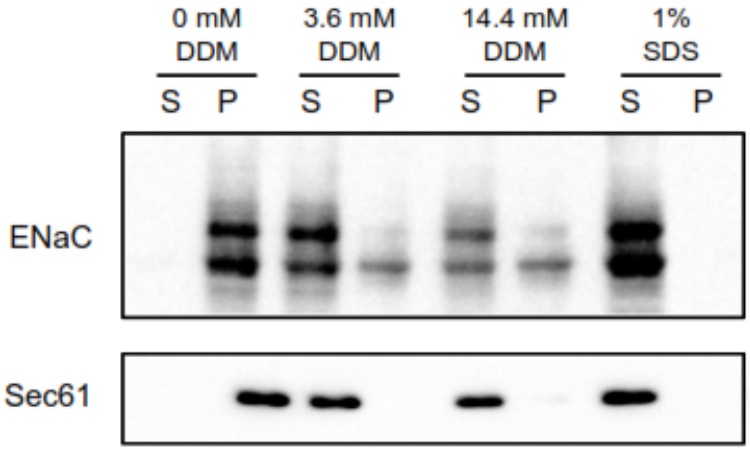
0 mM DDM
3.6 mM DDM
14.4 mM DDM
1% SDS
S P S P S P S P
ENaC
Sec61

B

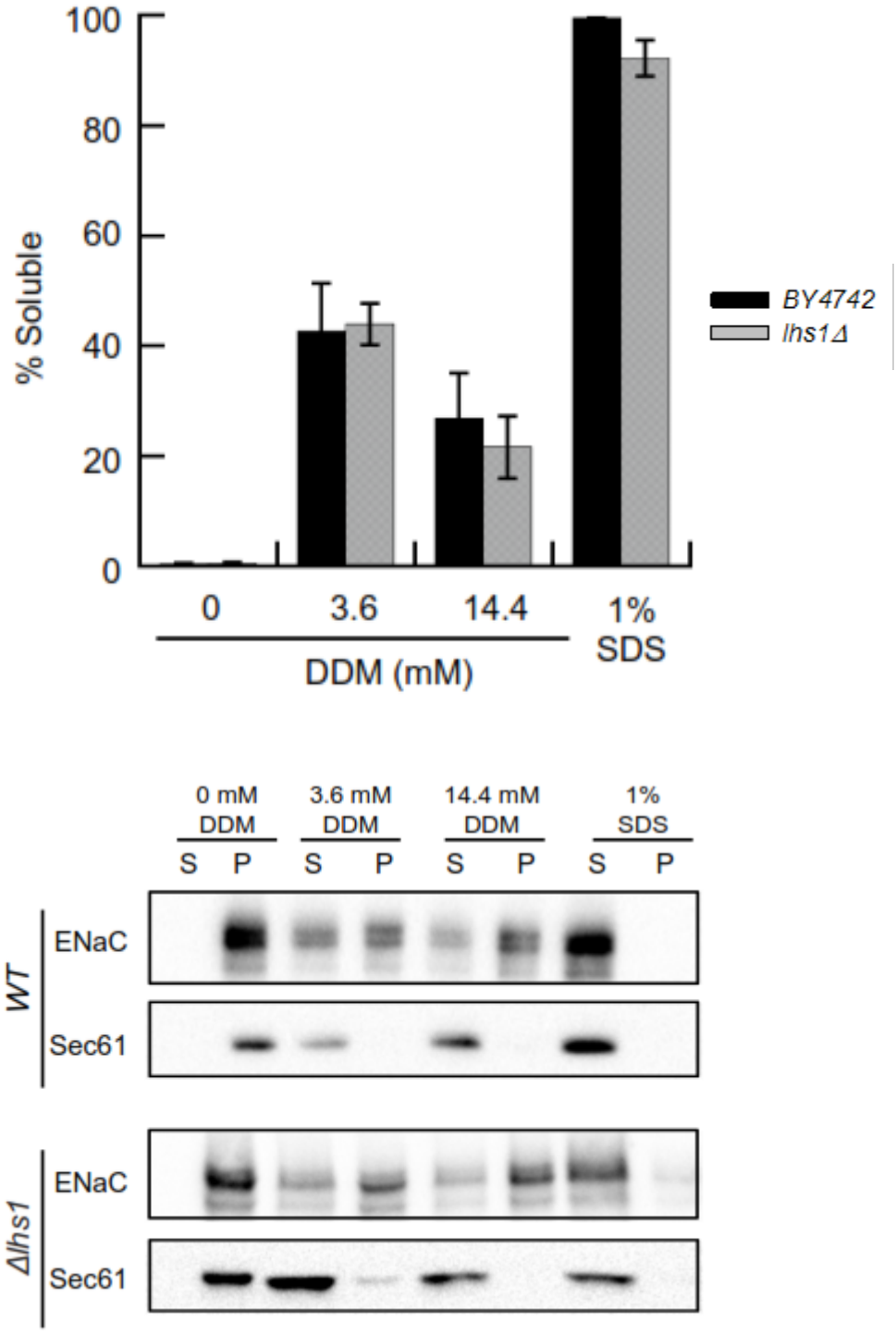
100
80
60
40
20
0
% Soluble
BY4742
lhs1Δ
0
3.6
14.4
1%
SDS
DDM (mM)
0 mM DDM
3.6 mM DDM
14.4 mM DDM
1% SDS
S P S P S P S P
WT
ENaC
Sec61
Δlhs1
ENaC
Sec61

C

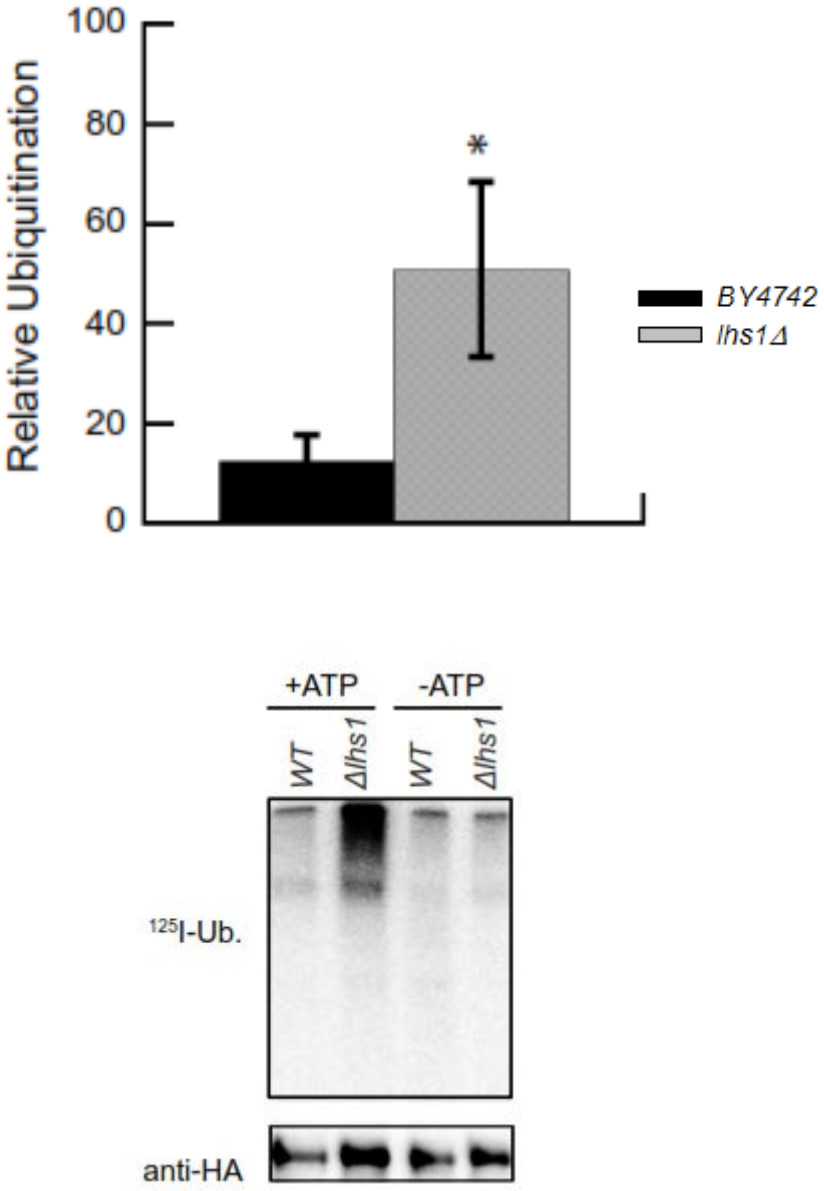
Relative Ubiquitination
100
80
60
40
20
0
*
BY4742
lhs1Δ
+ATP
-ATP
WT
Δlhs1
WT
Δlhs1
125I-Ub.
anti-HA

D

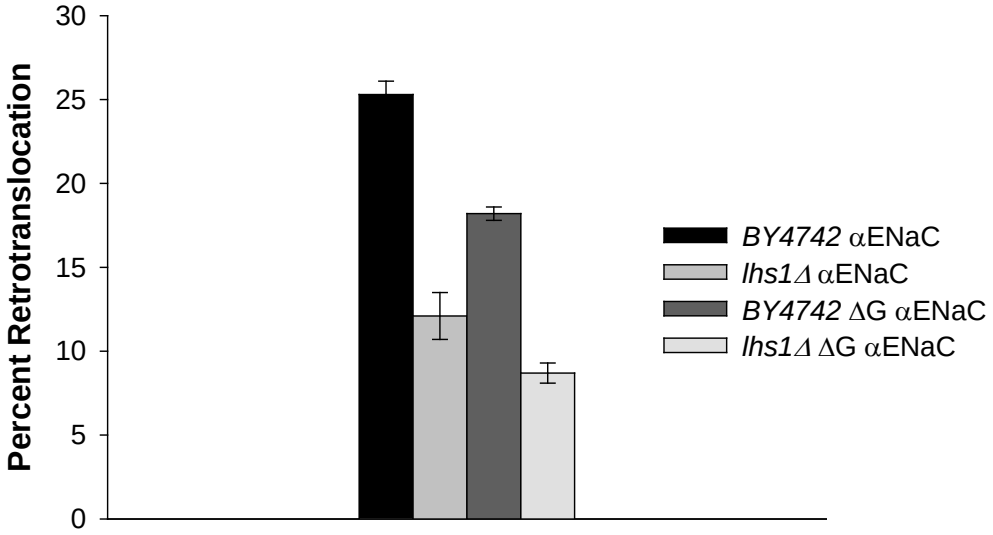
Percent Retrotranslocation
30
25
20
15
10
5
0
BY4742 αENaC
lhs1Δ αENaC
BY4742 ΔG αENaC
lhs1Δ ΔG αENaC

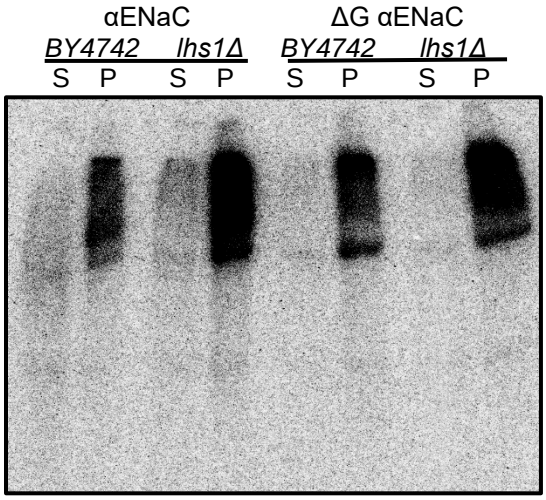
αENaC
ΔG αENaC
BY4742
lhs1Δ
BY4742
lhs1Δ
S P S P S P S P

Figure 22. Lhs1 recognizes a relatively insoluble population of αENaC and is required for the efficient retrotranslocation of αENaC.

(A) ER-enriched microsomes purified from the *lhs1Δ* yeast strain expressing the HA-tagged αENaC were treated with the non-ionic detergent, n-Dodecyl-β-D-maltoside (DDM). As controls, microsomes were incubated in buffer or in the presence of the strong ionic detergent, sodium dodecyl sulfate (SDS). Samples were centrifuged at 18,000 *x g* and 4°C for 10 min. Fractions were split and proteins were separated on polyacrylamide gels. αENaC was visualized using antisera against HA (ENaC) and Sec61, an ER-resident protein which served as a control for microsome solubilization. The data are representative of N = 4 +/-SEM, *p<0.01. (B) *lhs1Δ*-derived ER-enriched microsomes containing HA-tagged ΔG αENaC were treated similarly as in (A). The data are representative of N = 4 +/-SEM. (C) *In* vitro ^{125}I-ubiquitination assays were performed as described in Materials and Methods with ER-enriched microsomes containing ΔG αENaC purified from either wildtype (*BY4742*) or mutant (*lhs1Δ*) strains. Ubiquitinated ΔG αENaC was immunoprecipitated with anti-HA antisera and resolved on polyacrylamide gels. Data represent N = 6-9 experiments +/-SEM, *p<0.05. (D) *In vitro* ^{125}I-ubiquitination and retrotranslocation assays were completed as described in Materials and Methods using ER-enriched microsomes from wildtype (*BY4742*) and *lhs1Δ* strains containing either αENaC or ΔG αENaC. Data represent N = 2 +/- the range in the data.

B.4 DISCUSSION

During the ERAD of a misfolded substrate, a complex assembly of cellular machinery is responsible for recognition, ubiquitination, retrotranslocation, and the subsequent degradation of

the substrate. Many of these components have been investigated and their roles have been identified (for review, see Chapter 1). However, the list of factors that play a role in ERAD continues to expand. This expanding list could potentially be due to the large number of diverse substrates that undergo ERAD. For example, Lhs1, an ER luminal nucleotide exchange factor (NEF) for the ER luminal Hsp70, Kar2, is one such factor recently discovered to play a role in the degradation of the alpha subunit of the heterotrimeric protein, ENaC (345). Prior to this study, little was known about why αENaC is recognized by Lhs1 and what role Lhs1 plays in the degradation of αENaC. In order to address these questions, I worked with several members of the Brodsky lab.

The first question, why does Lhs1 recognize αENaC as a misfolded substrate, is an important question because much less is known about what characteristics lead to the selection of a protein for ERAD. Other labs have suggested that recognition of an ERAD substrate is due to the exposure of internal secondary protein structure (270-272), hydrophobicity (92, 273), or loss of post-translational modifications (274, 275). In order to test which characteristics of αENaC lead to the selection by Lhs1 for ERAD, I utilized a detergent solubility assay I developed in the lab. Interestingly, the non-glycosylated population of αENaC is roughly 50% less soluble than the glycosylated population (part A). Unexpectedly, the solubility of the non-glycosylated population of αENaC was not affected by Lhs1 (part B). This result was surprising as some ER luminal chaperones, such as Kar2, help maintain the solubility of ERAD substrates prior to degradation (346, 347). Similar functions in maintaining substrate solubility have been observed for the Kar2 mammalian homologue, BiP, as well, during ERAD (348).

Since Lhs1 does not appear to be important for maintaining the solubility of non-glycosylated αENaC, I investigated a potential role for Lhs1 in αENaC ubiquitination and retrotranslocation.

It is known that other Hsp70s and their cochaperones, such as the cytosolic Ssa1 and Ydj1, are required for integral membrane ERAD substrate ubiquitination (19, 141). However, in *in vitro* ubiquitination assays, the absence of Lhs1 led to a 3-4 fold increase in ΔG αENaC ubiquitination (part C). Instead, it appears that Lhs1 plays an important role in the efficient retrotranslocation of αENaC. In the absence of Lhs1, both ubiquitinated αENaC and ΔG αENaC were less efficiently retrotranslocated than in reactions using membranes from wildtype cells (part D). The mammalian homologue for Lhs1, GRP170, was also identified to be important for the retrotranslocation of ERAD substrate (349). However, one important difference between Lhs1 and GRP170 during ERAD is the lack of dependence on its nucleotide exchange factor activity for the degradation of αENaC (345, 349). Therefore, it will be important to identify the exact role of Lhs1 in the retrotranslocation of αENaC in the future.

BIBLIOGRAPHY

1. Vembar SS, Brodsky JL. One step at a time: endoplasmic reticulum-associated degradation. Nat Rev Mol Cell Biol. 2008;9(12):944-57.

2. Hershko A, Heller H, Elias S, Ciechanover A. Components of ubiquitin-protein ligase system. Resolution, affinity purification, and role in protein breakdown. J Biol Chem. 1983;258(13):8206-14.

3. Pickart CM. Mechanisms underlying ubiquitination. Annu Rev Biochem. 2001;70(1):503-33.

4. Varshavsky A. The ubiquitin system, an immense realm. Annu Rev Biochem. 2012;81:167-76.

5. Lee W-C, Lee M, Jung JW, Kim KP, Kim D. SCUD: Saccharomyces cerevisiae ubiquitination database. BMC Genomics. 2008;9(1):440.

6. van Wijk SJ, de Vries SJ, Kemmeren P, Huang A, Boelens R, Bonvin AM, et al. A comprehensive framework of E2–RING E3 interactions of the human ubiquitin–proteasome system. Mol Syst Biol. 2009;5(1):295.

7. Li W, Bengtson MH, Ulbrich A, Matsuda A, Reddy VA, Orth A, et al. Genome-wide and functional annotation of human E3 ubiquitin ligases identifies MULAN, a mitochondrial E3 that regulates the organelle's dynamics and signaling. PLoS One. 2008;3(1):e1487.

8. Huibregtse JM, Scheffner M, Beaudenon S, Howley PM. A family of proteins structurally and functionally related to the E6-AP ubiquitin-protein ligase. Proc Natl Acad Sci U S A. 1995;92(7):2563-7.

9. Scheffner M, Nuber U, Huibregtse JM. Protein ubiquitination involving an E1–E2–E3 enzyme ubiquitin thioester cascade. Nature. 1995;373(6509):81-3.

10. Cyr DM, Höhfeld J, Patterson C. Protein quality control: U-box-containing E3 ubiquitin ligases join the fold. Trends Biochem Sci. 2002;27(7):368-75.

11. Borden KL. RING domains: master builders of molecular scaffolds? J Mol Biol. 2000;295(5):1103-12.

12. Deshaies RJ, Joazeiro CA. RING domain E3 ubiquitin ligases. Biochemistry. 2009;78(1):399.

13. Chau V, Tobias J, Bachmair A, Marriott D, Ecker D, Gonda D, et al. A multiubiquitin chain is confined to specific lysine in a targeted short-lived protein. Science. 1989;243(1):576-83.

14. Pickart CM. Ubiquitin in chains. Trends Biochem Sci. 2000;25(11):544-8.

15. Komander D, Rape M. The ubiquitin code. Annu Rev Biochem. 2012;81:203-29.

16. Xu P, Duong DM, Seyfried NT, Cheng D, Xie Y, Robert J, et al. Quantitative proteomics reveals the function of unconventional ubiquitin chains in proteasomal degradation. Cell. 2009;137(1):133-45.

17. Koegl M, Hoppe T, Schlenker S, Ulrich HD, Mayer TU, Jentsch S. A novel ubiquitination factor, E4, is involved in multiubiquitin chain assembly. Cell. 1999;96(5):635-44.

18. Jarosch E, Taxis C, Volkwein C, Bordallo J, Finley D, Wolf DH, et al. Protein dislocation from the ER requires polyubiquitination and the AAA-ATPase Cdc48. Nat Cell Biol. 2002;4(2):134-9.

19. Nakatsukasa K, Huyer G, Michaelis S, Brodsky JL. Dissecting the ER-associated degradation of a misfolded polytopic membrane protein. Cell. 2008;132(1):101-12.

20. Richly H, Rape M, Braun S, Rumpf S, Hoege C, Jentsch S. A series of ubiquitin binding factors connects CDC48/p97 to substrate multiubiquitylation and proteasomal targeting. Cell. 2005;120(1):73-84.

21. Schuberth C, Buchberger A. Membrane-bound Ubx2 recruits Cdc48 to ubiquitin ligases and their substrates to ensure efficient ER-associated protein degradation. Nat Cell Biol. 2005;7(10):999-1006.

22. Neuber O, Jarosch E, Volkwein C, Walter J, Sommer T. Ubx2 links the Cdc48 complex to ER-associated protein degradation. Nat Cell Biol. 2005;7(10):993-8.

23. Ye Y, Meyer HH, Rapoport TA. Function of the p97-Ufd1-Npl4 complex in retrotranslocation from the ER to the cytosol: dual recognition of nonubiquitinated polypeptide segments and polyubiquitin chains. J Cell Biol. 2003;162(1):71-84.

24. Medicherla B, Kostova Z, Schaefer A, Wolf DH. A genomic screen identifies Dsk2p and Rad23p as essential components of ER-associated degradation. EMBO rep. 2004;5(7):692-7.

25. Elsasser S, Gali RR, Schwickart M, Larsen CN, Leggett DS, Müller B, et al. Proteasome subunit Rpn1 binds ubiquitin-like protein domains. Nat Cell Biol. 2002;4(9):725-30.

26. Elsasser S, Chandler-Militello D, Müller B, Hanna J, Finley D. Rad23 and Rpn10 serve as alternative ubiquitin receptors for the proteasome. J Biol Chem. 2004;279(26):26817-22.

27. Borodovsky A, Kessler BM, Casagrande R, Overkleeft HS, Wilkinson KD, Ploegh HL. A novel active site-directed probe specific for deubiquitylating enzymes reveals proteasome association of USP14. EMBO J. 2001;20(18):5187-96.

28. Yao T, Cohen RE. A cryptic protease couples deubiquitination and degradation by the proteasome. Nature. 2002;419(6905):403-7.

29. Verma R, Aravind L, Oania R, McDonald WH, Yates JR, Koonin EV, et al. Role of Rpn11 metalloprotease in deubiquitination and degradation by the 26S proteasome. Science. 2002;298(5593):611-5.

30. Leggett DS, Hanna J, Borodovsky A, Crosas B, Schmidt M, Baker RT, et al. Multiple associated proteins regulate proteasome structure and function. Mol Cell. 2002;10(3):495-507.

31. Guterman A, Glickman MH. Complementary roles for Rpn11 and Ubp6 in deubiquitination and proteolysis by the proteasome. J Biol Chem. 2004;279(3):1729-38.

32. Rubin DM, Glickman MH, Larsen CN, Dhruvakumar S, Finley D. Active site mutants in the six regulatory particle ATPases reveal multiple roles for ATP in the proteasome. EMBO J. 1998;17(17):4909-19.

33. Smith DM, Kafri G, Cheng Y, Ng D, Walz T, Goldberg AL. ATP binding to PAN or the 26S ATPases causes association with the 20S proteasome, gate opening, and translocation of unfolded proteins. Mol Cell. 2005;20(5):687-98.

34. Anfinsen CB, Haber E, Sela M, White FH, Jr. The kinetics of formation of native ribonuclease during oxidation of the reduced polypeptide chain. Proc Natl Acad Sci U S A. 1961;47:1309-14.

35. Kim PS, Baldwin RL. Specific intermediates in the folding reactions of small proteins and the mechanism of protein folding. Annu Rev Biochem. 1982;51:459-89.

36. Dill KA, MacCallum JL. The protein-folding problem, 50 years on. Science. 2012;338(6110):1042-6.

37. Gething MJ, Sambrook J. Protein folding in the cell. Nature. 1992;355(6355):33-45.

38. Dobson CM, Šali A, Karplus M. Protein folding: a perspective from theory and experiment. Angew Chem Int Ed. 1998;37(7):868-93.

39. Udgaonkar JB, Baldwin RL. NMR evidence for an early framework intermediate on the folding pathway of ribonuclease A. Nature. 1988;335(6192):694-9.

40. Dobson CM. Protein folding and misfolding. Nature. 2003;426(6968):884-90.

41. Hardesty B, Kramer G. Folding of a nascent peptide on the ribosome. Prog Nucleic Acid Res Mol Biol. 2001;66:41-66.

42. Stevens FJ, Argon Y. Protein folding in the ER. Semin Cell Dev Biol. 1999;10(5):443-54.

43. Berridge MJ, Bootman MD, Roderick HL. Calcium signalling: dynamics, homeostasis and remodelling. Nature reviews Molecular cell biology. 2003;4(7):517-29.

44. Hudson DA, Gannon SA, Thorpe C. Oxidative protein folding: From thiol–disulfide exchange reactions to the redox poise of the endoplasmic reticulum. Free Radical Biol Med. 2015;80:171-82.

45. Ellis RJ. Macromolecular crowding: an important but neglected aspect of the intracellular environment. Curr Opin Struct Biol. 2001;11(1):114-9.

46. Kim YE, Hipp MS, Bracher A, Hayer-Hartl M, Hartl FU. Molecular chaperone functions in protein folding and proteostasis. Annu Rev Biochem. 2013;82:323-55.

47. Hartl FU, Bracher A, Hayer-Hartl M. Molecular chaperones in protein folding and proteostasis. Nature. 2011;475(7356):324-32.

48. Cashikar AG, Duennwald M, Lindquist SL. A chaperone pathway in protein disaggregation. Hsp26 alters the nature of protein aggregates to facilitate reactivation by Hsp104. J Biol Chem. 2005;280(25):23869-75.

49. Denic V, Quan EM, Weissman JS. A luminal surveillance complex that selects misfolded glycoproteins for ER-associated degradation. Cell. 2006;126(2):349-59.

50. Gauss R, Jarosch E, Sommer T, Hirsch C. A complex of Yos9p and the HRD ligase integrates endoplasmic reticulum quality control into the degradation machinery. Nat Cell Biol. 2006;8(8):849-54.

51. Ross CA, Poirier MA. Protein aggregation and neurodegenerative disease. Nat Med. 2004;10 Suppl:S10-7.

52. Plemper RK, Bordallo J, Deak PM, Taxis C, Hitt R, Wolf DH. Genetic interactions of Hrd3p and Der3p/Hrd1p with Sec61p suggest a retro-translocation complex mediating protein transport for ER degradation. J Cell Sci. 1999;112(22):4123-34.

53. Okuda-Shimizu Y, Hendershot LM. Characterization of an ERAD pathway for nonglycosylated BiP substrates, which require Herp. Mol Cell. 2007;28(4):544-54.

54. Oda Y, Okada T, Yoshida H, Kaufman RJ, Nagata K, Mori K. Derlin-2 and Derlin-3 are regulated by the mammalian unfolded protein response and are required for ER-associated degradation. J Cell Biol. 2006;172(3):383-93.

55. Olivari S, Cali T, Salo KE, Paganetti P, Ruddock LW, Molinari M. EDEM1 regulates ER-associated degradation by accelerating de-mannosylation of folding-defective polypeptides and by inhibiting their covalent aggregation. Biochem Biophys Res Commun. 2006;349(4):1278-84.

56. Olivari S, Molinari M. Glycoprotein folding and the role of EDEM1, EDEM2 and EDEM3 in degradation of folding-defective glycoproteins. FEBS Lett. 2007;581(19):3658-64.

57. Ye Y, Meyer HH, Rapoport TA. The AAA ATPase Cdc48/p97 and its partners transport proteins from the ER into the cytosol. Nature. 2001;414(6864):652-6.

58. Ciehanover A, Hod Y, Hershko A. A heat-stable polypeptide component of an ATP-dependent proteolytic system from reticulocytes. Biochem Biophys Res Commun. 1978;81(4):1100-5.

59. Wilkinson K, Urban M, Haas A. Ubiquitin is the ATP-dependent proteolysis factor I of rabbit reticulocytes. J Biol Chem. 1980;255(16):7529-32.

60. Sommer T, Jentsch S. A protein translocation defect linked to ubiquitin conjugation at the endoplasmic reticulum. Nature. 1993;365(6442):176-9.

61. Ward CL, Omura S, Kopito RR. Degradation of CFTR by the ubiquitin-proteasome pathway. Cell. 1995;83(1):121-7.

62. Jensen TJ, Loo MA, Pind S, Williams DB, Goldberg AL, Riordan JR. Multiple proteolytic systems, including the proteasome, contribute to CFTR processing. Cell. 1995;83(1):129-35.

63. Hiller MM, Finger A, Schweiger M, Wolf DH. ER degradation of a misfolded luminal protein by the cytosolic ubiquitin-proteasome pathway. Science. 1996;273(5282):1725.

64. Chen P, Johnson P, Sommer T, Jentsch S, Hochstrasser M. Multiple ubiquitin-conjugating enzymes participate in the in vivo degradation of the yeast MATα2 repressor. Cell. 1993;74(2):357-69.

65. Vassal A, Boulet A, Decoster E, Faye G. QRI8, a novel ubiquitin-conjugating enzyme in Saccharomyces cerevisiae. Biochim Biophys Acta. 1992;1132(2):211-3.

66. Skalnik DG, Narita H, Kent C, Simoni RD. The membrane domain of 3-hydroxy-3-methylglutaryl-coenzyme A reductase confers endoplasmic reticulum localization and sterol-regulated degradation onto beta-galactosidase. J Biol Chem. 1988;263(14):6836-41.

67. Chun KT, Bar-Nun S, Simoni RD. The regulated degradation of 3-hydroxy-3-methylglutaryl-CoA reductase requires a short-lived protein and occurs in the endoplasmic reticulum. J Biol Chem. 1990;265(35):22004-10.

68. Hampton R, Gardner R, Rine J. Role of 26S proteasome and HRD genes in the degradation of 3-hydroxy-3-methylglutaryl-CoA reductase, an integral endoplasmic reticulum membrane protein. Mol Biol Cell. 1996;7(12):2029-44.

69. Bays NW, Gardner RG, Seelig LP, Joazeiro CA, Hampton RY. Hrd1p/Der3p is a membrane-anchored ubiquitin ligase required for ER-associated degradation. Nat Cell Biol. 2001;3(1):24-9.

70. Gardner RG, Swarbrick GM, Bays NW, Cronin SR, Wilhovsky S, Seelig L, et al. Endoplasmic reticulum degradation requires lumen to cytosol signaling transmembrane control of Hrd1p by Hrd3p. J Cell Biol. 2000;151(1):69-82.

71. Hampton RY, Bhakta H. Ubiquitin-mediated regulation of 3-hydroxy-3-methylglutaryl-CoA reductase. Proc Natl Acad Sci U S A. 1997;94(24):12944-8.

72. Nakatsukasa K, Brodsky JL, Kamura T. A stalled retrotranslocation complex reveals physical linkage between substrate recognition and proteasomal degradation during ER-associated degradation. Mol Biol Cell. 2013;24(11):1765-75.

73. Gauss R, Sommer T, Jarosch E. The Hrd1p ligase complex forms a linchpin between ER-lumenal substrate selection and Cdc48p recruitment. EMBO J. 2006;25(9):1827-35.

74. Wiertz EJ, Jones TR, Sun L, Bogyo M, Geuze HJ, Ploegh HL. The human cytomegalovirus US11 gene product dislocates MHC class I heavy chains from the endoplasmic reticulum to the cytosol. Cell. 1996;84(5):769-79.

75. Wiertz E, Tortorella D, Bogyo M, Yu J, Mothes W, Jones TR, et al. Sec61-mediated transfer of a membrane protein from the endoplasmic reticulum to the proteasome for destruction. Nature. 1996;384(6608):432-8.

76. Bordallo J, Plemper RK, Finger A, Wolf DH. Der3p/Hrd1p is required for endoplasmic reticulum-associated degradation of misfolded lumenal and integral membrane proteins. Mol Biol Cell. 1998;9(1):209-22.

77. Vashist S, Ng DT. Misfolded proteins are sorted by a sequential checkpoint mechanism of ER quality control. J Cell Biol. 2004;165(1):41-52.

78. Carvalho P, Goder V, Rapoport TA. Distinct ubiquitin-ligase complexes define convergent pathways for the degradation of ER proteins. Cell. 2006;126(2):361-73.

79. Vashistha N, Neal SE, Singh A, Carroll SM, Hampton RY. Direct and essential function for Hrd3 in ER-associated degradation. Proc Natl Acad Sci U S A. 2016;113(21):5934-9.

80. Horn SC, Hanna J, Hirsch C, Volkwein C, Schütz A, Heinemann U, et al. Usa1 functions as a scaffold of the HRD-ubiquitin ligase. Mol Cell. 2009;36(5):782-93.

81. Knop M, Finger A, Braun T, Hellmuth K, Wolf D. Der1, a novel protein specifically required for endoplasmic reticulum degradation in yeast. EMBO J. 1996;15(4):753.

82. Stolz A, Schweizer RS, Schafer A, Wolf DH. Dfm1 forms distinct complexes with Cdc48 and the ER ubiquitin ligases and is required for ERAD. Traffic. 2010;11(10):1363-9.

83. Sato BK, Hampton RY. Yeast Derlin Dfm1 interacts with Cdc48 and functions in ER homeostasis. Yeast. 2006;23(14-15):1053-64.

84. Biederer T, Volkwein C, Sommer T. Role of Cue1p in ubiquitination and degradation at the ER surface. Science. 1997;278(5344):1806-9.

85. Bagola K, von Delbrück M, Dittmar G, Scheffner M, Ziv I, Glickman MH, et al. Ubiquitin binding by a CUE domain regulates ubiquitin chain formation by ERAD E3 ligases. Mol Cell. 2013;50(4):528-39.

86. Friedlander R, Jarosch E, Urban J, Volkwein C, Sommer T. A regulatory link between ER-associated protein degradation and the unfolded-protein response. Nat Cell Biol. 2000;2(7):379-84.

87. Ye Y, Shibata Y, Yun C, Ron D, Rapoport TA. A membrane protein complex mediates retro-translocation from the ER lumen into the cytosol. Nature. 2004;429(6994):841-7.

88. Ye Y, Shibata Y, Kikkert M, van Voorden S, Wiertz E, Rapoport TA. Recruitment of the p97 ATPase and ubiquitin ligases to the site of retrotranslocation at the endoplasmic reticulum membrane. Proc Natl Acad Sci U S A. 2005;102(40):14132-8.

89. Lilley BN, Ploegh HL. Multiprotein complexes that link dislocation, ubiquitination, and extraction of misfolded proteins from the endoplasmic reticulum membrane. Proc Natl Acad Sci U S A. 2005;102(40):14296-301.

90. Mehnert M, Sommer T, Jarosch E. Der1 promotes movement of misfolded proteins through the endoplasmic reticulum membrane. Nat Cell Biol. 2014;16(1):77-86.

91. Wahlman J, DeMartino GN, Skach WR, Bulleid NJ, Brodsky JL, Johnson AE. Real-time fluorescence detection of ERAD substrate retrotranslocation in a mammalian in vitro system. Cell. 2007;129(5):943-55.

92. Stein A, Ruggiano A, Carvalho P, Rapoport TA. Key steps in ERAD of luminal ER proteins reconstituted with purified components. Cell. 2014;158(6):1375-88.

93. Baldridge RD, Rapoport TA. Autoubiquitination of the HRD1 ligase triggers protein retrotranslocation in ERAD. Cell. 2016;166(2):394-407.

94. Kikkert M, Doolman R, Dai M, Avner R, Hassink G, van Voorden S, et al. Human HRD1 is an E3 ubiquitin ligase involved in degradation of proteins from the endoplasmic reticulum. J Biol Chem. 2004;279(5):3525-34.

95. Kaneko M, Ishiguro M, Niinuma Y, Uesugi M, Nomura Y. Human HRD1 protects against ER stress-induced apoptosis through ER-associated degradation1. FEBS Lett. 2002;532(1-2):147-52.

96. Christianson JC, Shaler TA, Tyler RE, Kopito RR. OS-9 and GRP94 deliver mutant α1-antitrypsin to the Hrd1–SEL1L ubiquitin ligase complex for ERAD. Nat Cell Biol. 2008;10(3):272-82.

97. Alcock F, Swanton E. Mammalian OS-9 is upregulated in response to endoplasmic reticulum stress and facilitates ubiquitination of misfolded glycoproteins. J Mol Biol. 2009;385(4):1032-42.

98. Rose MD, Misra LM, Vogel JP. KAR2, a karyogamy gene, is the yeast homolog of the mammalian BiP/GRP78 gene. Cell. 1989;57(7):1211-21.

99. Katsanis N, Fisher EM. Identification, Expression, and Chromosomal Localization of Ubiquitin Conjugating Enzyme 7 (UBE2G2), a Human Homologue of theSaccharomyces cerevisiae Ubc7Gene. Genomics. 1998;51(1):128-31.

100. Mueller B, Klemm EJ, Spooner E, Claessen JH, Ploegh HL. SEL1L nucleates a protein complex required for dislocation of misfolded glycoproteins. Proc Natl Acad Sci U S A. 2008;105(34):12325-30.

101. Klemm EJ, Spooner E, Ploegh HL. Dual role of ancient ubiquitous protein 1 (AUP1) in lipid droplet accumulation and endoplasmic reticulum (ER) protein quality control. J Biol Chem. 2011;286(43):37602-14.

102. Schulze A, Standera S, Buerger E, Kikkert M, van Voorden S, Wiertz E, et al. The ubiquitin-domain protein HERP forms a complex with components of the endoplasmic reticulum associated degradation pathway. J Mol Biol. 2005;354(5):1021-7.

103. Christianson JC, Olzmann JA, Shaler TA, Sowa ME, Bennett EJ, Richter CM, et al. Defining human ERAD networks through an integrative mapping strategy. Nat Cell Biol. 2012;14(1):93-105.

104. Hagiwara M, Ling J, Koenig PA, Ploegh HL. Posttranscriptional Regulation of Glycoprotein Quality Control in the Endoplasmic Reticulum Is Controlled by the E2 Ub-Conjugating Enzyme UBC6e. Mol Cell. 2016;63(5):753-67.

105. Spandl J, Lohmann D, Kuerschner L, Moessinger C, Thiele C. Ancient ubiquitous protein 1 (AUP1) localizes to lipid droplets and binds the E2 ubiquitin conjugase G2 (Ube2g2) via its G2 binding region. J Biol Chem. 2011;286(7):5599-606.

106. Chen B, Mariano J, Tsai YC, Chan AH, Cohen M, Weissman AM. The activity of a human endoplasmic reticulum-associated degradation E3, gp78, requires its Cue domain, RING finger, and an E2-binding site. Proc Natl Acad Sci U S A. 2006;103(2):341-6.

107. Burr ML, Cano F, Svobodova S, Boyle LH, Boname JM, Lehner PJ. HRD1 and UBE2J1 target misfolded MHC class I heavy chains for endoplasmic reticulum-associated degradation. Proc Natl Acad Sci U S A. 2011;108(5):2034-9.

108. Liang J, Yin C, Doong H, Fang S, Peterhoff C, Nixon RA, et al. Characterization of erasin (UBXD2): a new ER protein that promotes ER-associated protein degradation. J Cell Sci. 2006;119(19):4011-24.

109. Lee JN, Zhang X, Feramisco JD, Gong Y, Ye J. Unsaturated fatty acids inhibit proteasomal degradation of Insig-1 at a postubiquitination step. J Biol Chem. 2008;283(48):33772-83.

110. Lim PJ, Danner R, Liang J, Doong H, Harman C, Srinivasan D, et al. Ubiquilin and p97/VCP bind erasin, forming a complex involved in ERAD. J Cell Biol. 2009;187(2):201-17.

111. Seok Ko H, Uehara T, Tsuruma K, Nomura Y. Ubiquilin interacts with ubiquitylated proteins and proteasome through its ubiquitin-associated and ubiquitin-like domains. FEBS Lett. 2004;566(1-3):110-4.

112. Wang Q, Liu Y, Soetandyo N, Baek K, Hegde R, Ye Y. A ubiquitin ligase-associated chaperone holdase maintains polypeptides in soluble states for proteasome degradation. Mol Cell. 2011;42(6):758-70.

113. Xu Y, Liu Y, Lee J-g, Ye Y. A ubiquitin-like domain recruits an oligomeric chaperone to a retrotranslocation complex in endoplasmic reticulum-associated degradation. J Biol Chem. 2013;288(25):18068-76.

114. Itakura E, Zavodszky E, Shao S, Wohlever ML, Keenan RJ, Hegde RS. Ubiquilins Chaperone and Triage Mitochondrial Membrane Proteins for Degradation. Mol Cell. 2016;63(1):21-33.

115. Ye Y, Shibata Y, Yun C, Ron D, Rapoport TA. A membrane protein complex mediates retro-translocation from the ER lumen into the cytosol. Nature. 2004;429(6994):841-7.

116. Ye Y, Shibata Y, Kikkert M, van Voorden S, Wiertz E, Rapoport TA. Recruitment of the p97 ATPase and ubiquitin ligases to the site of retrotranslocation at the endoplasmic reticulum membrane. Proc Natl Acad Sci U S A. 2005;102(40):14132-8.

117. Greenblatt EJ, Olzmann JA, Kopito RR. Derlin-1 is a rhomboid pseudoprotease required for the dislocation of mutant alpha-1 antitrypsin from the endoplasmic reticulum. Nat Struct Mol Biol. 2011;18(10):1147-52.

118. McGrath JP, Jentsch S, Varshavsky A. UBA 1: an essential yeast gene encoding ubiquitin-activating enzyme. EMBO J. 1991;10(1):227.

119. Handley-Gearhart PM, Stephen AG, Trausch-Azar JS, Ciechanover A, Schwartz AL. Human ubiquitin-activating enzyme, E1. Indication of potential nuclear and cytoplasmic subpopulations using epitope-tagged cDNA constructs. J Biol Chem. 1994;269(52):33171-8.

120. Handley-Gearhart PM, Trausch-Azar J, Ciechanover A, Schwartz AL. Rescue of the complex temperature-sensitive phenotype of Chinese hamster ovary E36ts20 cells by expression of the human ubiquitin-activating enzyme cDNA. Biochem J. 1994;304(3):1015-20.

121. Yamasaki S, Yagishita N, Sasaki T, Nakazawa M, Kato Y, Yamadera T, et al. Cytoplasmic destruction of p53 by the endoplasmic reticulum-resident ubiquitin ligase ‘Synoviolin’. EMBO J. 2007;26(1):113-22.

122. Biederer T, Volkwein C, Sommer T. Degradation of subunits of the Sec61p complex, an integral component of the ER membrane, by the ubiquitin-proteasome pathway. EMBO J. 1996;15(9):2069.

123. Ravid T, Kreft SG, Hochstrasser M. Membrane and soluble substrates of the Doa10 ubiquitin ligase are degraded by distinct pathways. EMBO J. 2006;25(3):533-43.

124. Wang Q, Chang A. Eps1, a novel PDI-related protein involved in ER quality control in yeast. EMBO J. 1999;18(21):5972-82.

125. Huyer G, Piluek WF, Fansler Z, Kreft SG, Hochstrasser M, Brodsky JL, et al. Distinct machinery is required in Saccharomyces cerevisiae for the endoplasmic reticulum-associated degradation of a multispanning membrane protein and a soluble luminal protein. J Biol Chem. 2004;279(37):38369-78.

126. Jungmann J, Reins HA, Schobert C, Jentsch S. Resistance to cadmium mediated by ubiquitin-dependent proteolysis. Nature. 1993;361(6410):369-71.

127. Stolz A, Besser S, Hottmann H, Wolf DH. Previously unknown role for the ubiquitin ligase Ubr1 in endoplasmic reticulum-associated protein degradation. Proc Natl Acad Sci U S A. 2013;110(38):15271-6.

128. Younger JM, Ren H-Y, Chen L, Fan C-Y, Fields A, Patterson C, et al. A foldable CFTRΔF508 biogenic intermediate accumulates upon inhibition of the Hsc70–CHIP E3 ubiquitin ligase. J Cell Biol. 2004;167(6):1075-85.

129. Kaneko M, Koike H, Saito R, Kitamura Y, Okuma Y, Nomura Y. Loss of HRD1-mediated protein degradation causes amyloid precursor protein accumulation and amyloid-β generation. J Neurosci. 2010;30(11):3924-32.

130. Younger JM, Chen L, Ren H-Y, Rosser MF, Turnbull EL, Fan C-Y, et al. Sequential quality-control checkpoints triage misfolded cystic fibrosis transmembrane conductance regulator. Cell. 2006;126(3):571-82.

131. Lenk U, Yu H, Walter J, Gelman MS, Hartmann E, Kopito RR, et al. A role for mammalian Ubc6 homologues in ER-associated protein degradation. J Cell Sci. 2002;115(14):3007-14.

132. Flierman D, Coleman CS, Pickart CM, Rapoport TA, Chau V. E2-25K mediates US11-triggered retro-translocation of MHC class I heavy chains in a permeabilized cell system. Proc Natl Acad Sci U S A. 2006;103(31):11589-94.

133. Yan L, Liu W, Zhang H, Liu C, Shang Y, Ye Y, et al. Ube2g2–gp78-mediated HERP polyubiquitylation is involved in ER stress recovery. J Cell Sci. 2014;127(7):1417-27.

134. Tiwari S, Weissman AM. Endoplasmic Reticulum (ER)-associated Degradation of T Cell Receptor Subunits involvement of ER-associated Ubiquitin-Conjugating Enzymes (E2s). J Biol Chem. 2001;276(19):16193-200.

135. Webster JM, Tiwari S, Weissman AM, Wojcikiewicz RJ. Inositol 1, 4, 5-trisphosphate receptor ubiquitination is mediated by mammalian Ubc7, a component of the endoplasmic

reticulum-associated degradation pathway, and is inhibited by chelation of intracellular Zn2+. J Biol Chem. 2003;278(40):38238-46.

136. Gardner RG, Shearer AG, Hampton RY. In vivo action of the HRD ubiquitin ligase complex: mechanisms of endoplasmic reticulum quality control and sterol regulation. Mol Cell Biol. 2001;21(13):4276-91.

137. Yang H, Zhong X, Ballar P, Luo S, Shen Y, Rubinsztein DC, et al. Ubiquitin ligase Hrd1 enhances the degradation and suppresses the toxicity of polyglutamine-expanded huntingtin. Exp Cell Res. 2007;313(3):538-50.

138. Apodaca J, Kim I, Rao H. Cellular tolerance of prion protein PrP in yeast involves proteolysis and the unfolded protein response. Biochem Biophys Res Commun. 2006;347(1):319-26.

139. Plemper RK, Egner R, Kuchler K, Wolf DH. Endoplasmic reticulum degradation of a mutated ATP-binding cassette transporter Pdr5 proceeds in a concerted action of Sec61 and the proteasome. J Biol Chem. 1998;273(49):32848-56.

140. Swanson R, Locher M, Hochstrasser M. A conserved ubiquitin ligase of the nuclear envelope/endoplasmic reticulum that functions in both ER-associated and Matα2 repressor degradation. Genes Dev. 2001;15(20):2660-74.

141. Han S, Liu Y, Chang A. Cytoplasmic Hsp70 promotes ubiquitination for endoplasmic reticulum-associated degradation of a misfolded mutant of the yeast plasma membrane ATPase, PMA1. J Biol Chem. 2007;282(36):26140-9.

142. Foresti O, Ruggiano A, Hannibal-Bach HK, Ejsing CS, Carvalho P. Sterol homeostasis requires regulated degradation of squalene monooxygenase by the ubiquitin ligase Doa10/Teb4. Elife. 2013;2:e00953.

143. Avci D, Fuchs S, Schrul B, Fukumori A, Breker M, Frumkin I, et al. The yeast ER-intramembrane protease Ypf1 refines nutrient sensing by regulating transporter abundance. Mol Cell. 2014;56(5):630-40.

144. Habeck G, Ebner FA, Shimada-Kreft H, Kreft SG. The yeast ERAD-C ubiquitin ligase Doa10 recognizes an intramembrane degron. J Cell Biol. 2015;209(2):261-73.

145. Haynes CM, Caldwell S, Cooper AA. An HRD/DER-independent ER quality control mechanism involves Rsp5p-dependent ubiquitination and ER-Golgi transport. J Cell Biol. 2002;158(1):91-102.

146. Haynes CM, Titus EA, Cooper AA. Degradation of misfolded proteins prevents ER-derived oxidative stress and cell death. Mol Cell. 2004;15(5):767-76.

147. Foresti O, Rodriguez-Vaello V, Funaya C, Carvalho P. Quality control of inner nuclear membrane proteins by the Asi complex. Science. 2014;346(6210):751-5.

148. Khmelinskii A, Blaszczak E, Pantazopoulou M, Fischer B, Omnus DJ, Le Dez G, et al. Protein quality control at the inner nuclear membrane. Nature. 2014;516(7531):410-3.

149. Wang H, Li Q, Shen Y, Sun A, Zhu X, Fang S, et al. The ubiquitin ligase Hrd1 promotes degradation of the Z variant alpha 1-antitrypsin and increases its solubility. Mol Cell Biochem. 2011;346(1-2):137-45.

150. Shmueli A, Tsai YC, Yang M, Braun MA, Weissman AM. Targeting of gp78 for ubiquitin-mediated proteasomal degradation by Hrd1: cross-talk between E3s in the endoplasmic reticulum. Biochem Biophys Res Commun. 2009;390(3):758-62.

151. Ballar P, Ors AU, Yang H, Fang S. Differential regulation of CFTRΔF508 degradation by ubiquitin ligases gp78 and Hrd1. Int J Biochem Cell Biol. 2010;42(1):167-73.

152. Shimizu Y, Okuda-Shimizu Y, Hendershot LM. Ubiquitylation of an ERAD substrate occurs on multiple types of amino acids. Mol Cell. 2010;40(6):917-26.

153. Kong S, Yang Y, Xu Y, Wang Y, Zhang Y, Melo-Cardenas J, et al. Endoplasmic reticulum-resident E3 ubiquitin ligase Hrd1 controls B-cell immunity through degradation of the death receptor CD95/Fas. Proc Natl Acad Sci U S A. 2016:201606742.

154. Tyler RE, Pearce MM, Shaler TA, Olzmann JA, Greenblatt EJ, Kopito RR. Unassembled CD147 is an endogenous endoplasmic reticulum-associated degradation substrate. Mol Biol Cell. 2012;23(24):4668-78.

155. Lee KA, Hammerle LP, Andrews PS, Stokes MP, Mustelin T, Silva JC, et al. Ubiquitin ligase substrate identification through quantitative proteomics at both the protein and peptide levels. J Biol Chem. 2011;286(48):41530-8.

156. Zavacki AM, e Drigo RA, Freitas BC, Chung M, Harney JW, Egri P, et al. The E3 ubiquitin ligase TEB4 mediates degradation of type 2 iodothyronine deiodinase. Mol Cell Biol. 2009;29(19):5339-47.

157. Zelcer N, Sharpe LJ, Loregger A, Kristiana I, Cook EC, Phan L, et al. The E3 ubiquitin ligase MARCH6 degrades squalene monooxygenase and affects 3-hydroxy-3-methyl-glutaryl coenzyme A reductase and the cholesterol synthesis pathway. Mol Cell Biol. 2014;34(7):1262-70.

158. Hassink G, Kikkert M, Van Voorden S, Shiow-Ju L, Spaapen R, COLEMAN CS, et al. TEB4 is a C4HC3 RING finger-containing ubiquitin ligase of the endoplasmic reticulum. Biochem J. 2005;388(2):647-55.

159. Fang S, Ferrone M, Yang C, Jensen JP, Tiwari S, Weissman AM. The tumor autocrine motility factor receptor, gp78, is a ubiquitin protein ligase implicated in degradation from the endoplasmic reticulum. Proc Natl Acad Sci U S A. 2001;98(25):14422-7.

160. Liang J-s, Kim T, Fang S, Yamaguchi J, Weissman AM, Fisher EA, et al. Overexpression of the tumor autocrine motility factor receptor Gp78, a ubiquitin protein ligase, results in

increased ubiquitinylation and decreased secretion of apolipoprotein B100 in HepG2 cells. J Biol Chem. 2003;278(26):23984-8.

161. Morito D, Hirao K, Oda Y, Hosokawa N, Tokunaga F, Cyr DM, et al. Gp78 cooperates with RMA1 in endoplasmic reticulum-associated degradation of CFTRΔF508. Mol Biol Cell. 2008;19(4):1328-36.

162. Song B-L, Sever N, DeBose-Boyd RA. Gp78, a membrane-anchored ubiquitin ligase, associates with Insig-1 and couples sterol-regulated ubiquitination to degradation of HMG CoA reductase. Mol Cell. 2005;19(6):829-40.

163. Shen Y, Ballar P, Fang S. Ubiquitin ligase gp78 increases solubility and facilitates degradation of the Z variant of α-1-antitrypsin. Biochem Biophys Res Commun. 2006;349(4):1285-93.

164. Tsai YC, Mendoza A, Mariano JM, Zhou M, Kostova Z, Chen B, et al. The ubiquitin ligase gp78 promotes sarcoma metastasis by targeting KAI1 for degradation. Nat Med. 2007;13(12):1504-9.

165. Kim S-M, Acharya P, Engel JC, Correia MA. Liver Cytochrome P450 3A Ubiquitination in Vivo by gp78/Autocrine Motility Factor Receptor and C Terminus of Hsp70-interacting Protein (CHIP) E3 Ubiquitin Ligases PHYSIOLOGICAL AND PHARMACOLOGICAL RELEVANCE. J Biol Chem. 2010;285(46):35866-77.

166. Connell P, Ballinger CA, Jiang J, Wu Y, Thompson LJ, Höhfeld J, et al. The co-chaperone CHIP regulates protein triage decisions mediated by heat-shock proteins. Nat Cell Biol. 2001;3(1):93-6.

167. Meacham GC, Patterson C, Zhang W, Younger JM, Cyr DM. The Hsc70 co-chaperone CHIP targets immature CFTR for proteasomal degradation. Nat Cell Biol. 2001;3(1):100-5.

168. Donnelly BF, Needham PG, Snyder AC, Roy A, Khadem S, Brodsky JL, et al. Hsp70 and Hsp90 multichaperone complexes sequentially regulate thiazide-sensitive cotransporter endoplasmic reticulum-associated degradation and biogenesis. J Biol Chem. 2013;288(18):13124-35.

169. Imai Y, Soda M, Hatakeyama S, Akagi T, Hashikawa T, Nakayama K-I, et al. CHIP is associated with Parkin, a gene responsible for familial Parkinson's disease, and enhances its ubiquitin ligase activity. Mol Cell. 2002;10(1):55-67.

170. Grove DE, Fan C-Y, Ren HY, Cyr DM. The endoplasmic reticulum–associated Hsp40 DNAJB12 and Hsc70 cooperate to facilitate RMA1 E3–dependent degradation of nascent CFTRΔF508. Mol Biol Cell. 2011;22(3):301-14.

171. Stagg HR, Thomas M, van den Boomen D, Wiertz EJ, Drabkin HA, Gemmill RM, et al. The TRC8 E3 ligase ubiquitinates MHC class I molecules before dislocation from the ER. J Cell Biol. 2009;186(5):685-92.

172. Lee JP, Brauweiler A, Rudolph M, Hooper JE, Drabkin HA, Gemmill RM. The TRC8 ubiquitin ligase is sterol regulated and interacts with lipid and protein biosynthetic pathways. Mol Cancer Res. 2010;8(1):93-106.

173. Boname JM, Bloor S, Wandel MP, Nathan JA, Antrobus R, Dingwell KS, et al. Cleavage by signal peptide peptidase is required for the degradation of selected tail-anchored proteins. J Cell Biol. 2014;205(6):847-62.

174. Chen CY, Malchus NS, Hehn B, Stelzer W, Avci D, Langosch D, et al. Signal peptide peptidase functions in ERAD to cleave the unfolded protein response regulator XBP1u. EMBO J. 2014;33(21):2492-506.

175. Hsu JL, van den Boomen DJ, Tomasec P, Weekes MP, Antrobus R, Stanton RJ, et al. Plasma membrane profiling defines an expanded class of cell surface proteins selectively targeted for degradation by HCMV US2 in cooperation with UL141. PLoS Pathog. 2015;11(4):e1004811.

176. Yoshida Y, Chiba T, Tokunaga F, Kawasaki H, Iwai K, Suzuki T, et al. E3 ubiquitin ligase that recognizes sugar chains. Nature. 2002;418(6896):438-42.

177. Ramachandran S, Osterhaus SR, Parekh KR, Jacobi AM, Behlke MA, McCray PB, Jr. SYVN1, NEDD8, and FBXO2 Proteins Regulate DeltaF508 Cystic Fibrosis Transmembrane Conductance Regulator (CFTR) Ubiquitin-mediated Proteasomal Degradation. J Biol Chem. 2016;291(49):25489-504.

178. Yoshida Y, Tokunaga F, Chiba T, Iwai K, Tanaka K, Tai T. Fbs2 is a new member of the E3 ubiquitin ligase family that recognizes sugar chains. J Biol Chem. 2003;278(44):43877-84.

179. Binette J, Dubé M, Mercier J, Halawani D, Latterich M, Cohen ÉA. Requirements for the selective degradation of CD4 receptor molecules by the human immunodeficiency virus type 1 Vpu protein in the endoplasmic reticulum. Retrovirology. 2007;4(1):1.

180. Mangeat B, Gers-Huber G, Lehmann M, Zufferey M, Luban J, Piguet V. HIV-1 Vpu neutralizes the antiviral factor Tetherin/BST-2 by binding it and directing its beta-TrCP2-dependent degradation. PLoS Pathog. 2009;5(9):e1000574.

181. Ahner A, Gong X, Schmidt BZ, Peters KW, Rabeh WM, Thibodeau PH, et al. Small heat shock proteins target mutant cystic fibrosis transmembrane conductance regulator for degradation via a small ubiquitin-like modifier–dependent pathway. Mol Biol Cell. 2013;24(2):74-84.

182. Maruyama Y, Yamada M, Takahashi K, Yamada M. Ubiquitin ligase Kf-1 is involved in the endoplasmic reticulum-associated degradation pathway. Biochem Biophys Res Commun. 2008;374(4):737-41.

183. Lu JP, Wang Y, Sliter DA, Pearce MM, Wojcikiewicz RJ. RNF170 protein, an endoplasmic reticulum membrane ubiquitin ligase, mediates inositol 1, 4, 5-trisphosphate receptor ubiquitination and degradation. J Biol Chem. 2011;286(27):24426-33.

184. El Khouri E, Le Pavec G, Toledano MB, Delaunay-Moisan A. RNF185 is a novel E3 ligase of endoplasmic reticulum-associated degradation (ERAD) that targets cystic fibrosis transmembrane conductance regulator (CFTR). J Biol Chem. 2013;288(43):31177-91.

185. Ron I, Rapaport D, Horowitz M. Interaction between parkin and mutant glucocerebrosidase variants: a possible link between Parkinson disease and Gaucher disease. Hum Mol Genet. 2010;19(19):3771-81.

186. Lerner M, Corcoran M, Cepeda D, Nielsen ML, Zubarev R, Pontén F, et al. The RBCC gene RFP2 (Leu5) encodes a novel transmembrane E3 ubiquitin ligase involved in ERAD. Mol Biol Cell. 2007;18(5):1670-82.

187. Altier C, Garcia-Caballero A, Simms B, You H, Chen L, Walcher J, et al. The Cav [beta] subunit prevents RFP2-mediated ubiquitination and proteasomal degradation of L-type channels. Nat Neurosci. 2011;14(2):173-80.

188. Guo X, Shen S, Song S, He S, Cui Y, Xing G, et al. The E3 ligase Smurf1 regulates Wolfram syndrome protein stability at the endoplasmic reticulum. J Biol Chem. 2011;286(20):18037-47.

189. van den Boomen DJ, Timms RT, Grice GL, Stagg HR, Skødt K, Dougan G, et al. TMEM129 is a Derlin-1 associated ERAD E3 ligase essential for virus-induced degradation of MHC-I. Proc Natl Acad Sci U S A. 2014;111(31):11425-30.

190. Neutzner A, Neutzner M, Benischke A-S, Ryu S-W, Frank S, Youle RJ, et al. A systematic search for endoplasmic reticulum (ER) membrane-associated RING finger proteins identifies Nixin/ZNRF4 as a regulator of calnexin stability and ER homeostasis. J Biol Chem. 2011;286(10):8633-43.

191. Fry WH, Simion C, Sweeney C, Carraway KL. Quantity control of the ErbB3 receptor tyrosine kinase at the endoplasmic reticulum. Mol Cell Biol. 2011;31(14):3009-18.

192. Bazirgan OA, Hampton RY. Cue1p is an activator of Ubc7p E2 activity in vitro and in vivo. J Biol Chem. 2008;283(19):12797-810.

193. Metzger MB, Maurer MJ, Dancy BM, Michaelis S. Degradation of a cytosolic protein requires endoplasmic reticulum-associated degradation machinery. J Biol Chem. 2008;283(47):32302-16.

194. Zhang Y, Nijbroek G, Sullivan ML, McCracken AA, Watkins SC, Michaelis S, et al. Hsp70 molecular chaperone facilitates endoplasmic reticulum-associated protein degradation of cystic fibrosis transmembrane conductance regulator in yeast. Mol Biol Cell. 2001;12(5):1303-14.

195. Youker RT, Walsh P, Beilharz T, Lithgow T, Brodsky JL. Distinct roles for the Hsp40 and Hsp90 molecular chaperones during cystic fibrosis transmembrane conductance regulator degradation in yeast. Mol Biol Cell. 2004;15(11):4787-97.

196. Messick TE, Russell NS, Iwata AJ, Sarachan KL, Shiekhattar R, Shanks JR, et al. Structural basis for ubiquitin recognition by the Otu1 ovarian tumor domain protein. J Biol Chem. 2008;283(16):11038-49.

197. Rumpf S, Jentsch S. Functional division of substrate processing cofactors of the ubiquitin-selective Cdc48 chaperone. Mol Cell. 2006;21(2):261-9.

198. Meacham GC, Lu Z, King S, Sorscher E, Tousson A, Cyr DM. The Hdj-2/Hsc70 chaperone pair facilitates early steps in CFTR biogenesis. EMBO J. 1999;18(6):1492-505.

199. Hagiwara M, Ling J, Koenig P-A, Ploegh HL. Posttranscriptional Regulation of Glycoprotein Quality Control in the Endoplasmic Reticulum Is Controlled by the E2 Ub-Conjugating Enzyme UBC6e. Mol Cell. 2016;63(5):753-67.

200. Matsumura Y, David LL, Skach WR. Role of Hsc70 binding cycle in CFTR folding and endoplasmic reticulum–associated degradation. Mol Biol Cell. 2011;22(16):2797-809.

201. Fisher EA, Zhou M, Mitchell DM, Wu X, Omura S, Wang H, et al. The degradation of apolipoprotein B100 is mediated by the ubiquitin-proteasome pathway and involves heat shock protein 70. J Biol Chem. 1997;272(33):20427-34.

202. Goldfarb SB, Kashlan OB, Watkins JN, Suaud L, Yan W, Kleyman TR, et al. Differential effects of Hsc70 and Hsp70 on the intracellular trafficking and functional expression of epithelial sodium channels. Proc Natl Acad Sci U S A. 2006;103(15):5817-22.

203. Needham PG, Mikoluk K, Dhakarwal P, Khadem S, Snyder AC, Subramanya AR, et al. The thiazide-sensitive NaCl cotransporter is targeted for chaperone-dependent endoplasmic reticulum-associated degradation. J Biol Chem. 2011;286(51):43611-21.

204. Yamamoto Y-h, Kimura T, Momohara S, Takeuchi M, Tani T, Kimata Y, et al. A novel ER J-protein DNAJB12 accelerates ER-associated degradation of membrane proteins including CFTR. Cell Struct Funct. 2010;35(2):107-16.

205. Sowa ME, Bennett EJ, Gygi SP, Harper JW. Defining the human deubiquitinating enzyme interaction landscape. Cell. 2009;138(2):389-403.

206. Liu Y, Soetandyo N, Lee J-g, Liu L, Xu Y, Clemons Jr WM, et al. USP13 antagonizes gp78 to maintain functionality of a chaperone in ER-associated degradation. Elife. 2014;3:e01369.

207. Hassink GC, Zhao B, Sompallae R, Altun M, Gastaldello S, Zinin NV, et al. The ER-resident ubiquitin-specific protease 19 participates in the UPR and rescues ERAD substrates. EMBO rep. 2009;10(7):755-61.

208. Blount JR, Burr AA, Denuc A, Marfany G, Todi SV. Ubiquitin-specific protease 25 functions in Endoplasmic Reticulum-associated degradation. PLoS One. 2012;7(5):e36542.

209. Jo Y, Hartman IZ, DeBose-Boyd RA. Ancient ubiquitous protein-1 mediates sterol-induced ubiquitination of 3-hydroxy-3-methylglutaryl CoA reductase in lipid droplet–associated endoplasmic reticulum membranes. Mol Biol Cell. 2013;24(3):169-83.

210. Ernst R, Mueller B, Ploegh HL, Schlieker C. The otubain YOD1 is a deubiquitinating enzyme that associates with p97 to facilitate protein dislocation from the ER. Mol Cell. 2009;36(1):28-38.

211. Wang Q, Li L, Ye Y. Regulation of retrotranslocation by p97-associated deubiquitinating enzyme ataxin-3. J Cell Biol. 2006;174(7):963-71.

212. Zhong X, Pittman RN. Ataxin-3 binds VCP/p97 and regulates retrotranslocation of ERAD substrates. Hum Mol Genet. 2006;15(16):2409-20.

213. Tsuchiya Y, Morita T, Kim M, Iemura S, Natsume T, Yamamoto M, et al. Dual regulation of the transcriptional activity of Nrf1 by beta-TrCP- and Hrd1-dependent degradation mechanisms. Mol Cell Biol. 2011;31(22):4500-12.

214. Bernardi KM, Williams JM, Inoue T, Schultz A, Tsai B. A deubiquitinase negatively regulates retro-translocation of nonubiquitinated substrates. Mol Biol Cell. 2013;24(22):3545-56.

215. Weber A, Cohen I, Popp O, Dittmar G, Reiss Y, Sommer T, et al. Sequential Poly-ubiquitylation by Specialized Conjugating Enzymes Expands the Versatility of a Quality Control Ubiquitin Ligase. Mol Cell. 2016;63(5):827-39.

216. Kreft SG, Wang L, Hochstrasser M. Membrane topology of the yeast endoplasmic reticulum-localized ubiquitin ligase Doa10 and comparison with its human ortholog TEB4 (MARCH-VI). J Biol Chem. 2006;281(8):4646-53.

217. Zhang T, Xu Y, Liu Y, Ye Y. gp78 functions downstream of Hrd1 to promote degradation of misfolded proteins of the endoplasmic reticulum. Mol Biol Cell. 2015;26(24):4438-50.

218. Ballar P, Shen Y, Yang H, Fang S. The role of a novel p97/valosin-containing protein-interacting motif of gp78 in endoplasmic reticulum-associated degradation. J Biol Chem. 2006;281(46):35359-68.

219. Bartel B, Wünning I, Varshavsky A. The recognition component of the N-end rule pathway. EMBO J. 1990;9(10):3179.

220. Blom D, Hirsch C, Stern P, Tortorella D, Ploegh HL. A glycosylated type I membrane protein becomes cytosolic when peptide: N-glycanase is compromised. EMBO J. 2004;23(3):650-8.

221. Suzuki T, Park H, Lennarz WJ. Cytoplasmic peptide: N-glycanase (PNGase) in eukaryotic cells: occurrence, primary structure, and potential functions. FASEB J. 2002;16(7):635-41.

222. Lam YA, Lawson TG, Velayutham M, Zweier JL, Pickart CM. A proteasomal ATPase subunit recognizes the polyubiquitin degradation signal. Nature. 2002;416(6882):763-7.

223. Thrower JS, Hoffman L, Rechsteiner M, Pickart CM. Recognition of the polyubiquitin proteolytic signal. EMBO J. 2000;19(1):94-102.

224. Boutet SC, Disatnik M-H, Chan LS, Iori K, Rando TA. Regulation of Pax3 by proteasomal degradation of monoubiquitinated protein in skeletal muscle progenitors. Cell. 2007;130(2):349-62.

225. Husnjak K, Elsasser S, Zhang N, Chen X, Randles L, Shi Y, et al. Proteasome subunit Rpn13 is a novel ubiquitin receptor. Nature. 2008;453(7194):481-8.

226. Kravtsova-Ivantsiv Y, Cohen S, Ciechanover A. Modification by single ubiquitin moieties rather than polyubiquitination is sufficient for proteasomal processing of the p105 NF-κB precursor. Mol Cell. 2009;33(4):496-504.

227. Lederkremer GZ, Glickman MH. A window of opportunity: timing protein degradation by trimming of sugars and ubiquitins. Trends Biochem Sci. 2005;30(6):297-303.

228. Meyer HH, Wang Y, Warren G. Direct binding of ubiquitin conjugates by the mammalian p97 adaptor complexes, p47 and Ufd1–Npl4. EMBO J. 2002;21(21):5645-52.

229. Meyer HH, Shorter JG, Seemann J, Pappin D, Warren G. A complex of mammalian Ufd1 and Npl4 links the AAA-ATPase, p97, to ubiquitin and nuclear transport pathways. EMBO J. 2000;19(10):2181-92.

230. Ye Y, Meyer HH, Rapoport TA. Function of the p97–Ufd1–Npl4 complex in retrotranslocation from the ER to the cytosol dual recognition of nonubiquitinated polypeptide segments and polyubiquitin chains. J Cell Biol. 2003;162(1):71-84.

231. Johnson ES, Ma PC, Ota IM, Varshavsky A. A proteolytic pathway that recognizes ubiquitin as a degradation signal. J Biol Chem. 1995;270(29):17442-56.

232. Liu Y, Ye Y. Roles of p97-associated deubiquitinases in protein quality control at the endoplasmic reticulum. Curr Protein Pept Sci. 2012;13(5):436-46.

233. Koch P, Breuer P, Peitz M, Jungverdorben J, Kesavan J, Poppe D, et al. Excitation-induced ataxin-3 aggregation in neurons from patients with Machado-Joseph disease. Nature. 2011;480(7378):543-6.

234. Wang G-h, Sawai N, Kotliarova S, Kanazawa I, Nukina N. Ataxin-3, the MJD1 gene product, interacts with the two human homologs of yeast DNA repair protein RAD23, HHR23A and HHR23B. Hum Mol Genet. 2000;9(12):1795-803.

235. Doss-Pepe EW, Stenroos ES, Johnson WG, Madura K. Ataxin-3 interactions with rad23 and valosin-containing protein and its associations with ubiquitin chains and the proteasome are consistent with a role in ubiquitin-mediated proteolysis. Mol Cell Biol. 2003;23(18):6469-83.

236. Boeddrich A, Gaumer S, Haacke A, Tzvetkov N, Albrecht M, Evert BO, et al. An arginine/lysine-rich motif is crucial for VCP/p97-mediated modulation of ataxin-3 fibrillogenesis. EMBO J. 2006;25(7):1547-58.

237. Todi SV, Winborn BJ, Scaglione KM, Blount JR, Travis SM, Paulson HL. Ubiquitination directly enhances activity of the deubiquitinating enzyme ataxin-3. EMBO J. 2009;28(4):372-82.

238. Lee J-G, Kim W, Gygi S, Ye Y. Characterization of the deubiquitinating activity of USP19 and its role in endoplasmic reticulum-associated degradation. J Biol Chem. 2014;289(6):3510-7.

239. Hatakeyama S, Yada M, Matsumoto M, Ishida N, Nakayama K-I. U box proteins as a new family of ubiquitin-protein ligases. J Biol Chem. 2001;276(35):33111-20.

240. Kaneko C, Hatakeyama S, Matsumoto M, Yada M, Nakayama K, Nakayama KI. Characterization of the mouse gene for the U-box-type ubiquitin ligase UFD2a. Biochem Biophys Res Commun. 2003;300(2):297-304.

241. Kim W, Bennett EJ, Huttlin EL, Guo A, Li J, Possemato A, et al. Systematic and quantitative assessment of the ubiquitin-modified proteome. Mol Cell. 2011;44(2):325-40.

242. Kravtsova-Ivantsiv Y, Ciechanover A. Non-canonical ubiquitin-based signals for proteasomal degradation. J Cell Sci. 2012;125(3):539-48.

243. Cadwell K, Coscoy L. Ubiquitination on nonlysine residues by a viral E3 ubiquitin ligase. Science. 2005;309(5731):127-30.

244. Wang X, Herr RA, Chua W-J, Lybarger L, Wiertz EJ, Hansen TH. Ubiquitination of serine, threonine, or lysine residues on the cytoplasmic tail can induce ERAD of MHC-I by viral E3 ligase mK3. J Cell Biol. 2007;177(4):613-24.

245. Magadan JG, Perez-Victoria FJ, Sougrat R, Ye Y, Strebel K, Bonifacino JS. Multilayered mechanism of CD4 downregulation by HIV-1 Vpu involving distinct ER retention and ERAD targeting steps. PLoS Pathog. 2010;6(4):e1000869.

246. Tokarev AA, Munguia J, Guatelli JC. Serine-threonine ubiquitination mediates downregulation of BST-2/tetherin and relief of restricted virion release by HIV-1 Vpu. J Virol. 2011;85(1):51-63.

247. Gustin JK, Douglas JL, Bai Y, Moses AV. Ubiquitination of BST-2 protein by HIV-1 Vpu protein does not require lysine, serine, or threonine residues within the BST-2 cytoplasmic domain. J Biol Chem. 2012;287(18):14837-50.

248. Ishikura S, Weissman AM, Bonifacino JS. Serine residues in the cytosolic tail of the T-cell antigen receptor α-chain mediate ubiquitination and endoplasmic reticulum-associated degradation of the unassembled protein. J Biol Chem. 2010;285(31):23916-24.

249. Read MA, Brownell JE, Gladysheva TB, Hottelet M, Parent LA, Coggins MB, et al. Nedd8 modification of cul-1 activates SCF(beta(TrCP))-dependent ubiquitination of IkappaBalpha. Mol Cell Biol. 2000;20(7):2326-33.

250. Eifler K, Vertegaal AC. Mapping the SUMOylated landscape. FEBS J. 2015;282(19):3669-80.

251. Flotho A, Melchior F. Sumoylation: a regulatory protein modification in health and disease. Annu Rev Biochem. 2013;82:357-85.

252. Tatham MH, Geoffroy M-C, Shen L, Plechanovova A, Hattersley N, Jaffray EG, et al. RNF4 is a poly-SUMO-specific E3 ubiquitin ligase required for arsenic-induced PML degradation. Nat Cell Biol. 2008;10(5):538-46.

253. Lallemand-Breitenbach V, Jeanne M, Benhenda S, Nasr R, Lei M, Peres L, et al. Arsenic degrades PML or PML–RARα through a SUMO-triggered RNF4/ubiquitin-mediated pathway. Nat Cell Biol. 2008;10(5):547-55.

254. Sun H, Leverson JD, Hunter T. Conserved function of RNF4 family proteins in eukaryotes: targeting a ubiquitin ligase to SUMOylated proteins. EMBO J. 2007;26(18):4102-12.

255. Gong X, Ahner A, Roldan A, Lukacs GL, Thibodeau PH, Frizzell RA. Non-native Conformers of Cystic Fibrosis Transmembrane Conductance Regulator NBD1 Are Recognized by Hsp27 and Conjugated to SUMO-2 for Degradation. J Biol Chem. 2016;291(4):2004-17.

256. Polevoda B, Sherman F. N-terminal acetyltransferases and sequence requirements for N-terminal acetylation of eukaryotic proteins. J Mol Biol. 2003;325(4):595-622.

257. Hwang C-S, Shemorry A, Varshavsky A. N-terminal acetylation of cellular proteins creates specific degradation signals. Science. 2010;327(5968):973-7.

258. Zattas D, Adle DJ, Rubenstein EM, Hochstrasser M. N-terminal acetylation of the yeast Derlin Der1 is essential for Hrd1 ubiquitin-ligase activity toward luminal ER substrates. Mol Biol Cell. 2013;24(7):890-900.

259. LaLonde DP, Bretscher A. The UBX protein SAKS1 negatively regulates endoplasmic reticulum-associated degradation and p97-dependent degradation. J Biol Chem. 2011;286(6):4892-901.

260. McNEILL H, Knebel A, Arthur JSC, Cuenda A, Cohen P. A novel UBA and UBX domain protein that binds polyubiquitin and VCP and is a substrate for SAPKs. Biochem J. 2004;384(2):391-400.

261. Ballar P, Zhong Y, Nagahama M, Tagaya M, Shen Y, Fang S. Identification of SVIP as an endogenous inhibitor of endoplasmic reticulum-associated degradation. J Biol Chem. 2007;282(47):33908-14.

262. Crosas B, Hanna J, Kirkpatrick DS, Zhang DP, Tone Y, Hathaway NA, et al. Ubiquitin chains are remodeled at the proteasome by opposing ubiquitin ligase and deubiquitinating activities. Cell. 2006;127(7):1401-13.

263. Aviram S, Kornitzer D. The ubiquitin ligase Hul5 promotes proteasomal processivity. Mol Cell Biol. 2010;30(4):985-94.

264. Kohlmann S, Schäfer A, Wolf DH. Ubiquitin ligase Hul5 is required for fragment-specific substrate degradation in endoplasmic reticulum-associated degradation. J Biol Chem. 2008;283(24):16374-83.

265. Sato BK, Schulz D, Do PH, Hampton RY. Misfolded membrane proteins are specifically recognized by the transmembrane domain of the Hrd1p ubiquitin ligase. Mol Cell. 2009;34(2):212-22.

266. Christianson JC, Ye Y. Cleaning up in the endoplasmic reticulum: ubiquitin in charge. Nat Struct Mol Biol. 2014;21(4):325-35.

267. Ruggiano A, Foresti O, Carvalho P. ER-associated degradation: Protein quality control and beyond. J Cell Biol. 2014;204(6):869-79.

268. Smith MH, Ploegh HL, Weissman JS. Road to ruin: targeting proteins for degradation in the endoplasmic reticulum. Science. 2011;334(6059):1086-90.

269. Guerriero CJ, Brodsky JL. The delicate balance between secreted protein folding and endoplasmic reticulum-associated degradation in human physiology. Physiol Rev. 2012;92(2):537-76.

270. Johnson PR, Swanson R, Rakhilina L, Hochstrasser M. Degradation signal masking by heterodimerization of MATα2 and MATa1 blocks their mutual destruction by the ubiquitin-proteasome pathway. Cell. 1998;94(2):217-27.

271. Arteaga MF, Wang L, Ravid T, Hochstrasser M, Canessa CM. An amphipathic helix targets serum and glucocorticoid-induced kinase 1 to the endoplasmic reticulum-associated ubiquitin-conjugation machinery. Proc Natl Acad Sci U S A. 2006;103(30):11178-83.

272. Furth N, Gertman O, Shiber A, Alfassy OS, Cohen I, Rosenberg MM, et al. Exposure of bipartite hydrophobic signal triggers nuclear quality control of Ndc10 at the endoplasmic reticulum/nuclear envelope. Mol Biol Cell. 2011;22(24):4726-39.

273. Gilon T, Chomsky O, Kulka RG. Degradation signals for ubiquitin system proteolysis in Saccharomyces cerevisiae. EMBO J. 1998;17(10):2759-66.

274. Shapira I, Charuvi D, Elkabetz Y, Hirschberg K, Bar-Nun S. Distinguishing between retention signals and degrons acting in ERAD. J Cell Sci. 2007;120(24):4377-87.

275. Mbonye UR, Wada M, Rieke CJ, Tang H-Y, DeWitt DL, Smith WL. The 19-amino acid cassette of cyclooxygenase-2 mediates entry of the protein into the endoplasmic reticulum-associated degradation system. J Biol Chem. 2006;281(47):35770-8.

276. Rabinovich E, Kerem A, Fröhlich K-U, Diamant N, Bar-Nun S. AAA-ATPase p97/Cdc48p, a cytosolic chaperone required for endoplasmic reticulum-associated protein degradation. Mol Cell Biol. 2002;22(2):626-34.

277. Bays NW, Wilhovsky SK, Goradia A, Hodgkiss-Harlow K, Hampton RY. HRD4/NPL4 is required for the proteasomal processing of ubiquitinated ER proteins. Mol Biol Cell. 2001;12(12):4114-28.

278. Nishikawa S-i, Fewell SW, Kato Y, Brodsky JL, Endo T. Molecular chaperones in the yeast endoplasmic reticulum maintain the solubility of proteins for retrotranslocation and degradation. The Journal of cell biology. 2001;153(5):1061-70.

279. Johnston JA, Ward CL, Kopito RR. Aggresomes: a cellular response to misfolded proteins. J Cell Biol. 1998;143(7):1883-98.

280. Garza RM, Sato BK, Hampton RY. In vitro analysis of Hrd1p-mediated retrotranslocation of its multispanning membrane substrate 3-hydroxy-3-methylglutaryl (HMG)-CoA reductase. J Biol Chem. 2009;284(22):14710-22.

281. Leichner GS, Avner R, Harats D, Roitelman J. Dislocation of HMG-CoA reductase and Insig-1, two polytopic endoplasmic reticulum proteins, en route to proteasomal degradation. Mol Biol Cell. 2009;20(14):3330-41.

282. Claessen JH, Ploegh HL. BAT3 guides misfolded glycoproteins out of the endoplasmic reticulum. PLoS One. 2011;6(12):e28542.

283. Xu Y, Cai M, Yang Y, Huang L, Ye Y. SGTA recognizes a noncanonical ubiquitin-like domain in the Bag6-Ubl4A-Trc35 complex to promote endoplasmic reticulum-associated degradation. Cell reports. 2012;2(6):1633-44.

284. Loayza D, Tam A, Schmidt WK, Michaelis S. Ste6p mutants defective in exit from the endoplasmic reticulum (ER) reveal aspects of an ER quality control pathway inSaccharomyces cerevisiae. Mol Biol Cell. 1998;9(10):2767-84.

285. Guerriero CJ, Weiberth KF, Brodsky JL. Hsp70 targets a cytoplasmic quality control substrate to the San1p ubiquitin ligase. J Biol Chem. 2013;288(25):18506-20.

286. Michaelis S, Herskowitz I. The a-factor pheromone of Saccharomyces cerevisiae is essential for mating. Mol Cell Biol. 1988;8(3):1309-18.

287. Ito H, Fukuda Y, Murata K, Kimura A. Transformation of intact yeast cells treated with alkali cations. J Bacteriol. 1983;153(1):163-8.

288. Berkower C, Loayza D, Michaelis S. Metabolic instability and constitutive endocytosis of STE6, the a-factor transporter of Saccharomyces cerevisiae. Mol Biol Cell. 1994;5(11):1185-98.

289. Mumberg D, Müller R, Funk M. Yeast vectors for the controlled expression of heterologous proteins in different genetic backgrounds. Gene. 1995;156(1):119-22.

290. Zhang Y, Michaelis S, Brodsky JL. CFTR expression and ER-associated degradation in yeast. Cystic Fibrosis Methods and Protocols. 2002:257-65.

291. Vembar SS, Jonikas MC, Hendershot LM, Weissman JS, Brodsky JL. J domain co-chaperone specificity defines the role of BiP during protein translocation. J Biol Chem. 2010;285(29):22484-94.

292. Amberg DC, Burke DJ, Strathern JN. Methods in Yeast Genetics. Cold Spring Harbor, NY, USA: Cold Spring Harbor Press; 2005.

293. Brodsky JL, Schekman R. A Sec63p-BiP complex from yeast is required for protein translocation in a reconstituted proteoliposome. J Cell Biol. 1993;123(6):1355-63.

294. Nakatsukasa K, Brodsky JL. In vitro reconstitution of the selection, ubiquitination, and membrane extraction of a polytopic ERAD substrate. Protein Secretion: Methods and Protocols. 2010:365-76.

295. Stirling C, Rothblatt J, Hosobuchi M, Deshaies R, Schekman R. Protein translocation mutants defective in the insertion of integral membrane proteins into the endoplasmic reticulum. Mol Biol Cell. 1992;3(2):129-42.

296. Nakatsukasa K, Kamura T. Subcellular Fractionation Analysis of the Extraction of Ubiquitinated Polytopic Membrane Substrate during ER-Associated Degradation. PLoS One. 2016;11(2):e0148327.

297. Kelley LA, Mezulis S, Yates CM, Wass MN, Sternberg MJE. The Phyre2 web portal for protein modeling, prediction and analysis. Nat Protocols. 2015;10(6):845-58.

298. Lee DH, Goldberg AL. Proteasome inhibitors: valuable new tools for cell biologists. Trends Cell Biol. 1998;8(10):397-403.

299. Helenius A, Simons K. Solubilization of membranes by detergents. Biochim Biophys Acta. 1975;415(1):29-79.

300. Niraula B, King TC, Misran M. Evaluation of rheology property of dodecyl maltoside, sucrose dodecanoate, Brij 35p and SDS stabilized O/W emulsion: effect of head group structure on rheology property and emulsion stability. Colloids Surf Physicochem Eng Aspects. 2004;251(1):59-74.

301. Luche S, Santoni V, Rabilloud T. Evaluation of nonionic and zwitterionic detergents as membrane protein solubilizers in two-dimensional electrophoresis. Proteomics. 2003;3(3):249-53.

302. Shorter J. The mammalian disaggregase machinery: Hsp110 synergizes with Hsp70 and Hsp40 to catalyze protein disaggregation and reactivation in a cell-free system. PLoS One. 2011;6(10):e26319.

303. Raviol H, Sadlish H, Rodriguez F, Mayer MP, Bukau B. Chaperone network in the yeast cytosol: Hsp110 is revealed as an Hsp70 nucleotide exchange factor. EMBO J. 2006;25(11):2510-8.

304. Kummer E, Szlachcic A, Franke KB, Ungelenk S, Bukau B, Mogk A. Bacterial and Yeast AAA+ Disaggregases ClpB and Hsp104 Operate through Conserved Mechanism Involving Cooperation with Hsp70. J Mol Biol. 2016;428(21):4378-91.

305. Glover JR, Lindquist S. Hsp104, Hsp70, and Hsp40: a novel chaperone system that rescues previously aggregated proteins. Cell. 1998;94(1):73-82.

306. Berman HM, Battistuz T, Bhat TN, Bluhm WF, Bourne PE, Burkhardt K, et al. The Protein Data Bank. Acta Crystallogr D Biol Crystallogr. 2002;58(Pt 6 No 1):899-907.

307. Li J, Jaimes KF, Aller SG. Refined structures of mouse P-glycoprotein. Protein Sci. 2014;23(1):34-46.

308. Sali A, Blundell TL. Comparative protein modelling by satisfaction of spatial restraints. J Mol Biol. 1993;234(3):779-815.

309. Haslbeck M, Miess A, Stromer T, Walter S, Buchner J. Disassembling protein aggregates in the yeast cytosol. The cooperation of Hsp26 with Ssa1 and Hsp104. J Biol Chem. 2005;280(25):23861-8.

310. Melville MW, McClellan AJ, Meyer AS, Darveau A, Frydman J. The Hsp70 and TRiC/CCT chaperone systems cooperate in vivo to assemble the von Hippel-Lindau tumor suppressor complex. Mol Cell Biol. 2003;23(9):3141-51.

311. Liou ST, Cheng MY, Wang C. SGT2 and MDY2 interact with molecular chaperone YDJ1 in Saccharomyces cerevisiae. Cell Stress Chaperones. 2007;12(1):59-70.

312. Mason AB, Allen KE, Slayman CW. C-terminal truncations of the Saccharomyces cerevisiae PMA1 H+-ATPase have major impacts on protein conformation, trafficking, quality control, and function. Eukaryot Cell. 2014;13(1):43-52.

313. von Bergen M, Barghorn S, Biernat J, Mandelkow EM, Mandelkow E. Tau aggregation is driven by a transition from random coil to beta sheet structure. Biochim Biophys Acta. 2005;1739(2-3):158-66.

314. Dawson RJ, Locher KP. Structure of a bacterial multidrug ABC transporter. Nature. 2006;443(7108):180-5.

315. Jones PM, George AM. Subunit interactions in ABC transporters: towards a functional architecture. FEMS Microbiol Lett. 1999;179(2):187-202.

316. Thibodeau PH, Brautigam CA, Machius M, Thomas PJ. Side chain and backbone contributions of Phe508 to CFTR folding. Nat Struct Mol Biol. 2005;12(1):10-6.

317. Tector M, Hartl FU. An unstable transmembrane segment in the cystic fibrosis transmembrane conductance regulator. EMBO J. 1999;18(22):6290-8.

318. Loo TW, Bartlett MC, Clarke DM. Processing mutations disrupt interactions between the nucleotide binding and transmembrane domains of P-glycoprotein and the cystic fibrosis transmembrane conductance regulator (CFTR). J Biol Chem. 2008;283(42):28190-7.

319. Berkower C, Michaelis S. Mutational analysis of the yeast a-factor transporter STE6, a member of the ATP binding cassette (ABC) protein superfamily. EMBO J. 1991;10(12):3777-85.

320. Neal SE, Mak R, Bennett EJ, Hampton R. A "Retrochaperone" Function for Cdc48: the Cdc48 Complex is Required for Retrotranslocated ERAD-M Substrate Solubility. J Biol Chem. 2017.

321. Paul S, Mahanta S. Association of heat-shock proteins in various neurodegenerative disorders: is it a master key to open the therapeutic door? Mol Cell Biochem. 2014;386(1-2):45-61.

322. Huyer G, Longsworth GL, Mason DL, Mallampalli MP, McCaffery JM, Wright RL, et al. A striking quality control subcompartment in Saccharomyces cerevisiae: the endoplasmic reticulum-associated compartment. Mol Biol Cell. 2004;15(2):908-21.

323. Ruan L, Zhou C, Jin E, Kucharavy A, Zhang Y, Wen Z, et al. Cytosolic proteostasis through importing of misfolded proteins into mitochondria. Nature. 2017;543(7645):443-6.

324. Rampelt H, Kirstein-Miles J, Nillegoda NB, Chi K, Scholz SR, Morimoto RI, et al. Metazoan Hsp70 machines use Hsp110 to power protein disaggregation. EMBO J. 2012;31(21):4221-35.

325. Lansbury PT, Jr., Costa PR, Griffiths JM, Simon EJ, Auger M, Halverson KJ, et al. Structural model for the beta-amyloid fibril based on interstrand alignment of an antiparallel-sheet comprising a C-terminal peptide. Nat Struct Biol. 1995;2(11):990-8.

326. Varley P, Gronenborn AM, Christensen H, Wingfield PT, Pain RH, Clore GM. Kinetics of folding of the all-beta sheet protein interleukin-1 beta. Science. 1993;260(5111):1110-3.

327. Goedert M. NEURODEGENERATION. Alzheimer's and Parkinson's diseases: The prion concept in relation to assembled Abeta, tau, and alpha-synuclein. Science. 2015;349(6248):1255555.

328. Jucker M, Walker LC. Self-propagation of pathogenic protein aggregates in neurodegenerative diseases. Nature. 2013;501(7465):45-51.

329. Spires-Jones TL, Attems J, Thal DR. Interactions of pathological proteins in neurodegenerative diseases. Acta Neuropathol. 2017.

330. Jackrel ME, DeSantis ME, Martinez BA, Castellano LM, Stewart RM, Caldwell KA, et al. Potentiated Hsp104 variants antagonize diverse proteotoxic misfolding events. Cell. 2014;156(1-2):170-82.

331. Zaarur N, Xu X, Lestienne P, Meriin AB, McComb M, Costello CE, et al. RuvbL1 and RuvbL2 enhance aggresome formation and disaggregate amyloid fibrils. EMBO J. 2015;34(18):2363-82.

332. Sanchez Y, Taulien J, Borkovich KA, Lindquist S. Hsp104 is required for tolerance to many forms of stress. EMBO J. 1992;11(6):2357-64.

333. Shaner L, Trott A, Goeckeler JL, Brodsky JL, Morano KA. The function of the yeast molecular chaperone Sse1 is mechanistically distinct from the closely related hsp70 family. J Biol Chem. 2004;279(21):21992-2001.

334. Olzscha H, Schermann SM, Woerner AC, Pinkert S, Hecht MH, Tartaglia GG, et al. Amyloid-like aggregates sequester numerous metastable proteins with essential cellular functions. Cell. 2011;144(1):67-78.

335. Sikorski RS, Hieter P. A system of shuttle vectors and yeast host strains designed for efficient manipulation of DNA in Saccharomyces cerevisiae. Genetics. 1989;122(1):19-27.

336. Becker J, Walter W, Yan W, Craig EA. Functional interaction of cytosolic hsp70 and a DnaJ-related protein, Ydj1p, in protein translocation in vivo. Mol Cell Biol. 1996;16(8):4378-86.

337. Caplan AJ, Cyr DM, Douglas MG. YDJ1p facilitates polypeptide translocation across different intracellular membranes by a conserved mechanism. Cell. 1992;71(7):1143-55.

338. Shaner L, Trott A, Goeckeler JL, Brodsky JL, Morano KA. The function of the yeast molecular chaperone Sse1 is mechanistically distinct from the closely related hsp70 family. J Biol Chem. 2004;279(21):21992-2001.

339. Ursic D, Culbertson M. The yeast homolog to mouse Tcp-1 affects microtubule-mediated processes. Mol Cell Biol. 1991;11(5):2629-40.

340. Haslbeck M, Braun N, Stromer T, Richter B, Model N, Weinkauf S, et al. Hsp42 is the general small heat shock protein in the cytosol of Saccharomyces cerevisiae. EMBO J. 2004;23(3):638-49.

341. Buck TM, Jordahl AS, Yates ME, Preston M, Cook E, Kleyman TR, et al. Interactions Between Intersubunit Transmembrane Domains Regulate the Chaperone Dependent Degradation of an Oligomeric Membrane Protein. Biochem J. 2016.

342. Canessa CM, Horisberger JD, Rossier BC. Epithelial sodium channel related to proteins involved in neurodegeneration. Nature. 1993;361(6411):467-70.

343. Schild L, Canessa CM, Shimkets RA, Gautschi I, Lifton RP, Rossier BC. A mutation in the epithelial sodium channel causing Liddle disease increases channel activity in the Xenopus laevis oocyte expression system. Proc Natl Acad Sci U S A. 1995;92(12):5699-703.

344. Grunder S, Firsov D, Chang SS, Jaeger NF, Gautschi I, Schild L, et al. A mutation causing pseudohypoaldosteronism type 1 identifies a conserved glycine that is involved in the gating of the epithelial sodium channel. EMBO J. 1997;16(5):899-907.

345. Buck TM, Plavchak L, Roy A, Donnelly BF, Kashlan OB, Kleyman TR, et al. The Lhs1/GRP170 chaperones facilitate the endoplasmic reticulum-associated degradation of the epithelial sodium channel. J Biol Chem. 2013;288(25):18366-80.

346. Nishikawa SI, Fewell SW, Kato Y, Brodsky JL, Endo T. Molecular chaperones in the yeast endoplasmic reticulum maintain the solubility of proteins for retrotranslocation and degradation. J Cell Biol. 2001;153(5):1061-70.

347. Kabani M, Kelley SS, Morrow MW, Montgomery DL, Sivendran R, Rose MD, et al. Dependence of endoplasmic reticulum-associated degradation on the peptide binding domain and concentration of BiP. Mol Biol Cell. 2003;14(8):3437-48.

348. Athanasiou D, Kosmaoglou M, Kanuga N, Novoselov SS, Paton AW, Paton JC, et al. BiP prevents rod opsin aggregation. Mol Biol Cell. 2012;23(18):3522-31.

349. Inoue T, Tsai B. The Grp170 nucleotide exchange factor executes a key role during ERAD of cellular misfolded clients. Mol Biol Cell. 2016;27(10):1650-62.